Solutions Manual

ADVANCED ENGINEERING DESIGN

Design for Reliability

Book: Advanced Engineering Design
Edition, 2012
www.engineering-abc.com

Solutions Manual
Last updated Feb 16, 2014

Dr.ir. Anton van Beek

Delft University of Technology
Mechanical Engineering

Recent updates:

Feb 27	Chapter 4, problem 4.1 and 4.4 updated, problem 4.2 new.
March 6	Chapter 3, problem 3.11, 3.12 and 3.15 new Chapter 3, problem 3.14 updated.
March 9	Chapter 3, Problem 3.5 new.
March 10	Chapter 3, Problem 3.24 new.
March 12	Chapter 3, Problem 3.3 solution updated Chapter 3, Problem 3.5 new Chapter 3, Problem 3.6 new
March 20	Chapter 6, Problem 6.3 and 6.4 Chapter 5, Problem 5.17
April 1	Chapter 3, Problem 3.13 solution updated Chapter 3, problem 3.12 solution updated

Problems Chapter 1

Problem 1.1: L_{10} service life

Consider a quantity of 10 components that all fail within a year of service. Calculate the L_{10} service life with 90% reliability and 10% failure probability assuming a normal failure distribution.

Months	1	2	3	4	5	6	7	8	9	10	11	12
Failures	0	0	0	0	0	1	2	4	2	1	0	0

Problem 1.2: Tolerance field

The diameter of a batch of shafts is normally distributed with 99.7% of the shafts within the tolerance field 20±0.2mm. Then 95% of the shafts will have a diameter within a tolerance field of 20 mm ±A mm.

a) What is A?

b) What is the coefficient of variation CV'?

CV' is defined as the maximum deviation of the mean divided by the mean.

Problem 1.3: Driving torque interference fit

An interference fit is realized with 20 H7/r6 hole/shaft tolerances. The dimensions of the components are assumed to be normally distributed. The standard deviation is calculated from the assumption that the tolerance interval is a ±3σ interval. Linear elastic deformation is to be considered which implies the torque that can be transmitted is proportional to the diametrical interference δ.

The torque that can be transmitted, based on the mean value of the diametrical interference, is T_{50} [Nm]. It is the torque with 50% failure probability. The torque that can be transmitted with 1% failure probability is denoted as T_1.

The variation of performance, relative to the mean, is a measure of reliability. The coefficient of variation is defined as CV'= deviation/mean. Calculate CV'= $(T_1-T_{50})/T_{50}$.

Problem 1.4: Driving torque tapered shaft hubs

The torque T that can be transmitted by a tapered shaft-hub connection is proportional to the clamping force, i.e. the bolt preload F_i. The preload F_i is proportional to M_A/μ where M_A is the tightening torque μ the coefficient of friction in the screw assembly. The coefficient of friction μ is managed by using a proper thread lubricant and varies between 0.12 and 0.16. Calculate the coefficient of variation CV'=$(T_{50}-T_{min})/T_{50}$ where T_{min} is the least torque that can be transmitted by the shaft-hub connection.

Problem 1.5: Interference fit with hollow shaft

A gear is to be press fitted over a hollow shaft of 20 mm diameter. Consider the interference δ=0.15±0.05 mm. The strain is that much that the hollow shaft will deform plastically.

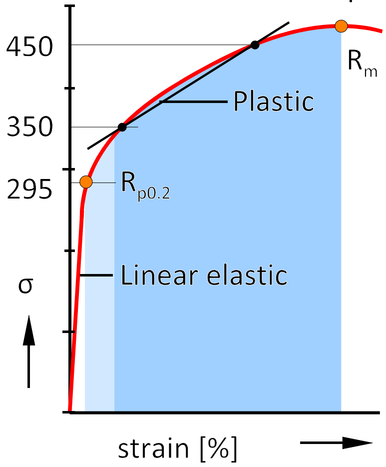

The tensile stress in the plastic regime varies much less with the strain than in the elastic regime.

The tensile stress in the plastic regime of the steel shaft is approximated by linear interpolation between σ(ε=0.005) = 350 MPa and σ(ε=0.01) = 450 MPa. Calculate the coefficient of variation CV'=(T_{50}-T_{min}) /T_{50} where T_{min} is the least torque that can be transmitted.

Problem 1.6: Chain dimensioning

The illustration below shows a simple drawing of a part made by milling. Calculate the symmetrical tolerance interval of A with 99% probability, assuming all tolerances are normally distributed within the ± 3σ interval and independent.

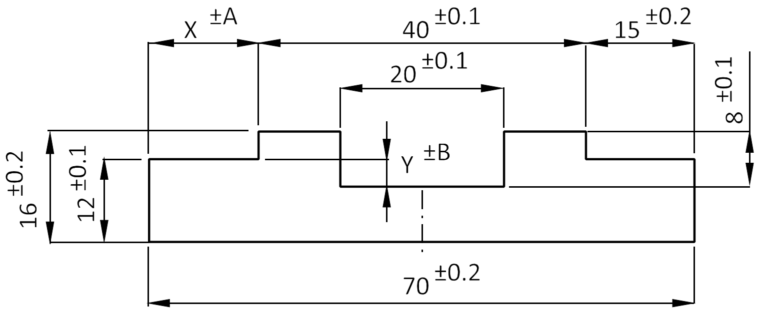

Problem 1.7: Number of measurements needed to obtain a reliable estimation

When the measurement of the coefficient of friction is repeated one will find a large variation. Consider the measured values 0.11, 0.12, 0.13, 0.14 and 0.15.

a) Calculate the 95% interval over which coefficient of friction may lie.

b) What number of measurements are needed to estimate the mean with 95% reliability within ±0.01 accuracy?

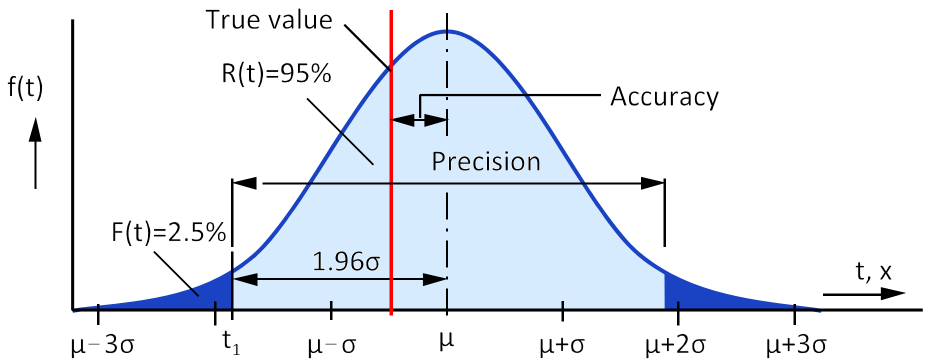

Problem 1.8: Estimation of service interval

From a series of experiments it is found that a component life is $\mu = 150 \cdot 10^3$ km and $\sigma = 20 \cdot 10^3$ km. A component reliability of 90% is specified with L_{10}, of 99% with L_1. Calculate the value L_{10} and L_1 and the ratio $a_1 = L_1/L_{10}$.

Problem 1.9: Conversion of MTBF to Reliability

a) Estimate the MTBF for N=10 devices that are tested for T_{test}=500 hours and during the test r=2 failures occur.

b) Estimate the probability that any one particular device will be operational at the time equal to the MTBF?

c) Estimate the probability that the component will work for 50% of the MTBF

d) Estimate the percentage of the MTBF where R(t)=0.95.

Problem 1.10: Fault Tree Analysis

Consider the fault tree with the component reliability given in the table below and calculate the failure probability F(t) of the system for a service life t.

	A	B	C	D	E	F	G
R(t)	0.9	0.85	0.9	0.7	0.95	0.8	0.99

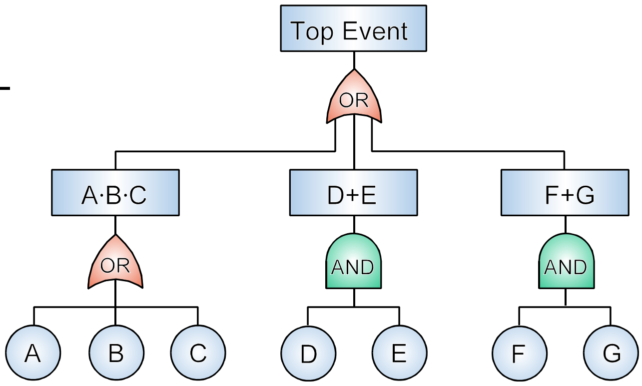

Problem 1.11: Bearing reliability, deep groove ball bearing

Calculate the operating reliability R(t=1000hr) of a deep groove ball bearing. The calculated L_{10} life expectancy of the ball bearing is $L_{10} = 500 \cdot 10^6$ rev. The rotational speed is 4000 rpm.

Hint: The life expectancy of the ball bearings is related to the L_{10} basic rating life according (eq. 4.66, page 129).

Problem 1.12: Reliability factor for Fatigue strength

A power supply is cooled by 3 fans. The correct functioning of at least one of the three fans is required to maintain sufficient cooling. The operating reliability of the system needs to be 99% for a service life of 10.000 hr, R_s (10.000 hr) = 0.99. The rotational speed is 4000 rpm.

a) Estimate the required operating reliability R_j of the individual fans.
b) Calculate the required L_{10h} of the individual bearings.
c) Calculate C/P

Problem 1.13: Reliability factor for Fatigue strength

Data published of the endurance strength are always mean values. In Norton (2000) is reported that the standard deviation of the endurance strength of steels seldom exceeds 8% of their mean. Estimate a correction factor for the endurance strength if a 99% probability is required.

Problem 1.14: Component reliability

Calculate the component reliability of a drive shaft (motor shaft) loaded in the High Cycle Fatigue (HCF) regime with $L_n = 2 \cdot 10^5$ load cycles.

Consider the calculated fatigue life of $L_{50} = 3 \cdot 10^5$ load cycles and a standard deviation of σ=0.2μ.

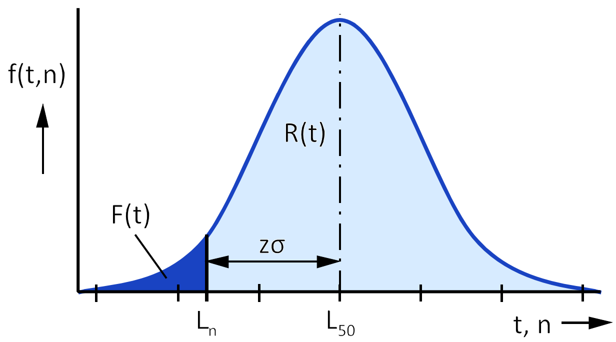

Problem 1.15: Stress concentration factor

"A chain is only as strong as its weakest link, regardless of the strength of the stronger links". Do you agree and what do you think about the reliability if the failure mode is fatigue?

Problem 1.16: System reliability

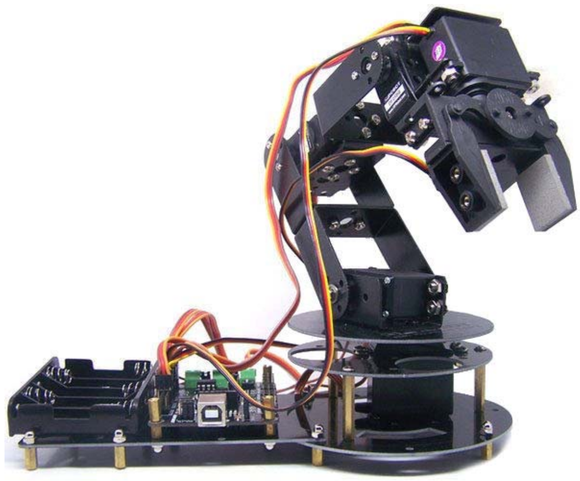

Calculate the failure probability F(100 hr) of two critical components of a system connected in series. From product catalogues it is found that the reliability of one component is specified with μ = 150 hr and σ = 30.5 hr, the other component is specified with μ = 120 hr and σ = 10.2 hr.

Hint: first step is to calculate R(t) of both components.

Problem 1.17: System reliability

A heavy-duty motorized frame features a quad drive system using two high power DC motors and four drive belts. All four belts are required to maintain optimal control. From field testing it is found that the service life of the belts under heavy duty operating conditions is normally distributed with a mean μ = 200 hr and a standard deviation of $\sigma = 0.2\mu$. Calculate the operating reliability of the set of 4 belts for a service life of 150 hr.

Problem 1.18: System reliability

There is a rule of thumb that says that the bearing load P related to the dynamic load rating of the bearing C is:

Normal loaded bearings P=0.06
Heavily loaded bearings P=0.12C

Consider a motor drive equipped with two ball bearings. One of the bearings is loaded with P=0.1C, where C is the dynamic load rating of bearing type 16004, C=7.28 kN. The motor rotates with n=1400 rpm during 8 hours a day, 5 days a week it is 1920 hr/year. Calculate the life expectancy [years] of this bearing with 1% failure probability.

Hint: First calculated L_{10} and L_{10h}. The life expectancy L_{na} of ball bearings is related to the L_{10} basic rating life according $L_{na} = a_1\, L_{10}$ (Table 4.6 page 129).

Problem 1.19: System reliability

Consider a motor drive equipped with two ball bearings. The life expectancy of the bearings is calculated as L_{10h}=12,000 hr and L_{10h}=16,000 hour respectively. Calculate the system (motor) reliability for a service life of 10,000 hour.

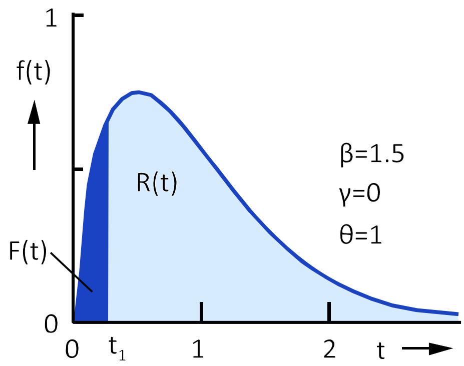

a) The life expectancy L_{na} of the ball bearings is related to the L_{10} basic rating life according $L_{na} = a_1 L_{10}$ (Table 4.6 page 129) where a_1 is the reliability factor derived from a statistical "Weibull distribution".

b) It is assumed that the failure distribution f(t) of the bearings is best fitted by a Weibull Failure Distribution function with shape factor β=1.5 (Eq. 1.5 page 12).

Problem 1.20: System reliability

The operating reliability of a production line needs to be estimated. The production line consists of 6 identical pick and place units with similar operating conditions.

The most critical components of the individual pick and place units are identified using an FMEA procedure. The operating reliability of these components are established and finally presented in a fault tree.

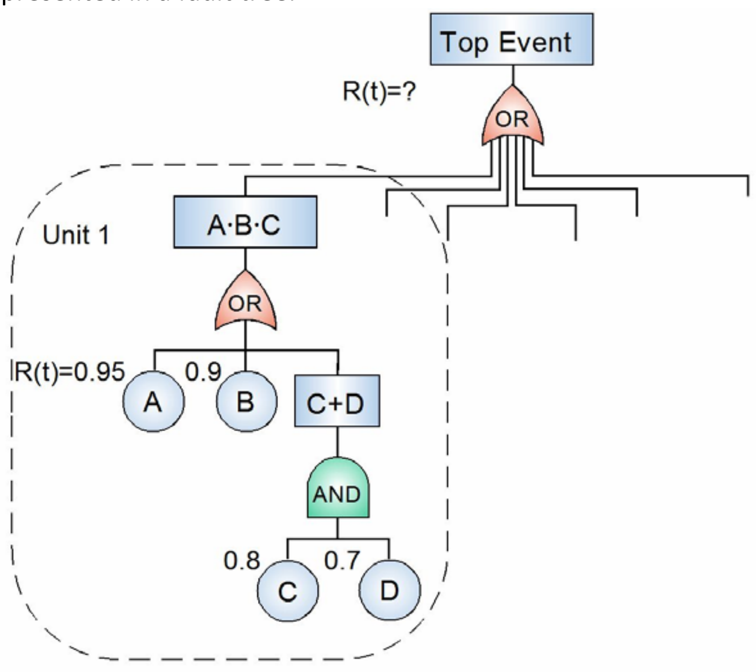

Calculated value of the operating reliability of the production line R(t).

Which of the components would you select to improve its operating reliability by 5 percent in order to improve the system reliability?

Problem 1.21: System reliability

A monitoring unit is applied to register as a function of time unexpected machine standstill which is caused by a specific component in the pick and place units. The service life t (hr) of this component is derived from the monitored data and listed in the table below.

Service life t (hr) of the critical component							
590	420	520	480	490	510	450	480

Calculate the required maintenance interval in order to replace this component in all pick and place units in time. The reliability of the individual pick and place units should be at least R(t)=0.99. What is t?

Problem 1.22: Precision and accuracy

Repeatability (precision) is the error between a number of successive attempts to move the machine to the same position. Repeatability can be represented by the interval which contains N% of the measured positions.

Accuracy is the difference between the intended position and the mean of the measured positions. The root-mean-square deviation (RMSD) or root-mean-square error (RMSE) is a frequently used measure for accuracy. The accuracy can be improved by adjusting the offset. The precision remains the same.

Resolution is the smallest possible movement of a system when actuated. Also known as the step size. The resolution of an instrument is the smallest increment that the gage displays.

$$RMSE = \sqrt{\frac{1}{N}\sum_{i=1}^{N}(x_i - x_{target})^2}$$

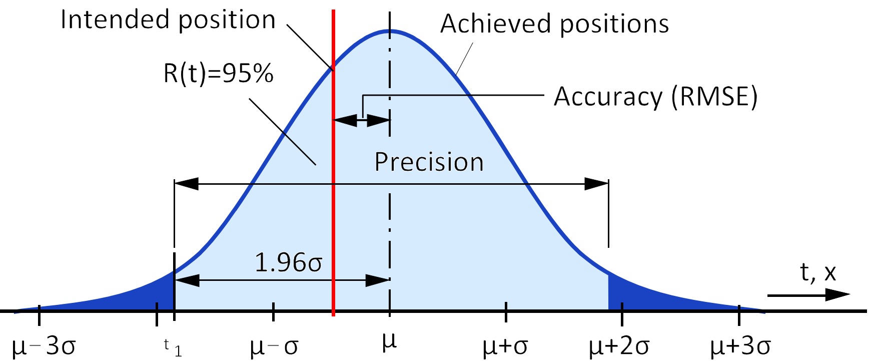

Consider an intended position of x_{target} = 40 mm and a range of measured x-data:
40.12, 40.07, 39.98 39.95 40.02 mm. Calculate the achieved accuracy and the repeatability within the 95% confidence interval. What is the resolution of the caliper shown above?

Answers

1.1)

$$\mu = \frac{1 \cdot 6 + 2 \cdot 7 + 4 \cdot 8 + 2 \cdot 9 + 1 \cdot 10}{n} = 8 \text{ months}$$

$$\sigma = \sqrt{\frac{(\mu-6)^2 + 2(\mu-7)^2 + 4(\mu-8)^2 + 2(\mu-9)^2 + (\mu-10)^2}{n-1}} = 1.155 \text{ months}$$

$$L_{10}: \quad z = 1.28 \qquad x = \mu - z\,\sigma \qquad x = 6.522 \text{ months}$$

1.2)

The mean value of the diameter of the shafts μ=20mm. The 99.7% interval is a ±3σ interval which results in σ = 0.2mm/3. The 95% symmetrical interval, with 2.5% on either side, corresponds to z=1.96 and A= 1.96σ = 0.13mm. The CV'-value is 1.96σ/μ = 0.65%.

1.3)

20H7: D_{max} = 20 mm + 21 µm, D_{min} = 20 mm + 0 µm, D_{mean} = 20 mm + 10.5 µm, σ_D= 21/6 µm
20r6 : d_{max} = 20 mm + 41 µm, d_{min} = 20 mm + 28 µm, d_{mean} = 20 mm + 34.5 µm, σ_d = (41-28)/6 µm

Interference mean δ_{50} = 34.5 µm - 10.5 µm = 24 µm, Interference SD $\sigma = \sqrt{(\sigma_D^2 + \sigma_d^2)} = 4.11\ \mu m$

The minimum value of δ with 1% failure probability $\delta_1 = \delta_{50} - z\,\sigma = 24 - 2.33\ 4.11 = 14.41\ \mu m$

Coefficient of variation, probabilistic: $CV' = \frac{\delta_{50} - \delta_1}{\delta_{50}} = 0.4$ thus, T_{min}=0.6 T_{mean}

The worst case scenario is obtained with the maximum bore diameter and the minimum shaft diameter.

The minimum value of δ (Deterministic): $\delta_{min} = D_{max} - d_{min} = 7\ \mu m$ and $CV' = \frac{\delta_{50} - \delta_{min}}{\delta_{50}} = 0.71$

1.4)

The mean value of the coefficient of friction μ_{50} = 0.14. The obtained preload F, with given tightening torque M, is minimal when the friction in fastener will have the highest value.

Torque ratio (worst case): $T = c\frac{M_a}{\mu} \qquad T\ \frac{1}{\mu} \qquad CV' = \frac{1/\mu_{mean} - 1/\mu_{max}}{1/\mu_{mean}} = 0.125$

where T is the torque the can be transmitted by the clamping action between the shaft - hub interface. Compared to the interference fit which is discussed in previous problem, a much smaller variation in the torque is obtained, and thus a more reliable connection is achieved. By controlling the friction, the reliability of the tapered shaft hub connection can be improved further. Besides special lubricants in the threaded area, washers are occasionally used as a means of minimising frictional scatter from the heat face friction during tightening.

1.5)

A small variation in the torque transmission is found, despite the large tolerance field on the diameter of the components.

Torque ratio (worst case): $CV' = \frac{T_{50} - T_{min}}{T_{50}} = \frac{p_{50} - p_{min}}{p_{50}} = \frac{\sigma(\varepsilon = 0.01) - \sigma(\varepsilon = 0.005)}{\sigma(\varepsilon = 0.01)} = \frac{400 - 350}{400} = 0.125$

1.6)

$$\mu_{15} = 15\ mm \qquad \mu_{40} = 40\ mm \qquad \mu_{70} = 70\ mm$$

$$\sigma_{15} = \frac{0.2\ mm}{3} \qquad \sigma_{40} = \frac{0.1\ mm}{3} \qquad \sigma_{70} = \frac{0.2\ mm}{3}$$

$$\mu_x = \mu_{70} - \mu_{40} - \mu_{15} \qquad \mu_x = 15\ mm$$

$$\sigma_x = \sqrt{\sigma_{15}^2 + \sigma_{40}^2 + \sigma_{70}^2} \qquad \sigma_x = 0.1\ mm$$

99% interval, 0.5% on both sides: $z = 2.58$

$$x_{\min} = \mu_x - z\sigma_x \qquad x_{\max} = \mu_x + z\sigma_x \qquad A = z\sigma_x = 0.258\ mm$$

A rule of thumb says that with chain dimensioning the probabilistic value can be estimated by the square root of the tolerances. This would result in: $A = \sqrt{(0.2^2 + 0.1^2 + 0.2^2)} = 0.3$

1.7)

The mean value is the same as the median in this case, μ=0.13.

$$\mu = \frac{0.11+0.12+0.13+0.14+0.15}{n} = 0.13$$

$$\sigma = \sqrt{\frac{(\mu-0.11)^2 + (\mu-0.12)^2 + (\mu-0.13)^2 + (\mu-0.14)^2 + (\mu-0.15)^2}{n-1}} = 0.016$$

The 95% interval of the COF of friction becomes $COF = \mu \pm 1.96\sigma = 0.13 \pm 0.031$

The standard deviation of the sample mean is $\sigma_m = \frac{\sigma}{\sqrt{n}} = 0.0071$

The 95% reliability interval of the sample mean is $COF = \mu \pm 1.96\sigma_m = \pm 0.014$

The number of experiments needed to have a 95% reliability of the estimation of the mean within ±0.01 accuracy is:

$$0.01 = 1.96\frac{\sigma}{\sqrt{n}} \qquad n = (\frac{1.96\sigma}{0.01})^2 \qquad n = 10$$

1.8)

Consider single side truncation of the probability density function

$$x_1 = \mu - z\sigma,\ z{=}2.33 \rightarrow x_1 = 103\ 10^3\ \text{km}$$

$$x_{10} = \mu - z\sigma,\ z{=}1.28 \rightarrow x_{10} = 124\ 10^3\ \text{km}$$

Note that with a 20% longer service the failure probability will increase to 10%.

1.9)

The Mean Time Between Failure MTBF = T/r = T_{test}·n / r = 10·500/2 = 2500 hr / failure
The failure rate λ is the inverse of the MTBF, λ = 1/MTBF = 1 / 2500 = 0.04% / hr
The reliability R(t)=exp(-λt) according (eq. 1.4 page 12), R(MTBF) = exp(-1) = 0.37 = 37%
The probability that the component will work for 50% of the MTBF is R(t)=exp(-0.5)=0.61
R(t)=0.95 is obtained with -ln(0.95)=0.0513 MTBF, only 5% of the MTBF.

1.10) F(t) = 1 - A·B·C · [1- (1-D) (1-E)] [1- (1-F) (1-G)] = 32%

1.11)

$$L_{10h} = \frac{L_{10}}{60n} = 2083\text{hr} \qquad L_{nh} = 1000\text{hr} \qquad a_1 = \frac{L_{nh}}{L_{10h}} = 0.48 \qquad R = \exp(-(a_1/4.48)^{3/2}) = 0.966$$

1.12)

$$R_s = 0.99 \quad n = 3 \quad R_j = 1-(1-R_s)^{1/n} \quad R_j = 0.785$$
$$L_{nh} = a_1 L_{10h} \quad a_1 = 4.48\ln(1/R_j)^2/3 \quad a_1 = 1.743$$
$$L_{10h} = 5738\,\text{hr} \quad n = 4000\,\text{rpm} \quad L_{10} = 1377\,10^6$$
$$C/P = (L_{10}/10^6)^{1/3} = 11.1 \quad P/C = 0.09$$

1.13)

Standard deviation σ = 0.08μ
L_n = μ-zσ, 99% reliability, n=1, z=2.33
L_{50} = μ, 50% reliability
C_{reliab} = L_n/L_{50}, L_1/L_{50}=(μ - z·σ)/μ = 0.814

Reliability factors C_{reliab} for σ=0.08μ

R(t)	50%	90%	99%	99.9%
C_{reliab}	1.000	0.897	0.814	0.753

1.14)

$$x = L_n,\ \mu = L_{50},\ \sigma = 0.2\mu \qquad z = \frac{\mu - x}{\sigma} \qquad z = 1.667 \quad \text{Table 1.2:} \quad R = 0.95$$

1.15)
A chain with 100 components (links) connected in series and component reliability 0.99 results in a system reliability of 0.99^{100}=0.366. If, one of the components has component reliability 0.95 (the weakest link in the chain), the system reliability becomes 0.99^{99}·0.95=0.351. The conclusion is that “A chain is only as strong as its weakest link” is valid in a deterministic approach, and it is the criterium for failure by overload. In the case of a probabilistic approach which is necessary for reliability analysis if the failure mode is fatigue, the reliability of all components matter.

1.16)

$$x = 100,\ \mu_1 = 150,\ \sigma_1 = 30.5,\ \mu_2 = 120,\ \sigma_2 = 10.2$$

$$z_i = \frac{\mu_i - x}{\sigma_i} \quad z_1 = 1.64 \quad z_2 = 1.96 \quad \text{Table 1.2:} \quad R_1 = 0.95 \quad R_2 = 0.975 \quad R_s = R_1 R_2 \quad F_s = 1 - R_s$$

1.17)

$$x = 150,\ \mu = 200,\ \sigma = 0.2\mu \qquad z = \frac{\mu - x}{\sigma} \qquad z = 1.25 \quad \text{Table 1.2:} \quad R = 0.9 \quad R_s = R^4 = 66\%$$

1.18)

$$C = 7.28\,kN,\; P = 0.1C,\; L_{10} = (C/P)^3 10^6 = 10^9\,\text{rev}$$
$$L_{10h} = L_{10}/60n = 11.9\,10^3\,\text{hr} = 6.2\,\text{year}$$
$$L_1 = a_1 L_{10}h,\; a_1 = 0.21,\; L_1 h = 1.3\,\text{year}$$

The ball bearing loaded with P=0.1C will have a life expectancy with 1% failure probability of 1.3 year.

1.19)

a)

$$\left.\begin{array}{l} a_1 = \dfrac{L_{nh}}{L_{10h}} = \dfrac{10{,}000}{16{,}000} = 0.625 \;\rightarrow\; R_1(10{,}000hr) = 0.949 \\ a_1 = \dfrac{L_{nh}}{L_{10h}} = \dfrac{10{,}000}{12{,}000} = 0.833 \;\rightarrow\; R_2(10{,}000hr) = 0.923 \end{array}\right\} R_s = R_1 R_2 = 0.876$$

b) Weibull's reliability function is (eq. 1.5 page 12)

$$R(t) = \exp\left(-\left(\frac{t}{\theta}\right)^{\beta}\right) \quad \text{solving } \theta \text{ results in:} \quad \theta = \frac{t}{(-\ln(R))^{1/\beta}}$$

Consider bearing 1: Substitution of β=1.5, R=0.9 and t=L_{10h}=16000 hr results in θ=71724 hr
The reliability of bearing 1 for the life of t=10000 hr can now be solved

$$R(t{=}10000) = \exp\left(-\left(\frac{t}{\theta}\right)^{\beta}\right) = 0.949$$

Repeating the method above for the other bearing result in the system reliability:

$$R_2 = 0.923,\; R_{system} = R_1 R_2 = 0.876$$

1.20)

A = 0.95, B = 0.9, C = 0.8, D = 0.7
R_{CD} = 1 - (1 - C) (1 - D) = 0.94
R_{unit} = A B (1 - (1 - C) (1 - D)) = 0.804
$R_{system} = R_{unit}^{\;6}$ = 0.27
The reliability of the components A and B dominate the system reliability.

1.21)

$$\mu = \frac{590 + 420 + 520 + 480 + \ldots}{8} = 492.5$$

$$\sigma = \sqrt{\frac{(\mu - 590)^2 + (\mu - 420)^2 + (\mu - 520)^2 + \ldots}{n-1}} = 50.64$$

$$99\%\ \text{reliability};\quad z = 2.33 \qquad t = \mu - z\,\sigma = 375\ \text{hr}$$

1.22)

N=5, μ = 40.028 mm, σ = 0.068 mm, RMSE = 0.067 mm
a) Accuracy: μ - x_{target} = 0.028 mm
b) Precision with 95% confidence interval: ±1.96σ = ± 0.134 mm
c) Resolution of the caliper is 0.01 mm

95% confidence interval of accuracy: $\pm 1.96\sigma_m,\; \sigma_m = \sigma/\sqrt{n} = 0.031,\; COF = \pm 0.062$

number of experiments needed to determine the accuracy within a 95% confidence interval of ±0.05

$$0.05 = 1.96\,\sigma/\sqrt{n},\; n = (1.96\sigma/0.05)^2 = 7$$

Problems Chapter 3

Problem 3.1: Fatigue of a bicycle front fork

A manufacturer of mountain bike components developed a light weight magnesium alloy front fork. Unfortunately, the fork cracked during field testing under normal loading conditions after only a few rough rides.

The design engineer was asked to check the fork design for stress concentrations. He made a solid model of the fork, performed 3D stress analysis in which the critical loading from braking and horizontal/vertical loading of the front wheel was set as input, optimized the model's surface mesh by creating a finer mesh around the small holes located at the brake connections and made the stress concentrations visible. The stress analysis proofed that the cracking experienced in the initial prototype testing was due to the part design, not the material properties of magnesium.

The first run showed areas of high stress beyond the critical failure point. The stress raisers were smoothened in some extra iterations, making modifications to the shape of the design and wall thickness. The modified design was manufactured and tested successfully. To evaluate the permissible stresses in design stage it is important to know in what fatigue regime the fork will operate during its life. Would it be in the LCF or in HCF regime?

Problem 3.2: Infinite life design cardan joint spline shaft loaded in torsion

Consider the cylindrical part of a drive shaft cyclically loaded in torsion. The ultimate tensile stress of the shaft is R_m=500 MPa. The shaft operates in the "infinite life" regime where σ'_e=0.5 R_m (Table 3.1 page 69) and σ_e=0.7σ'_e (eq. 3.3 page 68) and τ=0.58 σ_e. The yield stress of the shaft is $R_{p0.2}$=0.6R_m, the shear strength 0.58 $R_{p0.2}$.

Calculate D_{dyn}/D_{stat} where D_{dyn} is the shaft diameter required when dynamically loaded and D_{stat} when statically loaded.

a) Stress concentrations are left out of consideration.
b) The stress concentration in the shoulder fillet is K_t=1.7

Problem 3.3: Infinite life design drive shaft with transverse hole loaded in torsion

Consider a drive shaft with transverse hole cyclically loaded in torsion with T = ±10 Nm. The ultimate tensile stress of the shaft is R_m = 500 MPa, the yield stress of the shaft is $R_{p0.2}$ = 0.6R_m. The diameter of the transverse hole in the shaft is related to the diameter of the shaft according d/D = 0.2. Calculate the diameter of the shaft when:

a) statically loaded. Hint:

$$T=\frac{\pi}{16}D^3\left(1-1.7\frac{d}{D}\right)^3\tau \quad \tau=0.58R_{p0.2}$$

b) cyclically loaded in the "infinite life" regime where σ'_e = 0.5R_m (Table 3.1 page 69), σ_e= 0.7σ'_e and τ_e=0.58σ_e. The stress concentration factor can be calculated with the curve fit function K_t=1.5899-0.6355 log(d/D).

Problem 3.4: Infinite life design drive shaft under rotary bending

A stepped shaft is subjected to rotary bending M = 4 Nm. The ultimate tensile stress of the shaft is R_m = 500 MPa, the yield stress of the shaft is $R_{p0.2}$ = 0.6R_m. Calculate the diameter of the shaft when:

a) statically loaded.

b) cyclically loaded in the "infinite life" regime where σ'_e = 0.5R_m (Table 3.1 page 69), σ_e = 0.7σ'_e and K_t = 2.5.

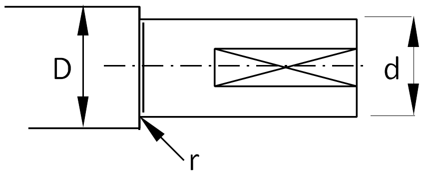

Problem 3.5: Infinite life design drive shaft under rotary bending

Calculate M_1/M_2 where
- M_1 is the endurance strength for rotary bending of a 12 mm diameter shaft without groove and
- M_2 is the endurance strength for rotary bending of a grooved shaft of d=20 mm, d_k=19 mm and K_t=5.

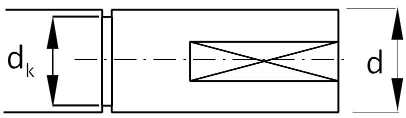

Problem 3.6: Infinite life design drive shaft under rotary bending

Consider a grooved shaft in rotary bending. The diameter of the shaft d = d_1 = 20 mm, the diameter of the groove d_k = 19 mm. The stress concentration factor K_t = 5. Calculate how much weight can be saved when this shaft is replaced by an un-grooved shaft of smaller diameter d_2 with the same endurance strength.

Calculate the percentage [%] of weight saving $(m_1-m_2)/m_1$ where m_1 is the mass of the grooved shaft and m_2 is the mass of the ungrooved shaft.

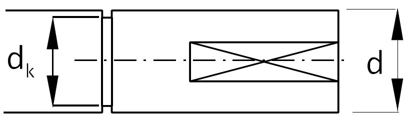

Problem 3.7: Cyclically loaded bolted structure

Consider a cyclically loaded bolted structure using M10-8.8 bolts. The joint stiffness $k_m=3k_b$ (Figure 3.18 page 80). All bolts are tightened by a preload between $0.6F_{0.2} < F_i < 0.8F_{0.2}$. Calculate:

a) the maximum external load P that is limited by the bolts yield strength.

b) the maximum external load P that is limited by the clamping force ($F_m \geq 0$).

c) the preload $F_i(F_{0.2})$ that will result in the maximum load capacity. In this case both the yield strength and clamping force needs to be considered.

d) the maximum external load P that is limited by the endurance strength of the bolts.

e) Give some reasons for why the preload is defined within a range. List some more influence factors that may affect the reliability of the load capability.

Problem 3.8: Spring model of a screw joint

Derive an equation for P_b/P expressed in k_b and k_m, where P_b is the load fluctuation in the threaded section between the nuts, P is the load fluctuation applied to the screw joint and k_m, k_b is the stiffness of the clamped material and the bolt respectively.

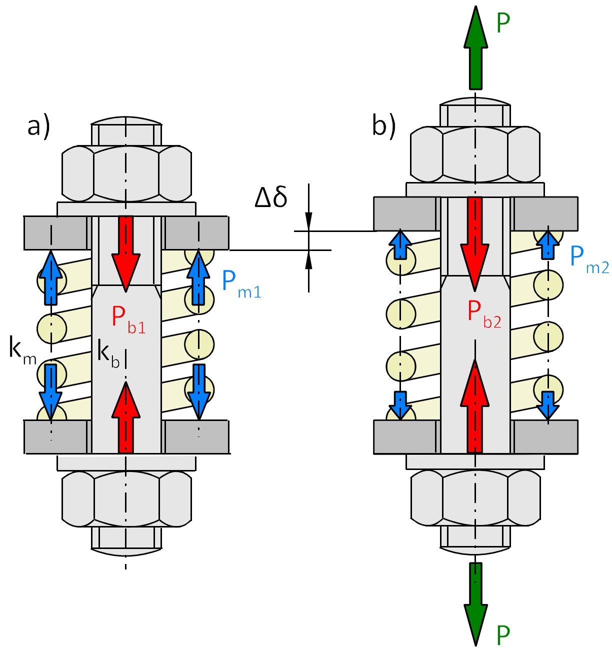

Problem 3.9: On the design of cyclically loaded screw joints

a) Calculate the fatigue strength P of the bolted structure as shown, where P is the maximum load fluctuation in the endurance strength regime of the bolt stress. Consider M24-8.8 bolts with a pretension of $0.6R_{p0.2}$ and a joint stiffness factor $C_m=1/4$.

b) In what way would you redesign the structure in order to obtain an improved fatigue strength?

Problem 3.10: Improved fatigue strength of a screw joint

Calculate the factor to which the fatigue strength P of the screw joint will increase by placing a ring below the nut, where P is the maximum load fluctuation in the endurance strength regime of the bolt stress.

Consider l_{m1}=2d and l_{m2}=3d.

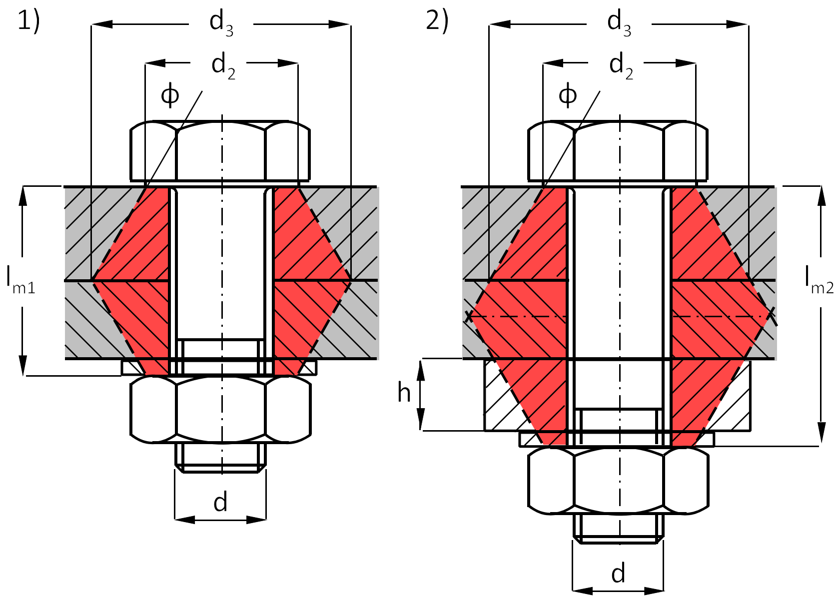

Problem 3.11: Improved fatigue strength of a screw joint

Calculate the factor to which the fatigue strength P of the screw joint will increase or decrease by replacing a metric M12-8.8 screw by a metric M10-10.9 screw. The thickness of the clamped members L_m=2d where d=12mm are kept the same.

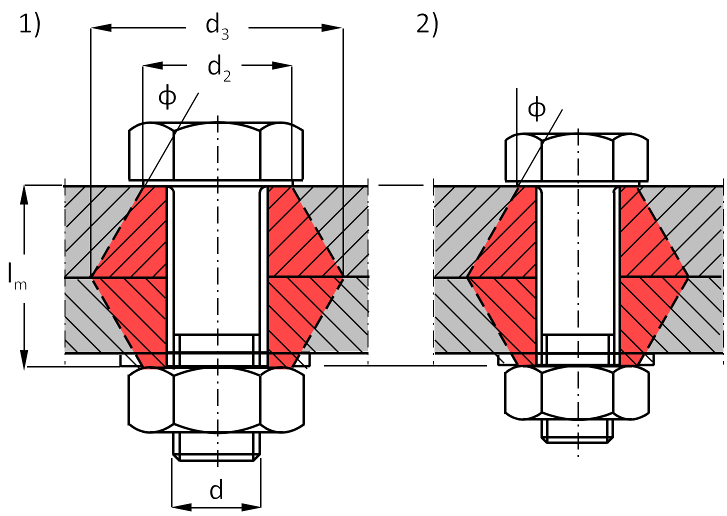

Problem 3.12: Improved fatigue strength mounting of a bearing housing

Consider two possible configurations for the mounting of a bearing housing. Both configurations are realised with M12 bolts sufficiently preloaded. The clamping length of the configuration 1 and 2 are $L_{m.1}$=0.8d and $L_{m.2}$=2d.

Calculate P_2/P_1, where P_1 and P_2 are the maximum load fluctuations on the bearings of configuration 1 and 2 respectively

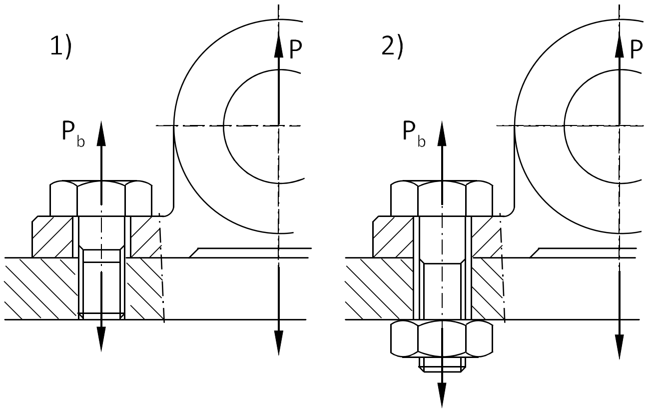

Problem 3.13: Improved fatigue strength piston - rod connection

Consider two possible configurations for a hydraulic piston - rod connection.
Configuration 1) M24-8.8, clamped over L_m=d, preloaded with $0.8F_{0.2}$
Configuration 2) M12-8.8, clamped over L_m=3d, preloaded with $0.8F_{0.2}$

Calculate the ratio of the fatigue strength P_2/P_1. P_1 and P_2 are the piston forces of configuration 1 and 2 respectively, that can be sustained for infinite life. The small letter p is the hydraulic pressure.

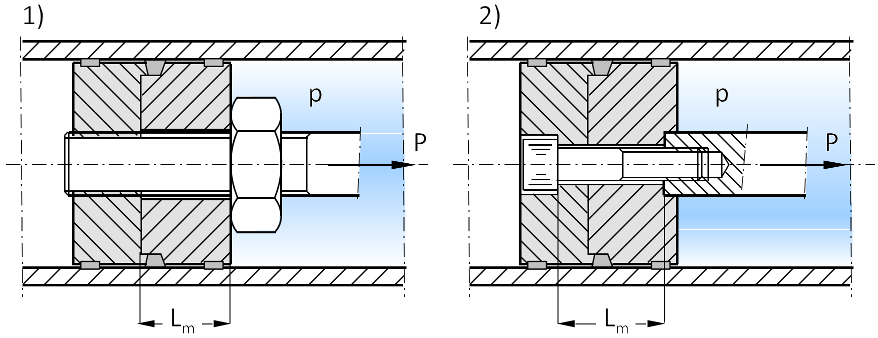

Problem 3.14: Fatigue failure probability of a screw joint

Consider a pneumatic cylinder that consists of an aluminium bushing with two end caps clamped by 4 steel bolt studs.

Bolt studs: d_b=4 mm, E_{steel}=210 GPa
Bushing: D_{cyl}=80mm, wall thickness s=6 mm, E_{alum}=70 GPa

a) Calculate the joint stiffness factor C_m.

b) The bushing is replaced by one with a 3 mm wall thickness. So, the joint stiffness factor of a screw joint is not C_m=1/4.2 but becomes C_m=1/2.6. What consequences will this deviation in joint stiffness have for the fatigue strength of the bolted connection.

Problem 3.15: Improved fatigue strength using stretch bolts

Stretch bolts are used by car manufacturers for several reasons; to accommodate LCF thermal expansion (thermo-mechanical fatigue TMF), to withstand HCF load and finally they can be prestressed accurately.

a) Calculate the stress concentration factor in the threaded section of the bolt. Consider a metric M12-8.8 bolt and an endurance strength of the steel when loaded in axial tension of σ'_e =0.4Rm. The fatigue strength of the threaded part σ_a=50 MPa is derived from Figure 3.16 page 79.

b) Calculate the minimal diameter of the shank, if the same fatigue strength [N] is asked for the shank and the threaded section. The stress concentration in the fillet on both ends of the shank is K_t=1.8. The strength reduction factors in the shank are $C_{surf} C_{reliab}$ = 0.8.

Problem 3.16: Infinite life design cylinder head studs

Cylinder head stud bolts clamp the cylinder head to the block. To maintain a tight leak-free seal, the bolts must be tightened in the proper sequence to specifications.

One of the methods to torque head bolds is called torque to yield (TTY). It means that the equivalent stress is increased until it reaches the yield strength during tightening. A rule of thumb says that the torsional stress increases the equivalent stress by approximately 20% and is released as a result of relaxation after tightening.

Calculate the maximum load fluctuation P_b that can be taken by each stud. Consider M10 threaded studs, A_t=58 mm^2, steel grade 12.9 and C_m=1/8.

Problem 3.17: Thermo Mechanical Fatigue (TMF) of cylinder head studs

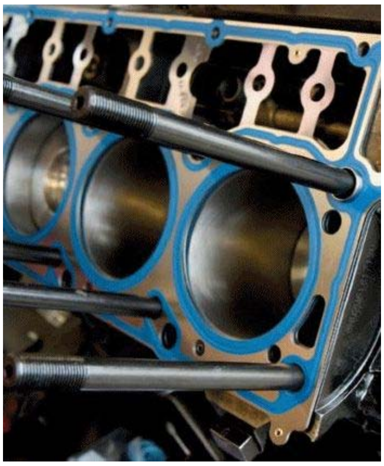

The overall clamp force generated by the cylinder head bolts/studs and its uniform distribution across the entire sealing system is a major issue. Various areas are to be sealed (gas, water and oil seal) and compression forces and thermal expansion must be accommodated while keeping an optimum clamping force over the gasket.

Each time the motor temperature increases from cold start to operating temperature the aluminium cylinder head expands. Because the cylinder head studs are made of steel and thermally expand to a lesser degree, the bolt stress varies each temperature cycle. Calculate to what extend the bolt stress will increase by thermal expansion of the head. Consider 10 mm diameter bolt studs and a clamping length of 150 mm.

Problem 3.18: Thermo Mechanical Fatigue (TMF) of solder joints

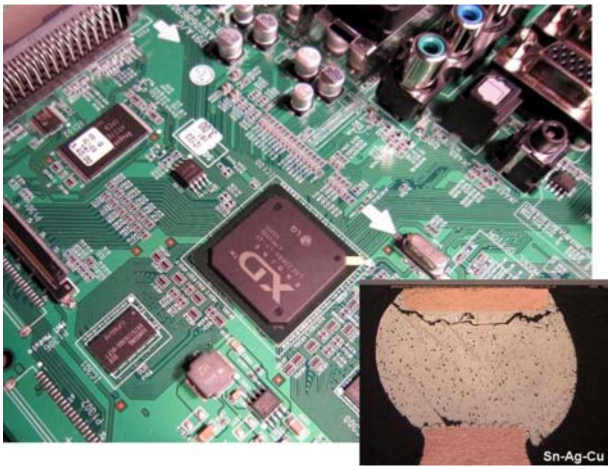

For environmental reasons tin-lead solders, for example Sn-37Pb, are replaced by lead free solders. Lead free solders, that are now being used are tin-silver-copper alloys. In the so called Ball Grid Array (BGA) packages in SMT these solder joints appear to suffer from Thermo Mechanical Fatigue.

The differences in the thermal expansion rates of the components and the printed circuit boards causes the solder joints to undergo cyclic elastic/plastic deformations. The plastic deformations can harden the solder and finally cause solder cracks and joint failure (cohesive bonding failure).

Derive an equation for the shear force acting on the solder joint, related to the thermo-mechanical properties of the components.

Problem 3.19: Infinite life design compression spring

Calculate the max amplitude of a compression spring for infinite life. Consider a wire diameter d=10 mm, number of winds n=8, radius of the winds r=50 mm, a shear modulus of G=80 GPa, R_m = 2220 - 820 log d where d [mm] and R_m [MPa], a fatigue strength for 10^7 stress cycles of τ_e / R_m=0.15. Approximate equations for spring stiffness of coil springs are listed in Table A4 page 526.

Problem 3.20: Finite life design of a welded chassis

Two hot rolled steel sections of S235 ($R_{p0.2}$ =235 MPa) are connected by welding. The fatigue strength of the welded zone is characterised σ_{HCF} ($N=10^7$) = 30 MPa (SN-diagram shown below).

Calculate the number of stress cycles that can be sustained with stresses as high as the yield strength of the structural steel itself.

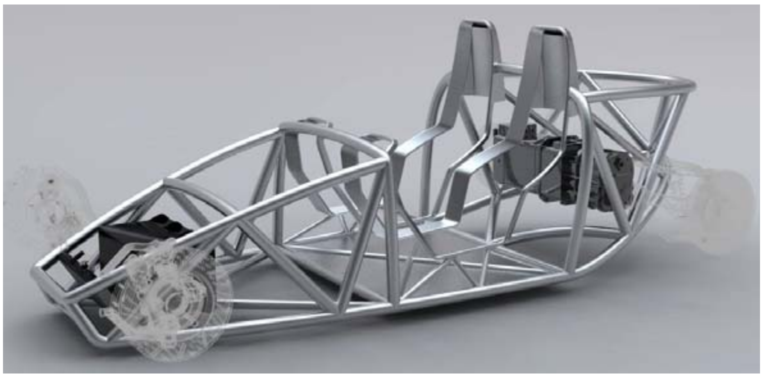

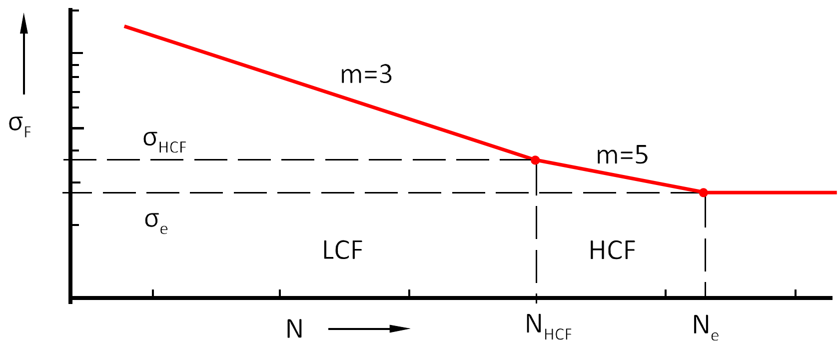

Problem 3.21: Finite life design of butt-weld connections in pipe flanges

Socket weld pipe flanges actually slip over the pipe. These pipe flanges are typically machined with an inside diameter slightly larger than the outside diameter of the pipe. Socket pipe flanges, are secured to the pipe with a fillet weld around the top of the flange.

Weld neck flanges attach to the pipe by welding the pipe to the neck of the pipe flange with u butt weld. The neck allows for the transfer of stress from the weld neck pipe flanges to the pipe itself. Weld neck pipe flanges are often used for high pressure applications. The inside diameter of a weld neck pipe flange is machined to match the inside diameter of the pipe.

Calculate the ratio of the fatigue life of the weld connection in a “socket weld pipe flange” with respect to the “weld neck pipe flange”, N_s/N_n. The Socket weld flange is typically a detail category with $\sigma_{HCF}(N=10^7)$=30 MPa, the weld neck flange with $\sigma_{HCF}(N=10^7)$=45 MPa (SN-diagram shown in previous problem). Consider a fatigue load inducing a stress over the cross section of the pipe of 50 MPa.

Problem 3.22: Finite life design of butt-weld connections using the Palmgren-Miner rule

Steel grades known as S235, S275 and S355 are non-alloy structural steels. The steel grades of the JR, JO, J2 and K2 categories are in general suitable for all welding techniques. The yield strength of S235 for example is 235 MPa. The strength of butt welds when statically loaded do not need to be calculated separately, since the strength of the weld material is at least as strong as that of the structural steel.

A reasonable estimation of the endurance strength of structural steels made of S235 subjected to cyclic bending is σ_e = 0.4Rm ≈ 160 MPa, which is 70% of the yield strength .

The endurance strength of welded connections is much less than the endurance strength of the structural steel members. For example, the endurance strength of butt welds is limited to approximately σ_e=0.55·45≈25 MPa (Figure 3.30 page 90 and Figure 3.27 page 87), which is less than 20% of the endurance strength of the structural steel S235.

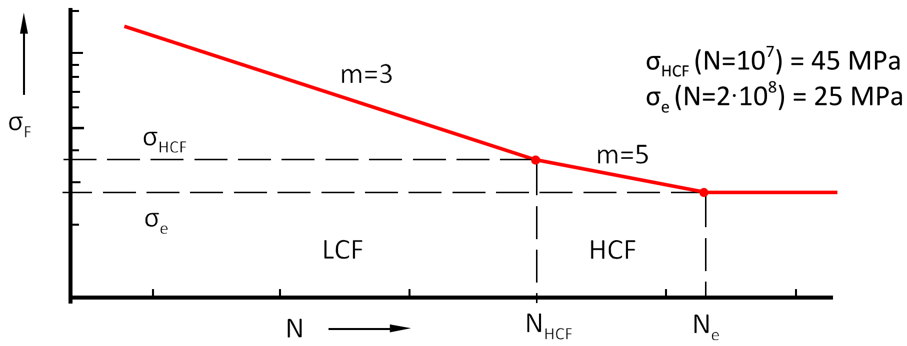

The relatively low value of the endurance strength of welded connections and the relative high stress peaks that must be sustained during life makes that most welded structures are designed in the “finite life regime”. Since parts are seldom stressed repeatedly at only one stress level, the cumulative damage effect of operations at various levels of stress need to be considered.

Calculate the fatigue life L(hr) of a welded connection located between the cylinder bushing and the end cap of a hydraulic cylinder.

The actual stresses in the weld are measured during one hour of service. The stress spectrum is simplified into the values which are listed in the table below.

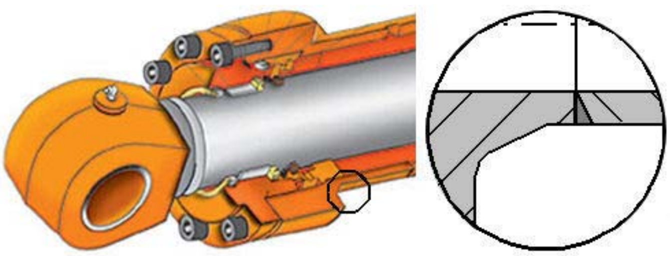

σ_F [MPa]	240	120	60	30	20
n_i [-]	10	20	40	400	1000

Problem 3.23: Finite life design of fillet-weld connections

A crane picks and place a load from position A to position B and back.

a) Calculate the static load F/(aL) that the fillet welds can sustain. L is the length of the weld over which the load is uniformly distributed and a is the cross section at the throat. The yield strength of the weld material is 235 MPa.

b) The stress spectrum in the welded zone of the lifting plates is simplified to n_{AB}=N/2 times σ and n_{BA}=N/2 times σ/3 where N is the fatigue life expressed in load cycles. Consider a stress σ=90 MPa and the SN-diagram of the fillet weld shown below. Calculate the fatigue life N

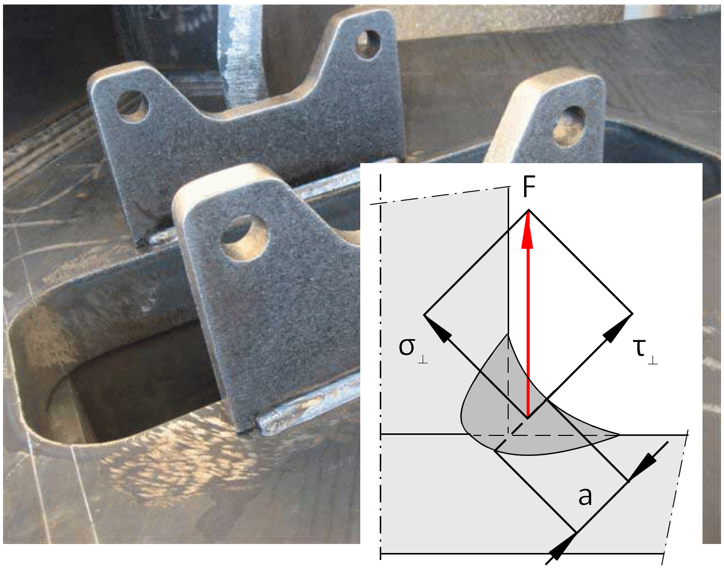

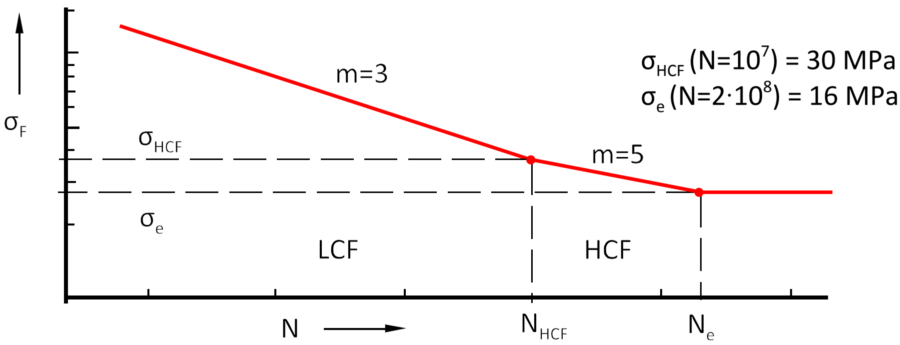

Problem 3.24: Finite life design of a fillet-weld subjected to bending

Consider the lift plate loaded in bending. Derive an equation for the maximum bending stress in the fillet weld. The left plate is welded with a double fillet weld with a cross section of the throat a.

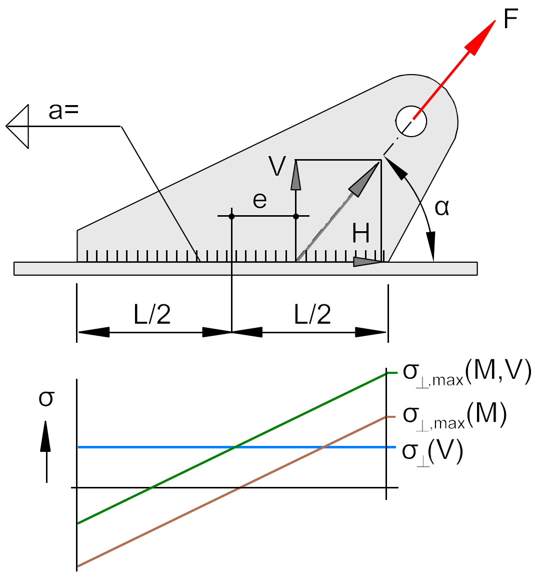

Problem 3.25: True or Untrue?

1. Finite element analysis will underestimate stress concentrations when applying a course grid.
2. It is always save to use the geometrical stress concentration factor Kt rather than the fatigue stress concentration factor K_f while $K_t \geq K_f$.
3. Fatigue failure might result form cyclic loading only if there is some tension in each stress cycle.
4. The introduction of residual compressive stresses to improve the fatigue strength can also be useful at shaft fillets and grooves, for example by impressing a hardened roller against a shaft as it is turned in a lathe.
5. Rotary machinery generally operate in the “infinite life regime” with stresses below endurance strength.
6. The ratio of endurance strength to ultimate tensile strength is taken 1/3 in a first approximation for steel shafts under rotary bending.
7. When a crack is formed it creates stresses larger than those from the original notch.
8. Fatigue fractured drive shafts in torsion typically show a fracture face under 45 degrees with the cross section.
9. The Smith diagram provides information about the influence of the mean stress on the endurance strength.
10. The Wöhler diagram also called SN diagram provides information about the fatigue strength in both the LCF as the HCF regime.

11. The stress concentration factor K_f can be determined by FEM calculation.
12. The Smith diagram provides information about the fatigue strength in the low cycle fatigue regime.
13. For steels the ratio of endurance strength σ_e to 0.2% yield strength $R_{p0.2}$ is taken 1/3 in a first approximation for steel shafts under rotary bending.
14. Smooth cylindrical drive shafts without any stress concentrations will not fail by fatigue.
15. Fatigue failure occurs typically at stresses below the endurance strength.
16. Fatigue failure only occurs at stresses below the yield strength of a material.

Answers

3.1) Mountain bikes exhibit a load spectrum that is quit variable due to braking, potholes and landings from jumping. The number of low magnitude stress cycles may be potentially large and in the HCF regime and thus less harmful. The number of high stress cycles in the magnitude up to local yielding are in the LCF regime (<10^3 load cycles, Figure 3.4 page 65) and will limit the life span of the front fork. The contribution of the low magnitude stress cycles could be estimated using Palmgren Miner's Rule (eq. 3.13 page 88).

3.2) The torque and shear stress are related according (eq. 3.2 page 68)

$$\frac{D_{dyn}}{D_{stat}} = \left(\frac{R_{p0.2}}{0.5\,0.7\,R_m}\right)^{1/3} = \left(\frac{0.6\,R_m}{0.5\,0.7\,R_m}\right)^{1/3} = 1.2$$

$$\frac{D_{dyn}}{D_{stat}} = \left(\frac{R_{p0.2}}{0.5\,0.7\,R_m}\right)^{1/3} = \left(\frac{0.6\,R_m}{0.5\,0.7\,R_m/1.7}\right)^{1/3} = 1.43$$

3.3)

a) Statically loaded

$$T = \frac{\pi}{16} D^3 \left(1 - 1.7\frac{d}{D}\right)\tau, \quad D = \left(\frac{T}{\frac{\pi}{16}\left(1-1.7\frac{d}{D}\right)\tau}\right)^{1/3} = 10.1\,\text{mm}$$

b) Dynamically loaded

$$T = \frac{\pi}{16} D^3 \left(1 - 1.7\frac{d}{D}\right)\frac{\tau_e}{K_t} \qquad \tau_e = 0.58 \cdot 0.7 \cdot 0.5 \cdot R_m \qquad K_t = 2.034 \qquad D = 15.3\text{ mm}$$

3.4)

a) Statically loaded

$$M = \frac{\pi}{32} D^3 \sigma, \quad D = \left(\frac{M}{(\pi/32)\,R_{p0.2}}\right)^{1/3} = 5.1\,\text{mm}$$

b) Dynamically loaded

$$M = \frac{\pi}{32} D^3 \sigma, \quad D = \left(\frac{M}{(\pi/32)\,0.7\,0.5\,R_m/K_t}\right)^{1/3} = 8.3\,\text{mm}$$

3.5) $M_1(d{=}12) = \frac{\pi}{32} d^3 \sigma_e, \quad M_2(d_k{=}19) = \frac{\pi}{32} d_k^3 \frac{\sigma_e}{K_t}, \quad \frac{M_1(d{=}12)}{M_2(d_k{=}19)} = \frac{d^3}{d_k^3/K_t} = 1.26$

3.6) $M = \frac{\pi}{32} d_2^3 \sigma_e \quad M = \frac{\pi}{32} d_k^3 \frac{\sigma_e}{K_t} \quad d_2 = \frac{d_k}{K_t^{1/3}} = 11.1\,\text{mm} \quad \frac{m_2}{m_1} = \left(\frac{d_2}{d_1}\right)^2 = 0.31$ weight saving 69%

3.7) a) The stress increase in the bolt is limited to the yield strength of the bolt.

$$P_b = 0.2\,F_{0.2} \quad P_m = 3P_b \quad P = P_b + P_m = 4\,P_b = 0.8F_{0.2} = 29.7\;kN$$

b) The stress increase in the bolt is limited by the minimum value of the clamping force F_m. If the bolt stress is increased further the clamped members become separated.

$$P_m = F_i = 0.6\,F_{0.2} \quad P_b = P_m/3 \quad P = P_b + P_m = 0.8\,F_{0.2} = 29.7\;kN$$

c) The maximum load capacity is obtained with $P_b+P_m=F_{0.2}$. With $P_b:P_m=k_b:km$ this results in

$$F_i = (1-C_m)F_{0.2} = 0.75\,F_{0.2} = 27.84\ kN \qquad P = F_{0.2} = 37.12\ kN$$

d) When cyclically loaded, the amplitude of bolt stress can further be limited by the endurance strength of the bolt. The endurance strength of the M10-8.8 bolt is σ_a=52.5 MPa (Figure 3.16 page 79). This results in

$$P_b = 2\,\sigma_a A_t \qquad P_m = 3P_b \qquad P = P_b + P_m = 4\,P_b = 24.4\ kN$$

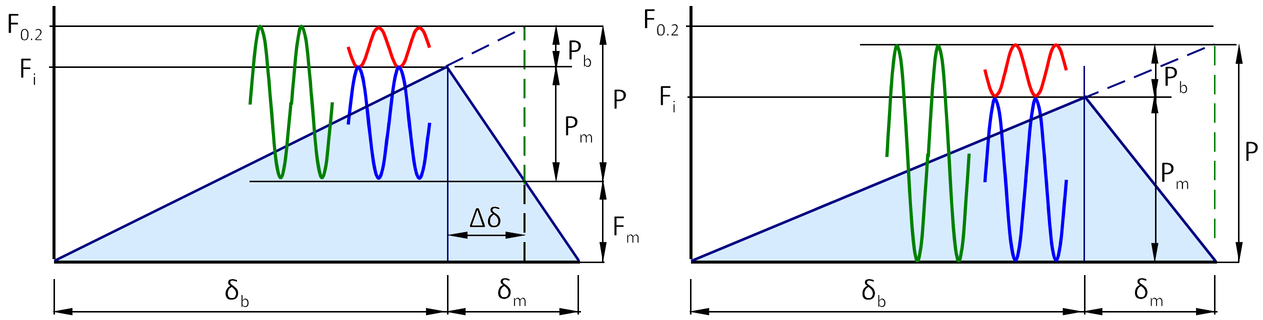

e) Variation on the preload is mainly caused by variation on the coefficient of friction during tightening. Other important influence factors are the accuracy of the tightening method and stress relaxation after tightening.

3.8) The physical model of the screw joint can be expressed as two springs connected in parallel.

$$\left.\begin{aligned} \Delta P_b &= \Delta\delta\, k_b \\ \Delta P_m &= -\Delta\delta\, k_m \\ P &= \Delta P_b - \Delta P_m \end{aligned}\right\} \begin{aligned} P &= \Delta\delta\,(k_b+k_m) \\ \Delta\delta &= \frac{P}{k_b+k_m} \end{aligned} \qquad \Delta P_b = \frac{k_b}{k_b+k_m}P = C_m\,P$$

3.9) The critical section of the screw joint is the part below the lower nut, not the prestressed section. The fatigue strength of the critical section is:

$$\left.\begin{aligned} P &= P_b = 2\sigma_e A_t \\ \sigma_e &= 0.75\left(\frac{180}{d}+52\right) \end{aligned}\right\} P = 31.5\ \text{kN}$$

A very small joint stiffness factor C_m can be obtained when using bolt studs anchored at a relative large depth (Figure b).

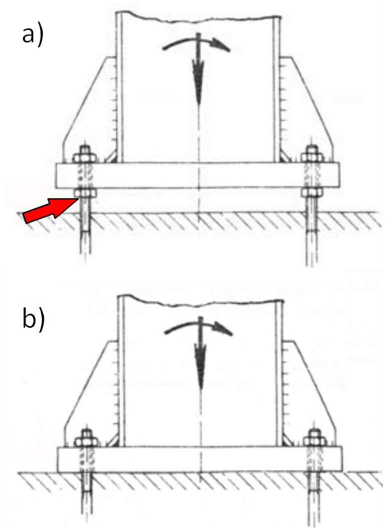

3.10) The load fluctuation P_b that can be taken by the bolt is the same for both configurations, since the steel grade and diameter of the bolts are the same. The load fluctuation that can be taken by the joint $P = P_b/C_m$ where C_m is the joint stiffness factor, it is the partition of the load P that is taken by the bolt. The factor to which the fatigue strength of the joint will increase is $P_2/P_1 = C_{m1}/C_{m2}$.

Substitution of $l_m/d=2$ in (3.11) page 81 gives $C_{m1} = 0.232$. Substitution of $l_m/d=3$ gives $C_{m2} = 0.178$.

The fatigue strength of the screw joint will increase by a factor $P_2/P_1 = C_{m1}/C_{m2}$=0.232/0.178=1.3. In other words, the external load that can be taken by the screw joint has increased by 30%.

3.11) The static strength of the bolt has decreased by a factor $\frac{(R_{p0.2}A_t)_2}{(R_{p0.2}A_t)_1} = \frac{0.9\ 1200\ 58}{0.8\ 800\ 84.3} = 0.97$

The fatigue strength of the bolt has decreased by a factor $\frac{(\sigma_a A_t)_2}{(\sigma_a A_t)_1} = \frac{52.5\ 70/60\ 58}{50.3\ 84.3} = 0.84$

where σ_a is calculated from (Figure 3.16-right page 79). The correction for the higher steel grade is 70/60 (Figure 3.16-left page 79). The tensile stress area is listed in Table A8 page 529.

The joint stiffness factor has decreased by a factor $\frac{C_{m2}}{C_{m1}} = \frac{0.208}{0.232} = 0.90$

Conclusion:
The static strength of the screw joint will increase by a factor 0.97/0.90=1.08.
The fatigue strength of the screw joint will decrease by a factor 0.84/0.90=0.95.

The fatigue strength of the screw joint has reduced by 10%. The situation is different when the diameter of the clamped material around the screw is limited (eq. 3.10 page 81), where a smaller screw diameter will improve the fatigue strength of the joint significantly.

3.12) Both mountings uses the same screws: $P_b = C_{m1} P_1 = C_{m.2} P_2$ $\quad \frac{P_2}{P_1} = \frac{C_{m.1}}{C_{m.2}} = \frac{0.334}{0.232} = 1.44$

3.13) The critical section of the screw joint in configuration 1 is the threaded part outside the clamped area, not the prestressed section. The fatigue strength of the critical area of the M24 is:

$$C_m = 1 \quad P_b = 2\sigma_e A_t \quad P_1 = P_b/C_m = 31.5\text{ kN}$$

The joint stiffness factor and the maximum load of the M12 screw joint in configuration 2 is:

$$C_m = 0.178 \quad P_b = 2\sigma_e A_t = 8.5\text{ kN} \quad P_2 = P_b/C_m = 47.5\text{ kN} \quad P_2/P_1 = 1.51$$

3.14)

$$\sigma = E\,\varepsilon \quad \frac{F}{A} = E\frac{dL}{L} \quad k = \frac{F}{dL} = \frac{A\,E}{L}$$

$$\frac{k_b}{k_m} = \frac{A_b E_b}{A_{st} E_{st}} = \frac{4\frac{\pi}{4} d^2 E_{steel}}{D\,s\,E_{alum}} = \frac{1}{3.18} \qquad C_m = \frac{1}{4.18}$$

The smaller the joint stiffness factor C_m, the smaller the part of external loading that is taken by the bolts, the better fatigue strength is achieved for the bolt joint.

In contrary, if the joint stiffness factor is larger than expected, C_m =1/2.6 and not 1/4.2, the fatigue strength of the bolted connection will be smaller than expected and the bolts may fail by fatigue prematurely.

3.15) The stress concentration factor is $K_f = \sigma_e/\sigma_a = 6.4$.

The fatigue strength of a metric M12-8.8 bolt is calculated form Figure 3.16 page 79, σ_a = 50.25 MPa. Multiplied by the tensile stress area A_t=84.26 mm^2 gives F_a = 4.23 kN.

The endurance strength of the steel in axial tension is 0.4R_m = 320 MPa. The required diameter of the shank becomes: $(\pi/4)\, d^2\, C_{surf}\, C_{reliab}\, \sigma_e / K_t = F_a$, d = 6.2 mm.

3.16) The maximum load fluctuation that can be taken by each stud can be limited by:
1) yielding of the bolt studs when exceeding the elastic limit

The load fluctuation that can be taken by each bolt stud
$P_b = 0.2\ A_t\ R_{p0.2} = 0.2\ F_{0.2} = 12.5$ kN (Figure 3.18 page 80), $P = P_b/C_m = 100$ kN

2) a minimum clamping force that is needed to ensure leak-free sealing and

When 20% of the yield strength of the bolt studs is needed as minimum clamping force then 60% of the preload remains for P_m, i.e. $P_m = 0.6\ F_{0.2}$
$P_b = C_m\ P$, $P_m = (1 - C_m)P$, then $P_b = (C_m/(1 - C_m))\ P_m = 5.4$ kN, $P = P_b/C_m = 43$ kN

3) the endurance strength of the bolt studs.

The endurance strength of the bolt studs is $P_b = 2\ \sigma_a\ A_t = 6.1$ kN, $P = P_b/C_m = 49$ kN.

Conclusion: The clamping force of the screw joint is most critical, $P_b = 5.4$ kN, $P = P_b/C_m = 43$ kN.

Bolt studs are always mounted using a solid lubricant (page 291) for several reasons. First of all to ensure a constant and low friction which is profitable to accurately apply the preload by tightening and to limit torsion stresses during tightening. Secondly, the solid lubricant prevents fretting corrosion which ensures that the bolted joint can be unscrewed, and, not less important that this avoids fatigue corrosion. Especially high strength steel alloys are very susceptible to stress corrosion.

3.17)

$$\left.\begin{aligned} dL &= L\,\alpha_m\,dT - \frac{dF}{k_m} \\ dL &= L\,\alpha_b\,dT - \frac{dF}{k_b} \end{aligned}\right\}\quad dF = \frac{\alpha_m - \alpha_b}{\frac{1}{k_m} + \frac{1}{k_b}}\,L\,dT$$

$$k_b = \frac{E\,A}{L} \qquad A = \frac{\pi}{4}d^2 \qquad \frac{k_m}{k_b} = \frac{1}{\left(\frac{1}{1.5 + 0.289\,L/d}\right)^2} - 1$$

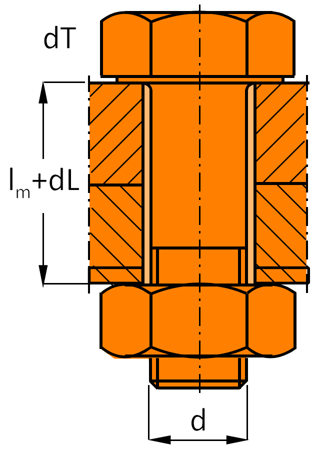

Substitution of d=10 mm, L=150 mm, E_{st}=210 GPa, α_{st}=12 10^{-6} /K, dT=150 K, E_{al}=70 GPa, α_{al} = 23 10^{-6} /K results in k_b = 1.1 10^5 N/m, k_m/k_b = 33, C_m=0.029, dF=17.6N, dσ=0.224 MPa.

The bolt is relatively elastic. The thermal expansion of the cylinder head is hardly limited by the bolts. The asymptotic solution for C_m=0 would result in free expansion of the head by $dL = L\alpha_{al}dT$ and an increase of stress in the bolts of $d\sigma = E_{st}\ dL/L = 0.231$ MPa.

With the bolts relatively elastic compared to the clamped material a very small part of the compression force is taken by the bolts keeping an optimum uniform and constant clamping force over the gasket.

3.18)

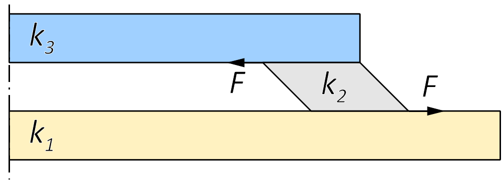

$$\left.\begin{aligned} u_1 &= L\,\alpha_1\,dT_1 - \frac{F}{k_1} \\ u_3 &= L\,\alpha_3\,dT_3 + \frac{F}{k_3} \\ u_2 &= \frac{F}{k_2} \qquad u_1 = u_2 + u_3 \end{aligned}\right\} \quad F = \frac{L\,(\alpha_1 T_1 - \alpha_3 T_3)}{\dfrac{1}{k_1}+\dfrac{1}{k_2}+\dfrac{1}{k_3}}$$

$$k_1 = \frac{E_1 A_1}{L} \qquad k_3 = \frac{E_3 A_3}{L} \qquad \tau = G\arctan\left(\frac{u_1-u_3}{h}\right) \approx G\frac{u_1-u_3}{h} \qquad \frac{F}{A} = G\frac{u_1-u_3}{h} \qquad k_2 = \frac{GA}{h}$$

This model can be useful to analyse the possibility of corrective actions.

3.19)

$$\left.\begin{aligned} & f = \frac{64 n\, r^3 F}{d^4 G}, \quad F = \frac{\pi}{16}\frac{d^3}{r}\tau : \quad f = 4\pi n \frac{r^2}{d}\frac{\tau}{G} \\ & \tau_e = 0.15\, R_m \qquad R_m = 2220 - 820 \log d \end{aligned}\right\} \; R_m = 1400\,\text{MPa} \qquad \tau_e = 210\,\text{MPa} \qquad f_{max} = 66\,\text{mm}$$

3.20) Substitution of σ_{HCF}=30 MPa, σ_i=235 MPa, m=3 in $N_i = (\frac{\sigma_{HCF}}{\sigma_i})^m 10^7$ gives $N_i = 20.8\,10^3$ cycles

3.21) The fatigue life expressed in the number of stress cycles N_i is calculated with eq. 3.12 page 87. $N_s/N_n=(30/45)^3=0.296$. The exponent m=3 for both flanges since $\sigma_i > \sigma_{HCF}$. Note that the fatigue life of the socked flange is only 30% of the fatigue life of the neck flange.

3.22) First step is to calculate the damage fraction D for one hour of service.

The damage fraction $D=n_i/N_i$ where N_i is the number of load cycles that could be accumulated when the amplitude of the stress cycles would remain constant over life (eq 3.12 page 87).

$\Delta\sigma_i$ [MPa]	240	120	60	30	20
n_i [-]	10	20	40	400	1000
N_i [-]	$(\frac{45}{240})^3 10^7$	$(\frac{45}{120})^3 10^7$	$(\frac{45}{60})^3 10^7$	$(\frac{45}{30})^5 10^7$	$(\frac{45}{20})^\infty 10^7$

Hypothetical: If in one hour $D = n_i/N_i = 0.1$, then 10% of the service life has passed and the service life would be L = 1/D = 10 hours.

The fatigue life is achieved when the cumulative damage D=1. So, the service life L becomes:

$$D = \sum_{i=1}^{5} \frac{n_i}{N_i} \qquad L = \frac{1}{D} = 4893\ hr$$

3.23)

a) The load is distributed over the length L:

$$\left.\begin{array}{c} \sigma_{eq} = \sqrt{\sigma_{\perp}^2 + 3(\tau_{\perp}^2 + \tau_{//}^2)} \le R_{p0.2} \\ \sigma_{\perp} = \tau_{\perp} = \dfrac{F\sqrt{2}}{aL} \\ \tau_{//} = 0 \end{array}\right] \quad \sigma_{eq} = R_{p0.2} = \frac{F\sqrt{2}}{aL} \qquad \frac{F}{aL} = \frac{R_{p0.2}}{\sqrt{2}}$$

b)

$$\left.\begin{array}{c} D = \dfrac{n_{AB}}{(\frac{30}{90})^3\, 10^7} + \dfrac{n_{BA}}{(\frac{30}{90/3})^3\, 10^7} = 1 \\ n_{AB} = n_{BA} \\ N = n_{AB} + n_{BA} \end{array}\right] \quad \begin{array}{l} n_{AB} = n_{BA} = 3.57\ 10^5 \\ N = 7.14\ 10^5 \text{ cycles} \end{array}$$

3.24) The maximum bending stress in the lift plate and the filled weld:

$$V = F\cos(\alpha) \qquad H = F\sin(\alpha) \qquad M = V\,e$$

lift plate thickness t $\quad M = \dfrac{1}{6}\, t\, L^2\, \sigma$

double fillet weld
with throad cross section a $\quad M = \dfrac{1}{6}\, a\, L^2\, \dfrac{\sigma}{2\sqrt{2}}$

The factor 2 in the denominator refers to the double fillet weld. The √2 is from σ_e in the cross section of the throat.

3.25) True 1 t/m 10.

Problems Chapter 4

Problem 4.1: Effective contact radius cam-roller system

Calculate the effective contact radius R’ of the cam roller supports shown in the figure. Consider a radius of the support of r_1=5mm and a curved cam with r_2=1.1r_1.

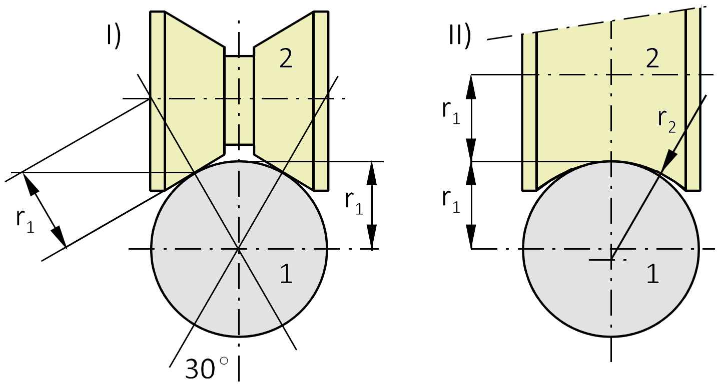

b) Calculate the static load rating C_0 of the point contact illustrated by configuration I according to ISO 76: 1987 (page 102). The cam and support are made of ball bearing steel 100Cr6, E=213 GPa, ν=0.29, p_{max} = 4.2 GPa, radius r_1 = 10 mm.

Problem 4.2: Calculation of the static safety factor to ensure smooth vibration free motion.

A contact load as large as the basic static load rating C_0 produces a permanent deformation of the rolling element and raceway, which is approximately 1/10,000 of the rolling element diameter. For smooth vibration free motion the required basic static load rating C_0, can be determined from $C_0 \geq s_0 P_0$ where s_0 is the static safety factor. Calculate s_0, when P_0 is the maximum load at which the contact deformation remains fully elastic.

a) Calculate C_0 with the maximum contact pressure p_{max} = 4.2 GPa for point contacts and p_{max} = 4 GPa for line contacts (according ISO 76: 1987 page 102). Consider both components made of ball bearing steel 100Cr6; E=213 GPa, ν=0.29, E’=233 GPa.
b) Calculate P_0 based on $p_{m.c}$ (eq. 4.9 page 100 for point contacts, eq 4.26 page 108 for line contacts).
c) Calculate s_0 for initial point contacts, elliptical contacts and line contacts.

Problem 4.3: Maximum contact pressure

Calculate the ratio between the load capacity of a steel ball and a ceramic ball running on a steel plane surface.

Steel ball: 100Cr6, E = 213 GPa, ν = 0.29
Ceramic ball: Si_3N_4, E = 300 GPa, ν = 0.28
Steel plane surface: 100Cr6, E = 213 GPa, ν = 0.29

Hint: The maximum contact pressure in the ceramic ball - steel contact is limited by the maximum contact pressure of steel, i.e. $p_{m.c} \approx R_{p0.2}$

Problem 4.4: Contact stiffness

Many tooling machines are equipped with cast iron slide surfaces because of the superior bearing stiffness and shock resistance. Rolling guides have advantage over slide surfaces when low friction is required.

The axial stiffness of rolling guides (eq. 4.5 and 4.6 page 99) can be increased by preload. Calculate the stiffness ratio S’ of a steel ball with diameter 5 mm running on a steel flat (E’=230 GPa), when loaded by 100 N preload and 10 N payload and when loaded by 10 N payload only. Payload is the load that is supported.

Problem 4.5.: Fatigue life of cam-roller supports

The dynamic load rating of commercial cam-roller systems is based on a surface hardness of the raceways between 58 to 64 HRC. If the hardness is lower than this range, the basic dynamic load rating C needs to be multiplied by the respective hardness factor (f_H). Calculate the factor of which the L_{10} fatigue life will decrease when the hardness of the support is HRC = 50 and f_H=0.6.

Problem 4.6.: Material selection of gears

Calculate the ratio of the maximum driving torque that can be transmitted by a set of spur gears (line contact) made of 16MnCr5 with σ_{Hlim} = 1400 MPa compared to a set made of 34CrMo4QT with σ_{Hlim} = 700 MPa (Hint: consider eq. 4.26 page 108, eq 4.82 page 144 and Table 4.7 page 141).

Problem 4.7: Brinell hardness test

a) In the Brinell Hardness test, the indentation made by a 10mm ball should lie between 0.24D and 0.6D. The load can be chosen in the range of 1, 2.5, 5, 10, 15 and 30kN. Examine the minimum and maximum hardness that can be measured for each load.

b) Calculate the load F_c whereby deformation can still just be considered to be purely elastic. Do the calculation for a steel ball as well as a “hard metall” tungsten carbide ball. For the steel ball take E = 213 GPa, ν = 0.29 and for the tungsten carbide ball E = 640 GPa and ν = 0.26. Assume that the material in the experiment has a hardness of 600HBW and that p_c = H/3. Explain the result of the calculation.

c) Use the details in the previous question to calculate F/F_c for 600HBW, F = 30 kN for both the steel ball and the hard metal ball. What can you conclude about the accuracy of the measurements?

Problem 4.8: Load carrying capacity of a roller guide

The load capacity of a guiding system needs to be calculated. The outer rings of the track rollers are made of ball bearing steel ($R_{p0.2}$ =1.85 GPa, E=206 GPa, ν=0.3). The rails are made of carbon steel ($R_{p0.2}$ = 1080 MPa, same E and ν) . The diameter of the rollers and the rails are the same, D=16 mm.

a) Calculate the load capacity of the guiding system when the deformation in the Hertzian contacts needs to remain fully elastic.

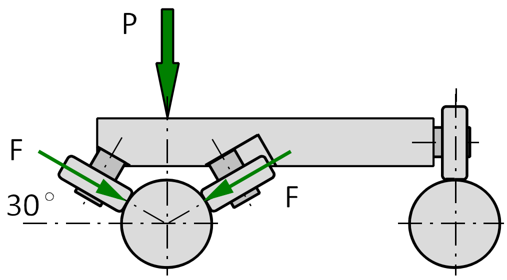

b) During a running in phases a running track is created on the rail surface by plastic deformation. Calculate the load P that creates almost fully plastic deformation during running in (p_m = H, $H/R_{p0.2}$ = 3).

c) Calculate the track width (flattening of the rail) that remains after the running in phase.

Problem 4.9: High speed hybrid ball bearing

Ceramic balls are applied in ball bearings to enable higher rotational speed. The lower density of the ceramic balls (silicon nitride) decline the centrifugal force.

a) Find out by what percentage the centrifugal force $F = -m\omega^2 R$ declines when using ceramic balls. By what percentage can the rotation speed be increased? The density of steel is 7800 kg/m^3, while the density of silicon nitride is 3200 kg/m^3.

b) Because the E-modulus of silicon nitride is approximately 1.5 time that of steel, an equal load will lead to higher contact pressure. The advantage of a smaller centrifugal force is hence limited. How big is this effect? For ball bearing steel E = 213 GPa, ν = 0.29, for silicon nitride E = 315GPa, ν = 0.26.

c) By what percentage can the rotation speed be increased when both effects are combined?

d) What other effects will be advantageous with respect to the higher rotation speed by using ceramic balls?

Problem 4.10: Cone on ring CVT / Hertzian line contact subjected to rolling with traction

Consider the line contact of a cone on ring cvt subjected to rolling with traction, both components are made of carburised steel in accordance with DIN17210, with E = 200 GPa, ν = 0.3, $R_{p0,2}$ = 835 MPa. Consider the contra form contact between the ring and cone: $R_1 = R_2$=30 mm, L = 10 mm. What is the maximum normal load

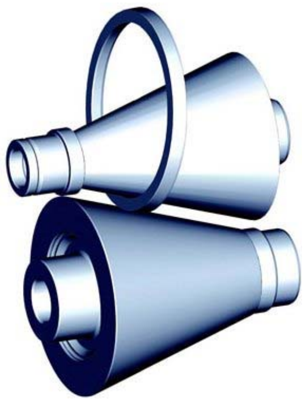

a) for pure rolling under which no plastic deformation occurs?
b) for rolling when the traction force amounts to 30% of the normal force and no plastic deformation is allowed to occur?

The normal load calculated above is based on the so called “static load rating”, it is the maximum load that can be transmitted without initiating plastic deformation. For surface durability reasons, the so called “dynamic load rating”, the fatigue strength and lubrication conditions need to be considered (Case 4.11 page 149).

Problem 4.11.: Surface durability of a gear set

The calculation of the surface durability is based on the Hertzian contact pressure p_{max} which may not exceed the allowable stress number $\sigma_{H.lim}$ of gear materials (Table 4.7 page 141).

a) The contact pressure of a carburised and hardened spur gear set needs to be verified. The pinion is driven by a torque of T_1 = 750 Nm. From the information on the drawing in accordance with NEN2366 follows that z_1 = 15, z_2 = 71, m = 7 mm, α = 20° and b = 44 mm. Calculate p_{max}.
b) What would be the factor of safety for the driving torque when selecting a steel with σ_{Hlim} is 1.2 times the calculated value of p_{max}.

Problem 4.12: Contact friction

The friction force between two surfaces in sliding motion can be written as $F_f = \tau A$ where τ is the interfacial shear stress. The shear stress is assumed to be a constant and will be discussed in the next chapter. The contact area A of a Hertzian point contact is a function of F (eq. 4.10 page 101). Derive an equation for $F_f(F) = C F^B$. What is B and what is C?

Problem 4.13: True or Untrue?

1. The Hertzian formulae are derived on the basis of linear elastic deformation, the stresses below the surface are not affected by finite dimensions of the contacting bodies and the contacting surfaces are assumed to be frictionless.

2. The Hertzian formulae can be applied for stationary concentrated contacts as well for rolling contacts.

3. In concentrated contacts the normal stresses are the greatest at the surface.

4. In concentrated contacts the normal stresses lead to shear stresses below the surface.

5. In concentrated contacts first inelastic yielding takes place just below the surface. This is where the shear stresses are maximum.

6. In concentrated initial point contacts the load at which first inelastic yielding will take place is proportional to the critical contact pressure $p_{m.c}^3$.

7. The load capacity of a point contact is proportional to $R_{p0.2}^3$.

8. Doubling the load on a deep groove ball bearing will decrease the fatigue life by a factor 2^3=8.

9. The slip between the side surfaces of a cylinder roller with its track is typically an example of Heathcote slip.

10. In the ball-raceway contact of angular contact ball bearings a combination of rolling and spinning takes place.

11. In rolling bearings the balls and raceways become separated during service by elasto-hydrodynamic lubrication, dependent on load, speed and surface roughness.

12. Rolling bearings in motion, loaded up to the static load rating show initial plastic deformation which is limited to the running in period.

13. Plastic deformation in concentrated contacts of rolling mechanisms may vanish during running in by work hardening of the steel and an increase of contact conformity by inelastic yielding.

14. The surface durability (fatigue strength) in gear transmissions is based on the Hertzian contact pressure.

15. --- The static load rating of deep groove ball bearings is defined by the Hertzian contact load at which a contact pressure occurs of 4.2 GPa. This contact pressure is the maximum contact pressure at which the deformation is still elastic.

16. --- Brinell hardness is measured as the depth of an indentation of a hard metal ball under prescribed load.

17. --- The rolling resistance in a steel ball – ring contact is solely defined by the time dependent elastic recovery, called hysteresis loss.

18. --- Reynolds slip typically occurs in a rolling contact under traction.

19. --- Elasto hydrodynamic lubrication must be avoided in traction drives in order to prevent macro slip.

20. --- The dynamic load rating of deep groove ball bearings is defined as the load at which a maximum contact pressure will occur of 4.2 GPa.

21. --- In groove ball bearings the dynamic load rating is smaller than the static load rating.

22. --- When considering elastic deformation it can be stated that; the load capacity of a ceramic ball running on a steel flat is higher than that of a steel ball running on the same steel flat.

Answers

4.1)

a) The effective contact radius is calculated using eq. 4.3 page 99

I) $r_{1x} = \infty,\ r_{1y} = r_1,\ r_{2x} = r_1,\ r_{2y} = \infty:\ R' = r_1/2 = 2.5$ mm

II) $r_{1x} = \infty,\ r_{1y} = r_1,\ r_{2x} = r_1,\ r_{2y} = -r_2:\ R' = 4.583$ mm

a minus sign is because of the concave surface as explained on page 99.

b) If the cam roller diameter is equal to the diameter of the rail guide, then the radius of the Hertzian contact $r_x = r_y = r$. Substitution of $p_m = p_{max}/1.5$, $p_{max} = 4.2$ GPa, R' = 2.5 mm and E'=233 GPa in eq. 4.10 page 101 results in the static load rating of the point contact of $C_0 = 708$ N. The contact pressure of 4.2 GPa corresponds to a plastic indentation of 1/10,000 of the roller diameter.

If the rolling contact should remain fully elastic then the load capacity is limited by $p_{m.c} = R_{p0.2} =$ 1850 MPa and results in F_c=204 N, a factor 3.5 less. This can be written as $F_c = s_0 C_0$ where $s_0 = 3.5$.

4.2)

a) Point contact: The maximum contact load is proportional to $p_{m.c}^3$ (eq. 4.10 page 101).

$$s_0 = \frac{P_0}{C_0} = \left(\frac{p_{m.C0}}{p_{m.c}}\right)^3 = \left(\frac{p_{max}/1.5}{R_{p0.2}}\right)^3 = 3.5$$

When running in the same track the plastic deformation will vanish in a few load cycles.

b) Line contact: The maximum contact load is proportional to $p_{m.c}^2$ (eq. 4.26 page 108).

$$s_0 = \frac{P_0}{C_0} = \left(\frac{p_{m.C0}}{p_{m.c}}\right)^2 = \left(\frac{\frac{\pi}{4} p_{max}}{\frac{0.5}{0.387} R_{p0.2}}\right)^2 = 1.7$$

Rolling elements with line contacts and loaded up to C_0 will fail by ratcheting (page 114).

4.3) The load capacity is calculated using eq. 4.10 page 101. The critical value of the maximum contact pressure is limited by the steel surface for both material combinations. The only parameter that matters in this equation is the effective E-modulus (eq. 4.2 page 98):

$$\left.\begin{aligned} E'_{steel-steel} &= 233\text{ GPa} \\ E'_{steel-ceramic} &= 271\text{ GPa} \end{aligned}\right\} \frac{F_{steel-steel}}{F_{steel-ceramic}} = \left(\frac{E'_{steel-ceramic}}{E'_{steel-steel}}\right)^2 = 1.36$$

4.4) The contact stiffness is related to indentation (eq. 4.6 page 99), with the contact radius (eq. 4.5 page 99) and with the load (eq. 4.1 page 98):

$$\frac{S_1}{S_2} = \left(\frac{\delta_1}{\delta_2}\right)^{0.5} \qquad \frac{\delta_1}{\delta_2} = \left(\frac{r_1}{r_2}\right)^2 \qquad \frac{r_1}{r_2} = \left(\frac{F_1}{F_2}\right)^{1/3}$$

This can be written as S(F):

$$\frac{S_1}{S_2} = \left(\frac{F_1}{F_2}\right)^{1/3} = \left(\frac{110}{10}\right)^{1/3} = 2.224$$

The contact stiffness has increased by a factor 2.224. The fatigue life however will decrease dramatically with this heavy preload, starting and running friction will also be higher and as a consequence the bearing temperature will be higher. To eliminate running noise in ball bearings an axial preload is advised of 0.01C (a mean contact pressure of 1 GPa).

4.5) With a surface hardness of HRC50 the dynamic load rating will decrease from C to 0.5C. The fatigue life will decrease with $(1-0.6^3)100\% = 78.4\%$ (eq. 4.62 page 129).

4.6) From eq. 4.82 page 144 it follows that the maximum contact load is related to σ_{Hlim}^2. This results for the maximum driving torque:

$$\frac{T_1}{T_2} = \frac{F_{t.1}}{F_{t.2}} = \left(\frac{\sigma_{h.lim1}}{\sigma_{H.lim2}}\right)^2 = \left(\frac{1400}{700}\right)^2 = 4$$

Note that the Hertz equation for line contacts (eq. 4.26 page 108) would give the same result.

4.7)

a) Substitution of the numerical data in eq. 4.14 page 103 gives HBW in 10^7 MPa (30HB ≈300MPa)

	1	2.5	5	10	15	30 kN
d=0.6D	3	8	16	32	48	95HBW
d=0.24D	22	54	109	218	327	653HBW

b) Substitution of the numerical data in (eq. 4.10 page 101) gives:

steel - steel	$E' = 233$GPa	$F_c = 258$N	$F/F_c = 116$
steel - diamond	$E' = 347$GPa	$F_c = 116$N	$F/F_c = 260$

The hard metal ball flattens less and consequently has a smaller contact surface as a function of the load.

c) With a steel ball it appears that $F/F_c < 200$, indicating that the deformation is not fully plastic (Figure 4.4 page 102). Because of the flattening of the steel balls these are unsuitable to determine the hardness of hard objects (>450HBW).

4.8)

a) The Hertzian load is limited by the yield strength of the rail guides. The Hertzian contact will be a circular point contact with radius r since the roller diameter and the diameter of the rail guide are the same. Substitution of $p_{m.c} = R_{p0.2} = 1080$ MPa and R' = 4 mm in (eq. 4.10 page 101) results in F_c = 32 N. The maximum value of the payload becomes P = 2 F_c sin 30 = F_c

b) It is shown in Figure 4.4 page 102 that the relation $p_m \sim F^{1/3}$ according Hertz holds reasonably good up to $p_m = H$. Substitution of $p_m = H$ in (eq. 4.10 page 101) results in $F_H = 860$ N.

c) The contact area $A = F_H / H = 0.265$ mm^2. With by approximation a circular contact the contact width 2r = 0.58 mm.

4.9)

a) The weight of a silicon nitride ball is 60% less than that of a steel ball, resulting in a centrifugal force that is 60% lower. The rotation speed could consequently be increased by a factor of $\omega_2/\omega_1 = (1/0.6)^{1/2} = 1.3$ or 30%.

b) For steel-steel $E'_1 = 230$ GPa, for steel-silicon nitride it follows that $E'_2 = 272$ GPa. The maximum contact pressure is constrained by the less hard steel ring. For the load ratio of both material combinations, it follows from (eq. 4.19 page 106) that: $F_c/F_H = (E'_2/E'_1)^2 = 0.7$. This means the maximum load for the steel-silicon nitride contact is 30% less.

c) A 60% lower centrifugal force and a 30% lower load rating therefore means the advantage of the lower density will be halved. The rotational speed can consequently be increased not by 30% for ceramic balls but only by 15%.

d) Ceramic balls create a smaller contact surface and hence a lower resistance to rolling with less heat development as a result. This positively affect the maximum rotational speed for hybrid ball bearings, which would in total lie between 15% and 30% higher than for steel ball bearings.

4.10)

a) The maximum contact load of a line contact in pure rolling is given by eq. 4.24 page 108. Substitution of $p_m = p_{m.c} = (0.5/0.387)R_{p0.2}$, $R' = 15$ mm and $E' = 220$ GPa gives $F_c = 8.1$ kN.

b) For rolling with traction and F_{tan}/F => 1/9 the maximum shear stress occurs at the surface. From Table 4.1 page 111 it follows with $F_{tan}/F = 0.3$ that $\tau_{max}/p_m = 0.51$. Substitution in eq 4.25 page 108 gives $p_{m.c} = 0.5/0.51\ R_{p0.2}$ and from eq. 4.10 page 101 that $F_c = 4.7$ kN. This means the maximum normal force has decreased by 42%. The drive torque that can be applied is $M = 0.3 \cdot F_c \cdot R = 41.9$ Nm.

4.11)

a) Consider eq. 4.77 page 142. Firstly, factors Z_H, Z_E and Z_ε are determined. From (eq. 4.79 page 143) it follows that $Z_E = 1.9 \cdot 10^5\ Pa^{1/2}$ and $Z_H = 2.495$. To establish Z_ε (4.79), the necessary gear dimensions must be determined first (eq. 4.75 page 142). For the contact ratio, it follows that $\varepsilon = 1.646$ and for the contact ratio factor $Z_\varepsilon = 0.886$. The tangential force follows from $T = F_t d_1/2$, this is $F_t = 14.3$ kN. Substitution of the numerical data in (eq. 4.77 page 142) gives $p_{max} = 0.8$ GPa.

From Table 4.7 page 141 it follows for carburised and hardened steel that p_{max}=1.3...1.5 GPa. It means that the fatigue strength of the tooth flanks may be sufficient. The impact of imperfect alignment, peak loads from the drive and other possible effects still have to be incorporated into the calculation.

b) The relation between the limiting contact stress σ_{Hlim} and the maximum tangential force is presented in (eq. 4.82 page 144), i.e. $\sigma_{Hlim} \sim F_t^{1/2}$. Because $T_{max} \sim F_t$, it follows $\sigma_{Hlim} \sim T_{max}^{1/2}$. With $\sigma_{Hlim} = 1.2 \cdot p_{max}$ a factor of safety for the driving torque would be $1.2^2 = 1.44$.

4.12)

From eq. 4.10 page 101 it follows

$$F_f = \tau A \qquad A = \frac{F}{p_m} \qquad p_m = C_1 F^{1/3} \qquad C_1 = \frac{1}{\pi}\left(\frac{1}{3}\right)^{2/3}\left(\frac{E'}{R'}\right)^{2/3}$$

$$F_f = \tau \frac{F}{C_1 F^{1/3}} = \frac{\tau}{C_1} F^{2/3} = C_2 F^{2/3} \qquad C_2 = \frac{\tau}{C_1} \qquad \mu = \frac{C_2}{F^{1/3}}$$

The contact area A and $F_f = \tau A$ increases less than proportional with F.
The coefficient of friction is a constant when F_f increases proportional with F.
For the spherical contact the coefficient of friction decreases with F.

Problems Chapter 5

Problem 5.1: Self locking of metric thread and nut

Flange nuts are more resistant to vibration loosening. The wider effective bearing area result with the same friction force in a larger torque needed for self loosening. Sometimes the bearing surface is serrated to provide some extra locking action. Various alternative locking mechanisms may be employed; adhesives, safety pins, nylon inserts. Lugnuts, tapered or spherical nuts are applied to centre the nut accurately and to reduce the tendency for the nut to loosen.

Fine threads have less tendency to loosen under vibration because of their smaller helix angle. Calculate the minimum value of the coefficient of friction needed for a M10x1.5 thread and that of an M10x1 metric fine thread in order to ensure it is self-locking.

Problem 5.2: Torque controlled tightening

Calculate the percentage of the tightening torque needed to overcome a) the friction in the threaded contact of an M10x1.5 bolt, b) the head face contact and c) the percentage needed to develop the clamping force. Consider the coefficient of friction of μ=0.15 and the effective bearing diameter of the nut of d_k=1.3d

Problem 5.3: Torque Angle controlled tightening

Torque-controlled tightening results in bolt force / clamping force deviations of ± 20% due to variation on the torque applied and the scatter on the coefficient of friction, despite special MoS_2 based lubricants are used. Therefore more advanced combined torque/angle-controlled tightening methods are applied.

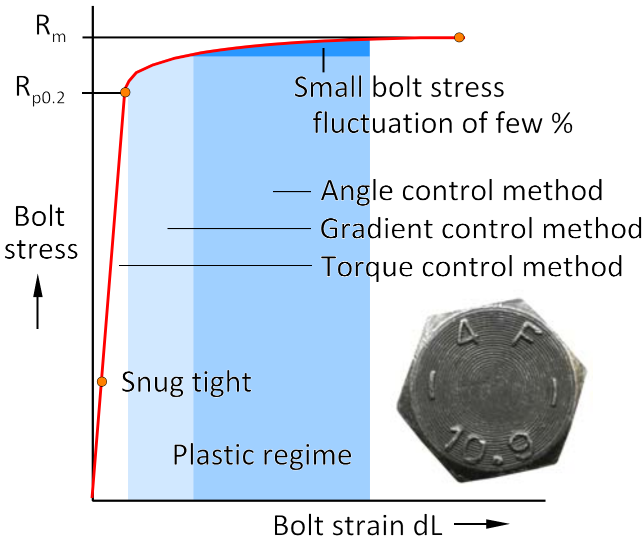

Angle control tightening is a procedure in which a fastener is pre-tightened by a so called snug torque to eliminate play, and in a next step it is further tightened by giving the nut an additional controlled rotation.

Bolts are tightened beyond their yield point by this method in order to ensure that a precise preload is achieved.

a) Calculate the bolt strain when tightened to $\sigma_i = R_{p0.2}$.

b) Calculate the bolt strain when tightened in two steps, first snug tight to 25% of the yield strength and then tightened with a 90 degrees rotation angle. Consider M10-10.9 bolt and a clamped material of L=5d.

Problem 5.4: Friction loss in Bowden cables

Calculate the percentage of loss of actuation force over the bended part of the Bowden cable shown in the figure below. Consider a coefficient of friction in a lubricated steel-steel contact of μ=0.15.

Problem 5.5: Wedge effect in belt pulley drives

Calculate the drive torque ratio T_a/T_b, where T_a is the is the torque that can be transmitted when the belt is supported on the pulley wall surfaces and T_b is the torque when the belt is supported on the groove bottom surface. Consider a pulley groove angle of β=40°.

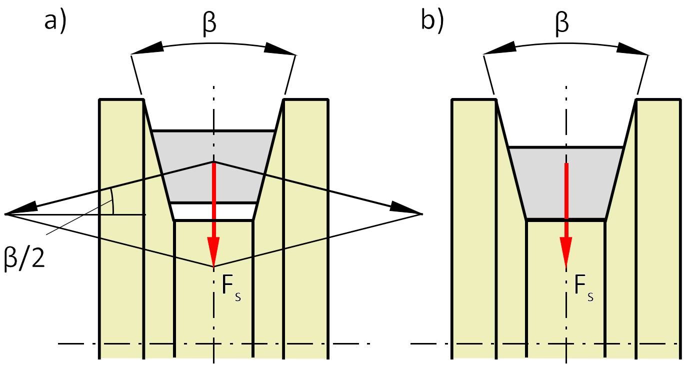

Problem 5.6: Jamming of a piston in a cylinder

Consider a piston moving in a cylinder, as represented in Figure 5.31 page 191. The piston has a diameter D and a length L. If the load F_1 acts at the piston with a maximum eccentricity of e=D/2, how long should the piston be to prevent it from jamming?

Problem 5.7: Stick slip motion

A mass of m=0.5 kg is pulled along a surface using a spring balance. The spring balance is moved with a constant velocity of v=0.1 m/s. The motion exhibits a clear stick-slip behaviour. The reading of the spring balance varies between 8 N and 14 N. The stiffness of the spring k = 1 N/mm.

a) Calculate the ratio between the static and dynamic coefficient of friction.
b) Calculate the amplitude of motion.
c) Calculate the frequency of motion.
d) Calculate the natural frequency of the mass spring system.

Problem 5.8: Stick slip motion

One of the options in a morphological matrix to fulfil the actuator function in a linear motion drive system is a pneumatic cylinder. The friction between the piston seals and the cylinder typically results in a friction as modelled in Figure 5.24 page 183.

The seal friction is highest in the static position of the piston and falls down to a very low level by elasto-hydrodynamic lubrication when the piston moves.

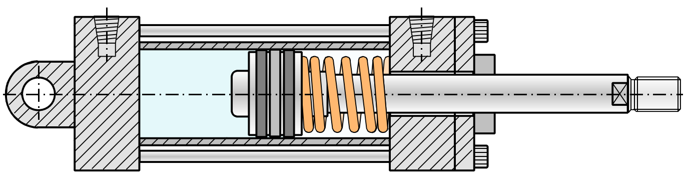

Consider a pneumatic cylinder - spring system. The static friction between the piston and cylinder wall can be expressed as a percentage of the piston force F_{stat} = 10% F_{piston}. The piston is actuated by air pressure. The air pressure is increased until the piston starts to move. When the piston starts to move the friction falls down to approximate zero level. The piston will make a step forward. This process is repeated.

Calculate the smallest possible step size in a step by step movement of the piston. Start from a position in which there is equilibrium between the air pressure and the spring force (zero friction). In this position F_0 = 500 N. Next the air pressure is increased until the piston starts to move etc. The spring stiffness k=10 N/mm.

Problem 5.9: PV-value

Consider a polymer bearing with a PV-value of PV = 0.2 MPa ·m/s. The shaft diameter d=20 mm, the bearing width L=d, rotational speed n=477 rpm.

a) Calculate the load that this bearing can sustain.
b) Calculate power loss in this bearing at the moment of failure, assuming a coefficient of friction μ=0.2

Problem 5.10: Operating clearance

If a bearing bushing is press fitted in a metal housing a cumulation of machining tolerances result in a large variation of the bearing busing inside diameter. To ensure a positive clearance under the most unfavourable conditions the minimum value of the operating clearance in generally is taken to be 0.5% of the shaft diameter. The operating clearance is defined as the minimum clearance during operation. Effects resulting in a decrease of clearance during operation are thermal dimensional changes and for some polymers moisture-related dimensional changes.
Calculate the decrease of the bearing clearance [%] of a PA plain bearing busing with a shaft diameter of d=12 mm and a wall thickness of t=3 mm. Consider a temperature increase of the polymer of dT=80 degrees and a linear expansion coefficient of PA of α=80 10^{-6} /K

Problem 5.11: Hysteresis error from friction in the drive spindle

In the figure below a linear motion axis of a milling machine is shown actuated by a servo motor. The system accuracy suffers from the “Wind-up” of the lead screw. The “Wind-up” of drive shafts is defined as the torsion angle. It is assumed that the displacement of the carriage is set by the rotation angle of a stepper motor. The drive torque is present in <u>one direction of motion</u>.

Screw length L = 1 m
Trapezoidal thread Tr12 x P3
Pitch diameter d_2 = 10.5 mm
Shear modulus G = 80 GPa
Drive torque T_{dyn} = 26 Nm
Drive torque T_{stat} = 1.2 T_{dyn}
v = 0.1 m/s

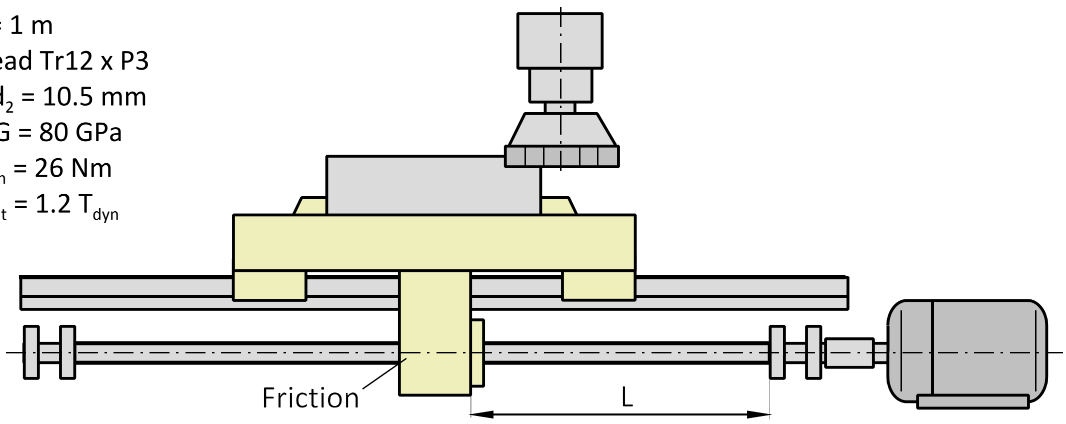

a) Calculate the hysteresis error resulting from the friction in the drive spindle.

b) Calculate the amplitude and frequency of the stick-slip movement assuming that the driving torque is 20% higher by static friction, before the motion starts. The carriage is driven with v=0.1 m/s (Hint: Figure 5.25 page 183).

c) Calculate the displacement of the carriage by frictional heating in the nut-spindle interface. One of the bearings in the motor drive is the locating bearing of the drive spindle. Consider a mean value of temperature increase over the spindle of 10°C. The thermal expansion coefficient is $\alpha=12\ 10^{-6}$ /K.

Problem 5.12: Hysteresis error from friction in the dovetail slide

In the figure below a linear motion axis of a milling machine is shown actuated by a servo motor. The system accuracy suffers from the "friction in the dovetail slide" of the carriage and the resulting hysteresis error. It is assumed that the displacement of the carriage is set by the rotation angle of a stepper motor. The friction is present in both directions of motion.

Screw length L = 1 m
Trapezoidal thread Tr12 x P3
Pitch diameter d_2 = 10.5 mm
E modulus E = 210 GPa
Coefficient of friction μ=0.15
Normal load F = 2000 N

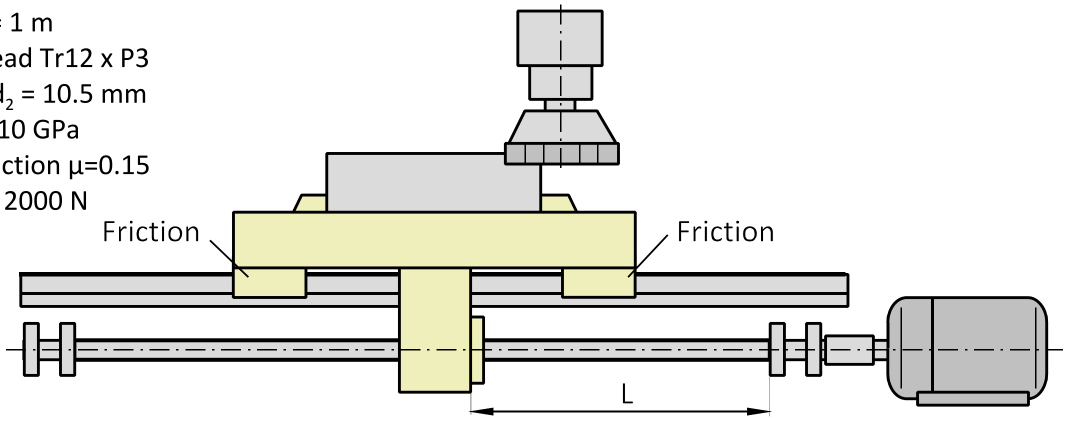

a) Calculate the hysteresis error resulting from the friction in the dovetail slide.
b) Calculate the amplitude and frequency of the stick-slip movement that occurs if the coefficient of friction varies between μ_s=0.25 and μ_d=0.1 and the sliding velocity v=0.1 m/s (Hint: Figure 5.25 page 183).

Problem 5.13: Hysteresis error from friction in a friction joint

Many work lamps use friction joints, so you can easily direct the light where you want it. Consider a lamp arm with two legs of unequal length in the position as illustrated. The friction joints should maintain a fixed clamping for a load up to F=10 N and will slip when the lamp arm is loaded with a higher load. Calculate the hysteresis of this mechanism (virtual play, bidirectional).

Consider: Arm lengths L_1=0.3 m and L_2=0.3 m. The arms are made of hollow steel pipes, E = 210 GPa, D=10 mm and d=8 mm.

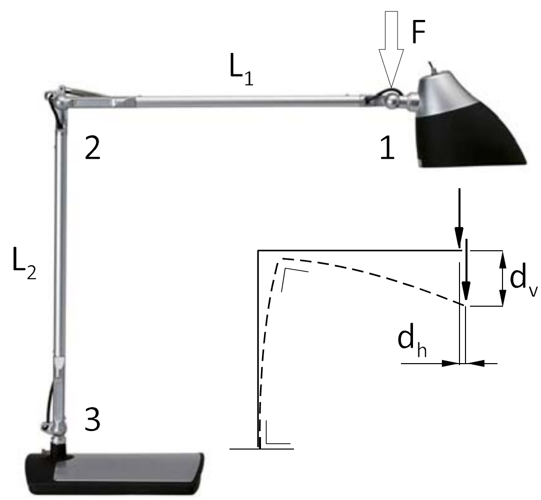

Problem 5.14: Frictional heating of a disk brake

In order to save weight, pearlitic cast iron disk brakes could be replaced by aluminium disks. Aluminium is also a better heat conductor than cast iron. With surface treatment, the aluminium can be made very resistant to wear. A possible disadvantage is that the maximum allowable temperature of aluminium is lower than that of cast iron. Examine the performance of an aluminium brake disk by answering the following questions.

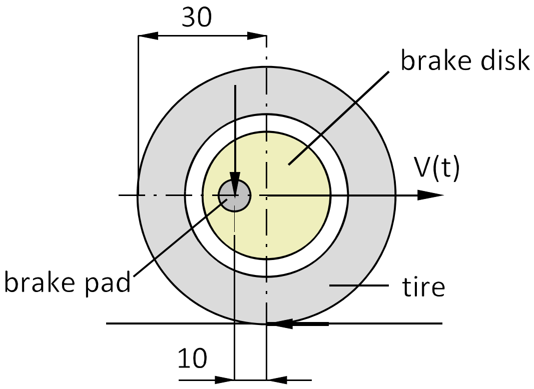

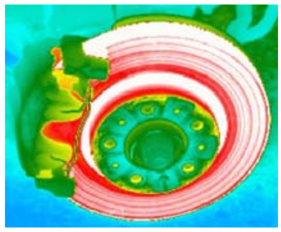

a) If the car comes to a stop from a driving speed of V_t=100 km/h with a constant deceleration, the braking distance appears to be S = 100 m (standard for cars). What is the deceleration before the stop and how long will it take to stop?

b) The mass of the car is m = 1000 kg. What is the required friction coefficient μ between the tires and the road surface to prevent slip?

c) Approximately 80% of the braking energy is absorbed by the front wheels. Both front wheels are equipped with a single brake disk and a brake pad on each side of the disk. The wheel diameter is 0.6 m. The distance between the centre of the brake pad and the wheel centre is 0.1 m. The friction coefficient between the brake disk and the brake pad is μ = 0.4. How great is the pressure force on the brake pads?

d) What temperature does the brake disk reach when all friction energy is absorbed by the brake disk? Consider both the cast iron and aluminium brake disks. The brake disk has a diameter of 300 mm and a thickness of 12 mm. For cast iron ρ = 7300 kg/m^3, c = 0.50 kJ/(kg K), k = 60 W/(m K), T_{melt} = 1450 K, while for aluminium ρ = 2700 kg/m^3, c = 0.88kJ/(kgK), k = 237 W/(m K), T_{melt} = 932 K.

Note: Since braking only occurs for short periods, little heat will be dissipated through convection. The brake disk absorbs much more heat than the pads, firstly because the contact surface of the brake disk is much bigger (non-stationary contact) and also because it is a better conductor for heat than the pads. For a first approximation, it is justifiable to assume that all heat goes into the disk.

Problem 5.15: Tire width Formula 1 - racing car

The first classical law of friction states: “The size of the contact surface does not influence the friction”. Why, then, are tires for the Formula 1 racing cars so wide?

According to the “FIA Technical Commission”, the organisation that decides on the technical rules for Formula 1, the front tires should not be wider than 355 mm (i.e. 14 inches) and the rear tires no wider than 380 mm (15 inch).

Problem 5.16: Acceleration of Formula 1 racing car [1]

A modern Formula 1 racing car manages approximately 1.5 km/liter (or 1 :1.5). To complete the Grand Prix distance, it would need approximately 180 liters of fuel. Since the time gain from a lower mass exceeds the disadvantage of a refuelling stop, the tank contents are much smaller. The weight of a car, including a full tank and the driver, is approximately 600 kg. A Formula 1 car accelerates six to ten times as quickly as a normal car. Acceleration of 0-100 km/h in 2 seconds, 0-160 km/h in 3.5 seconds and 0-250 km/h in less than 6 seconds is typical. The top speed of an F1 racer is around 370 km/h. Accelerating from 0-160 km/h and braking to a complete halt takes approximately 6.5 seconds. This means the car speeds up and slows down at the same rate. What is the required friction coefficient between the tire and the road surface to make this acceleration possible?

Problem 5.17: True or untrue?

1. Coulomb's friction law - if the load is doubled the friction is doubled - can be explained by the elastic deformation in the micro contacts, i.e. in the real contact area. U
2. Coulombs friction law, that says that the friction in a dry sliding contact is independent of the visible area, do not apply to polymers.
3. Coulombs friction law can be explained on the basis of plastic deformation in the roughness summits, that transfer the load between two surfaces in dry sliding.
4. The Ra surface roughness sometimes called the Arithmetical mean or Centre Line Average is independent of the length scale of the surface profile. For example, a surface profile described by sin(x) and sin(2x) respectively would result in the same Ra-value.
5. In polymer-metal contacts the real contact area increases more than proportional with the load which explains the larger friction coefficient at higher load. U
6. The real contact area is formed by the micro contacts between roughness peaks of the surfaces. Friction in dry sliding or boundary lubricated contacts is a result of ploughing and adhesion forces in these micro contacts.
7. Metallurgical compatible materials are sensitive to adhesion.
8. The ploughing component of friction in a steel-steel contact can be decreased by selecting both materials of the same high hardness.
9. The adhesion component of friction can be decreased by applying a soft coating.
10. The backlash is defined as the virtual play that a mechanical structure exhibit when actuated by reversed loading. U
11. Alloyed steel is generally beneficial in respect to have low friction, because it reduces surface energy and at the same time increases hardness.
12. The friction in dry sliding polymer - metal contacts is independent on the sliding velocity. U
13. The static coefficient of friction is generally normative in clamping joints and interference fits, explained by the stiffness of the clamped material which is in most cases smaller than the stiffness of the structure. U

[1] Test Method for Friction Coefficient Measurements between tire and pavement using a variable slip technique ASTM E 1859-97 and E 1844-96

14. The flash temperature is defined as the contact temperature in the micro contacts formed between interacting asperities.
15. In polymer - metal contacts the friction remains minimal when the polymer surface has a roughness of around Ra=0.2 µm.
16. One of the measures to eliminate stick-slip in polymer - steel contacts is by making the steel surfaces smoother (super finishing). U
17. The coefficient of friction between metals operating in vacuum environment is much higher than in the regular atmosphere which can be explained by the adhesion component of friction.
18. The coefficient of friction is always smaller than $\mu \leq 1$. U
19. The coefficient of friction in polymer metal contacts decreases with the contact pressure.
20. The friction force in polymer metal contacts decreases with the contact pressure. U
21. The friction force in polymer metal contacts increases with the contact pressure.
22. The friction force by ploughing is dependent on the radius of the asperities (roughness summits).
23. The friction force by ploughing can be decreased by super finishing techniques in which the rounding of the asperities are enlarged.
24. The friction by ploughing is dominated by the roughness of the less harder surface when two body's of different hardness are in contact. U
25. Stainless steel fasteners are sensitive for adhesive wear by the very thin oxide layer on stainless steel.
26. The friction in zinc plated fasteners is limited by the low shear strength of the zinc.
27. With a Brinell hardness of HB300 is the maximum contact pressure 300 kgf/mm2 = 3000 MPa
28. Friction in a hydrodynamic lubricated contact is a result of viscous shearing.
29. The backlash is defined as the geometric play that a mechanical structure exhibit when actuated by reversed loading.

Answers

5.1) The thread is self-locking if ρ′ > φ where ρ′ = atan (μ / cos(β/2)), β = 60° and φ = tan (P / π d_2), d_2 = d - 0.649519 P.

$$\frac{\mu}{\cos(\beta/2)} = \frac{P}{\pi d_2}$$

Substitution of d = 10 mm, P = 1.5 mm gives μ > 0.046, with P = 1 mm then μ > 0.029.
It can be concluded that fine threads are less susceptible to vibration loosening.

5.2) Total friction

$$M = F_i \frac{d_2}{2} \tan[\, atan(\frac{P}{\pi d_2}) + atan(\frac{\mu}{\cos(\beta/2)})] + \mu F_i \frac{d_k}{2}$$

- Percentage head face friction: $\dfrac{\mu F_i \frac{d_k}{2}}{M} = 49\%$
- Percentage thread friction: $\dfrac{F_i \frac{d_2}{2} \tan[atan(\frac{\mu}{\cos(\beta/2)})]}{M} = 39\%$
- Percentage clamping: $\dfrac{F_i \frac{d_2}{2} \tan[\, atan(\frac{P}{\pi d_2})]}{M} = 12\%$

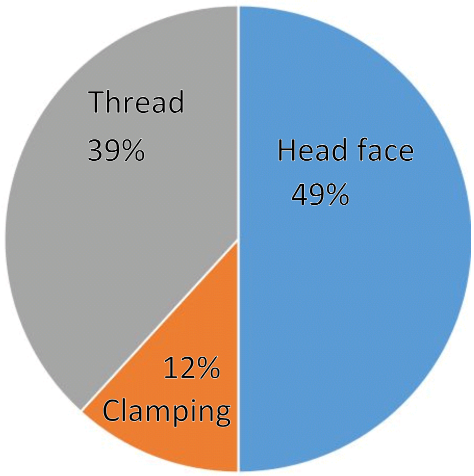

5.3)

$$\varepsilon = \frac{R_{p0.2}}{E_{st}} = \frac{0.9\ 1000\ 10^6}{210\ 10^9} = 0.43\%$$

$$\varepsilon = \frac{1}{4}\frac{R_{p0.2}}{E_{st}} + \frac{60}{360}\frac{P}{3d} = \frac{0.43\%}{4} + 0.83\% = 0.94\%$$

5.4)

$$\frac{T_1}{T_2} = e^{\mu\alpha} \qquad \frac{T_1 - T_2}{T_1} = 1 - \frac{T_2}{T_1} = 1 - e^{-\mu\alpha} = 0.376$$

5.5)

$$F_\perp = \frac{F}{2}\frac{1}{\sin(\beta/2)} \qquad F_{f.a} = 2\mu F_\perp \qquad F_{f.b} = \mu F \qquad \Bigg\} \qquad \frac{F_{f.a}}{F_{f.b}} = \frac{1}{\sin(\beta/2)}$$

5.6) The system jams when μ > ½ h/e. Substitution of h = L and e = D/2 gives μ > L/D. This means that with L/D > μ the piston will not jam in the circumstances given.

5.7)

a) $$F_{\max} = \mu_s F \quad F_{mean} = \frac{F_{\max} + F_{\min}}{2} \quad \mu_s = \frac{F_{\max}}{F} \quad \mu_d = \frac{F_{mean}}{F} \quad \frac{\mu_s}{\mu_d} = \frac{F_{\max}}{F_{mean}} = \frac{14}{11} = 1.27$$

b) $$\Delta X = \frac{F_{\max} - F_{\min}}{k} = 6\,\mathrm{mm} \qquad \text{amplitude} = \frac{\Delta X}{2} = 3\,\mathrm{mm}$$

c,d) $T=\dfrac{\Delta X}{v}=0.06\text{sec}$ $f=\dfrac{1}{T}=16.7\,\text{Hz}$ $f_0=\dfrac{1}{2\pi}\sqrt{\dfrac{k}{m}}=7.1\,\text{Hz}$

5.8) Figure 5.25 page 183: $X_0=\dfrac{F_0}{k}=50\,\text{mm}$ $X_1(1.1F_0)=55\,\text{mm}$ $X_1-X_0=5\,\text{mm}$

5.9)

a) $F=\dfrac{PV}{v}A$ $A=d^2$ $v=\pi d n$ $v=0.5\,\text{m/s}$ $F=160\,\text{N}$

b) $P=F_f v$ $F_f=\mu F$ $P=16\text{ W}$

5.10) $\Delta t=t\alpha dT=0.019\,mm$ $\Delta d=2\Delta t$ $\Delta d/d=0.32\%$

5.11)

a) $I_p=\dfrac{\pi}{32}d^4$ $\varphi=\dfrac{TL}{GI_p}$ $s_v=\dfrac{\varphi}{360°}P=0.13\text{ mm}$

b) $\Delta M=2\ 20\%\ 26\,\text{Nm}=10.4\text{ Nm}$ $\Delta X=2\ 20\%\ 0.13=0.052\text{ mm}$ $T=\Delta X/v=1.9\text{ kHz}$

Amplitude of motion is ΔX/2 = 0.026 mm

The same result can be found by considering the velocity in screw nut interface:

$v_{carriage}=0.1\,\text{m/s},\ P=3\text{ mm},\ n=v_{carriage}/P,\ n=2000\,\text{rpm}$

$v_{contact}=\pi d_2 n=1.1\,\text{m/s},\ T=\dfrac{(d_2/2)\Delta\varphi}{v_{contact}},\ f=\dfrac{1}{T}=1.9\,\text{kHz}$

c) $\Delta L=L\alpha\Delta T=0.12\text{ mm}$

5.12)

a) $\sigma=\dfrac{F_f}{A}$ $A=\dfrac{\pi}{4}d^2$ $d=10.5\,\text{mm}$ $\sigma=3.465\,\text{MPa}$ $dL=L\dfrac{\sigma}{E}=0.016\text{ mm}$ $s_v=2dL=0.033\text{ mm}$

b) $k=\dfrac{AE}{L}=18.2\,10^6\,\text{N/m}$ $\Delta F=2P(\mu_s-\mu_d)=600\,\text{N}$ $\Delta X=\dfrac{\Delta F}{k}=0.033\,\text{mm}$ $\Delta t=\dfrac{\Delta X}{v}$ $f=\dfrac{1}{\Delta t}=3\,\text{kHz}$

5.13) $\delta_1=\dfrac{FL_1^3}{3EI}$ $M=FL_1$ $\phi_2=\dfrac{ML_2}{EI}$ $\delta_2=\phi_2 L_1$ $\delta_{tot}=\delta_1+\delta_2$ $s_v=2\delta_{tot}$

5.14)

a) $a=-\dfrac{1}{2}\dfrac{V_t^2-V_0^2}{s},$ $t=\dfrac{V_t-V_0}{a};$ $a=-3.858\ m/s^2,$ $t=7.2\ \text{sec}$

b) $F_a=ma=3858\ N$ $F=mg=9.81\ kN$ $\mu=F_a/F=0.393$

c) $F_{wheel}=\dfrac{0.8\,F_a}{2},$ $\mu F_{pad}=\dfrac{30}{10}\dfrac{F_{wheel}}{2},$ $\mu=0.4;$ $F_{pad}=5787\ N$

d) $E=½\,mV_t^2=386\ kJ$

cast iron: $m_{schijf}=\rho V=6.2\text{ kg}$ $Q=m_{schijf}\,c\,dT=E$ $dT=125\text{ K}$

aluminium: $m_{schijf} = \rho V = 2.3$ kg $\quad Q = m_{schijf}\, c\, dT = E \quad dT = 191$ K

The aluminium brake disk proves to be warmer after braking once than the cast iron brake disk. Furthermore the maximum allowable temperature of the aluminium is much lower. It means that the heat conduction of the brake disk must be fully exploited for it to make aluminium a suitable material for the purpose.

From further research with thermal network analysis and practical experiments it appears that wheel bearings get substantially warmer due to the good heat conductivity of aluminium, which makes them critical components. The carbon fibre brake disks used in Formula 1 can be loaded up to 1000 degrees Celsius.

5.15) The classical friction laws apply to materials that undergo mainly plastic deformation in the asperity summits. Polymers display a lower friction coefficient at a high nominal contact pressure. A high friction force can consequently only be achieved with a large surface area. Other advantages of a wide surface are that the wear is distributed over a larger area, heat development per unit of surface is lower and the result is a larger heat-radiating surface.

In machine construction, where low friction is mostly considered desirable, high surface pressure are desirable. For instance, halving the diameter of a shaft can double the surface pressure. If the friction force was in proportion to $p^{2/3}$, the friction coefficient would be reduced to 63% of the original value. The friction torque would consequently be reduced to 31.5% of its original value!

5.16) To arrive at V=100 km/h in t=2 seconds, an acceleration is needed of $a=V/t=14 m/s^2$. To this end a traction force of $F_f=ma$ is needed. The necessary traction coefficient follows from $\mu=F_f/F=ma/mg\approx1.4$. The distance required to reach the speed is then only $S=½a\, t^2=28$m.

When accelerating and braking, the coureur experience an acceleration of approximately 1.4g. When turning a corner at speed, drivers can only undergo up to 4g for a few seconds before they become unconscious. Accelerations are limited by a prescribed maximum tire width with four circumferential grooves. Wet weather tires also have axial grooves to dissipate water sideways.

5.17) True: 2 - 3 - 4 - 6 - 7 - 8 - 9 - 11 - 14 - 15 - 17 - 18 - 19 - 21 - 22 - 23 -25 -26 -27

Problems Chapter 6

Problem 6.1: Service life of a lead screw

Consider a lead screw assembly that operates with a contact pressure in the threaded area of p = 5 MPa. The pitch diameter d_2=10.5 mm. The stroke over which the nut is displaced is 20 times the nut height. The number of loaded turns during service life is n=100 10^3 rev.

The specific wear rate of the bronze nut and the spindle are $k_{nut} = k_{spindle}$ = 10 10^{-15} m^2/N. Calculate the increase of backlash h [mm] in the screw-nut interface of a trapezoidal lead screw

a) caused by wear of the bronze nut.

b) caused by wear of the spindle.

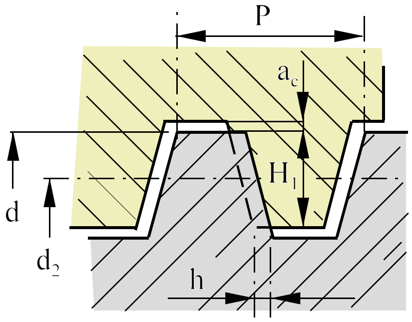

Problem 6.2: Investigation to hard wearing materials for knee replacements

In order to assess the wear performance of different materials of total knee replacements (TKR), a block on ring test rig will be used. The ring is actuated in reciprocating motion.

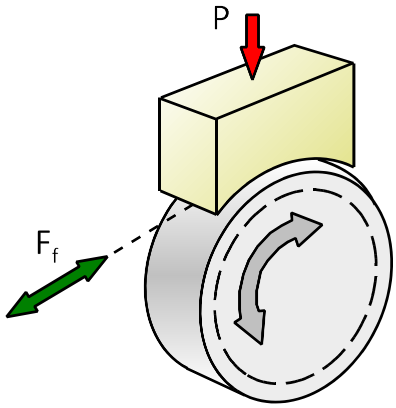

a) Calculate the required test duration in hours.

The ring is made of steel, the block from ultra high weight molecular polyethylene (UHMWPE). The density of UHMWPE is ρ = 945 kg/m^3. A specific wear rate k=10·10^{-15} m^2/N of the PE block is expected. A minimum wear of the polymer block of 0.1 gram is to be obtained to establish the wear rate. The contact surface A=100 mm^2, the surface pressure is p=2 MPa, the total sliding distance in one cycle is s_i = 30 mm and n=2 cycles per second are made.

b) What temperature will the ring get when the frictional heating is to be transferred by convection only.

The coefficient of friction μ=0.12, the heat convection coefficient of the rotating disc in free air h_c = 80 W/ m^2K and the effective heat convection surface area of the ring A = 7 10^{-3} m^2.

Problem 6.3: Service life of a linear axis using plain bearings

A linear guide's travel smoothness and tolerance variations are key concerns for machine designers. But, the most important design factor is how well the guide resists deflection. Linear support rails in combination with open design bearings are best suited to sustain heavy loads and to provide high stiffness.

Linear plain bearings are the better choice compared to linear ball bearings when the bearing arrangement is subjected to heavy shock loads, vibrations or high accelerations in the unloaded state however, increased friction must be expected.

Calculate over what sliding distance s [km] the bearing will wear down over h=0.1 mm. Consider a mean value of the contact pressure of p = 3 MPa and the specific wear rate of k= 10^{-15} m^2/N. Consider good conformity between the plain bearing and the linear support.

Problem 6.4: Service life disk brake

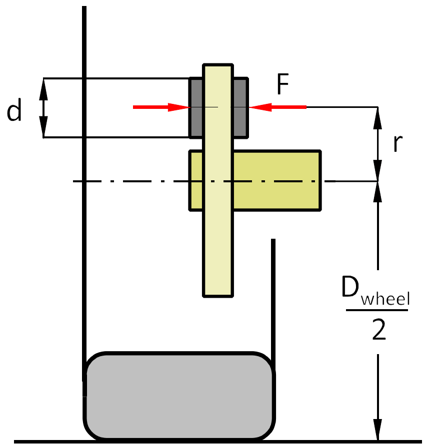

a) Calculate the service life of disk brake pads, expressed in numbers of brake times. The contact area of the brake pad is approached by a round disk with a diameter of d=60mm located at centre distance r=100mm, the thickness of the brake lining is t=10mm, the specific wear rate k=50 10^{-15} m^2/N (class 5), the normal force F=6000N, the wheel diameter D=0.6m and the brake distance S=100 m.

b) How much thinner will the brake disk worn down during the service life of the brake pads if the specific wear rate of the brake disk equals that of the brake lining?

c) What is the perfect ratio of k_{pad}/k_{disk} that makes that the pad and disk are worn after the same sliding distance if h_{pad}/h_{disk} = 5?

Problem 6.5: True or untrue?

1. Lapping is based on three body abrasion.
2. Metals with good metallurgical compatibility are less sensitive to adhesive wear.
3. In a polymer-steel contact under sliding the wear rate of the polymer will always exceed the wear rate of the metal surface.
4. When lapping a hardened steel surface using a pearlitic cast iron disc and diamond powder in a mixture of petrol and oil, the relative soft cast iron disc doesn't suffer from wear while the hard steel surface becomes finished to a high polish.
5. Hard wear particles that abrade a sliding surface may originate from the slide surface itself.
6. Three body abrasive wear refers to erosion, which is the predominant wear mechanism in sand-slurry pumps.
7. Carburizing of low carbon steels creates a beneficial non metallic surface character that makes the steel less sensitive to adhesive wear.
8. Scuffing is a type of adhesive wear that typically occurs in dry sliding.
9. Accumulation of work piece material on the cutting edge of a tool can be characterized by galling, a severe form of adhesion.
10. False Brinelling is a result of plastic deformation in concentrated contacts creating shallow indents.
11. The dimension of the specific wear rate k is $m^3/Nm = m^2/N$, the wear factor K is dimensionless.
12. The "stationary contact" is defined as the contact surface that is stationary with the load vector.
13. Scuffing, cold welding and galling are specific forms of adhesive wear.
14. A steel part can be made less sensitive to three body abrasion by making it from a lower grade steel.
15. PTFE bearings are favourable over many other polymers because of the very low friction and high wear resistance.
16. Fretting wear typically occurs by reciprocating motion such as in a piston - liner contact.
17. Adhesive, abrasive and corrosive wear are the three fundamental wear mechanisms in sliding contacts. In rolling contacts surface fatigue is generally the predominant wear mechanism.
18. The main difference between surface grinding and super finishing techniques like polishing, lapping and honing is that super finishing is limited to the smoothening of roughness summits.
19. The wear rate of metals subjected to abrasive wear is in a large range of operating conditions by approximation inversely proportional to their hardness.
20. Materials that show relatively low friction have high wear resistance.

Answers

6.1)

a) Sliding distance $s = \pi\, d_2\, n = 3.3\ km$ $\quad h_{nut} = k\, p\, s = 0.165\ mm$

b) Sliding distance $h_{spindle} = k\, p\, s\, A_{nut}/A_{spindle} = 0.165/20\ mm$

6.2)

a) Substitution of F=pA and V=m/ρ in Archard's equation (eq. 6.1 page 232) gives s=53 km, and t=245 hours = 10.2 days.

b) Equating the frictional heating to the heat transfer by convection gives $Q = F_f\, v = h_c\, A\, dT$, where $F_f = \mu F$ and $v = n\, s_i$. This results in Q=1.44 W and a temperature increase of dT=2.6°C. The mass temperature is much lower than that of the human body and consequently the test frequency can be increased.

6.3) $h = k\, p\, s \qquad s = \dfrac{h}{kp} = 33\,\text{km}$

6.4)

a) $h = k\, p\, s,\quad p = F/(\pi\, 30^2),\quad s = S/3;\quad h = 3.5\ 10^{-3}\,mm,\quad 10/h \approx 2827$ stops.

b) $$V_{pad} = V_{disk};\quad \frac{A_{disk}}{A_{pad}} = \frac{\pi\,(100+30)^2 - \pi\,(100-30)^2}{\pi\, 30^2} = 13.3,\qquad h_{disk} = \frac{A_{pad}}{A_{disk}}\, h_{pad} = 0.75\ mm$$

alternative method: $$h_{disk} = \frac{k\, F\, s}{A_{disk}} = 0.75\ \text{mm}$$

c) $$h_{pad} = k_{pad}\frac{F}{A_{pad}}s \qquad h_{disk} = k_{disk}\frac{F}{A_{disk}}s$$

$$\frac{k_{pad}}{k_{disk}} = \frac{h_{pad}}{h_{disk}}\frac{A_{pad}}{A_{disk}}$$

Braking is one of the biggest strengths of a Formula One car. The brake disks of Formula 1 cars are made of a composite material reinforced with carbon fibre. The coefficient of friction between the pads and the discs can be as much as 0.6 when the brakes are up to temperature. Steel brake disks are heavier and would exhibit a higher wear rate at these high temperatures.

The temperature of an F1-brake disk varies between 400 and 1000°C. You can often see the brake discs glowing during a race. If the racing driver hits the brakes full on before the brake disks have reached a temperature of approximately 400 degrees, the disks could explode under the thermal stresses created. These stresses are the result of large temperature gradients leading to expansion which causes large stress gradients.

As the heat created in the modern Formula One brake disk is so high, there is a constant demand to find more and more cooling. In 2001, Ferrari conceived an original way of dealing with the heat problem in brakes. The brake-duct, conducting the slipstream wind along the brake disks, is equipped with a kind of turbo. This is a rotor mounted on the wheel shaft, providing additional suction to get even more air into the brake-duct. Thanks to the rotor, the brake-duct can be made smaller, benefiting the aerodynamics. The other F1 teams have now copied the idea.

In F1 the maximum dimensions of the brake disks are laid down in regulations. During qualification, relatively thin and hence light brake disks are used because the cars only need to complete 12 laps. For the race itself the thickest possible discs are fitted on the car. It means the incurred heat can be better distributed over the brake disk material. During the race a sensor continuously measures the thickness of the brake disks. The measurements will help the driver to know when he has to go easy on the brakes to make it across the finishing line. A set of disks and pads costs as much as a compact car. For every Grand Prix race each team reckons on using twenty sets of brake disks and pads per car.

6.4)

True: 1- 4 - 5 - 7 - 9 -11- 12- 13 - 14 - 17 - 18 - 19

Problems Chapter 7

Problem 7.1: Design considerations plastic plain bearings

a) A designer is faced with a choice between a plain bearing with small shaft diameter in combination with a long bushing or a larger shaft diameter in combination with a short bushing, so that the projected contact area LD is the same for both bearings. Which considerations will determine the choice?

b) In order to reach a higher PV-value, the designer selected a thin plastic bushing, increasing the heat dissipation to the environment via the bushing. In experiments, the LPV-value turned out to be smaller than anticipated. Explain this result.

c) Explain why a plastic bearing loaded with high p and low v exhibit a larger LPV-value than one loaded with low p and high v.

Problem 7.2: Material selection metal plain bearings

One guideline for material selection of boundary lubricated metallic bearings is a high hardness ratio between the two mating surfaces. Explain this measure.

Problem 7.3: Deep drawing

The tool life of a drawing die strongly depends on the lubricant used, the blank material and the surface coating on the forming die.

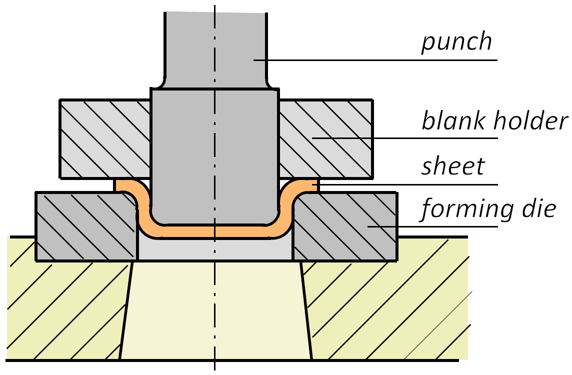

During pressing operations, the punch and forming die are continuously in contact with new material (open system). A pin-on-disk tribometer can therefore not be used in its standard form for this application, since this implies that the pin always runs in the same track on the disk rather than come into contact with new material.

ASTM G 132-96 contains the description of a "standard test method for pin abrasion testing". In this standard various configurations are given whereby the pin makes a specific movement over the counter surface so as to continuously make a fresh track. The configuration of choice is one with a spherical pin moving over a steel plate, drawing parallel tracks 1 mm apart. The pin has a radius of 5 mm. The average contact stress lies in the region of the hardness of the plate material (steel plate: 64HBW or 640 MPa, aluminium plate: 36HBW or 360 MPa).

a) Calculate the track width in the steel plate with a load of F= 150 N.

b) The drawing tool's steel pin is provided with a CVD-TiC coating. How can it be determined during the experiment whether the coating is worn away?

c) The pin is provided with a CVD-TiC coating of 8µm thickness. What is the expected life of the coating when $k = 0.1 \cdot 10^{-15}\ m^2/N$? Express the expected life in meters track length and in the experiment duration when the sliding velocity is 0.01 m/s.

d) If the friction suddenly increases, without the coating having worn out, what could have caused it?

Problem 7.4: Preselection of materials in high temperature applications

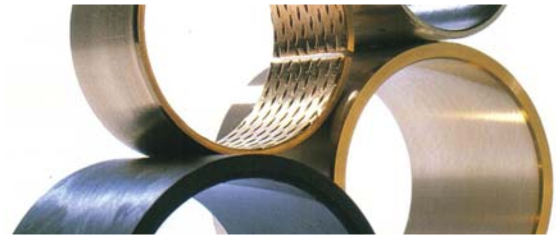

What causes and are the major temperature limitations in sliding contacts considering polymer-metal, metal-metal and ceramic-metal combinations?

Problem 7.5: Tire temperature Formula 1 racing car

A racing tire performs optimally at an operation temperature of 100°C-110°C. During racing, the tire temperature is measured constantly and the data passed on to the driver. If the F1-car is getting ready for the race, the tires' temperature is raised with tire heaters. A sort of electric blanket is used to pre-heat the tires to 80°C. Why is the tire temperature so important and what would happen if the temperature would become too high?

Problem 7.5: True or untrue?

1. Typical abrasion effects are characterised by irregular friction with large peaks and material transfer from one surface to the other.
2. Poisson's ratio is the ratio of lateral to axial stiffness of an anisotropic material, for rubbers v =0.5, for polymers v = 0.3 to 0.45.
3. In dry sliding metal to metal combinations the coefficient of friction is maximal for materials with high shear strength.
4. Lubrication of metal-to-metal contacts in relative motion is generally essential to prevent severe adhesive wear that ruins the surface quality and to prevent very high friction.
5. Steel shafts running in combination with sinter bronze bearings impregnated with solid lubricants do not need any further lubrication until the solid lubricant is worn away.
6. In order to minimize the tendency to adhesive wear materials are selected which are metallurgical incompatible.
7. A good material selection factor for the Hertzian load capacity of a concentrated circular contact is (Rp0.2/E')2.
8. In order to minimize the tendency to adhesive wear, materials are selected which are metallurgical compatible.
9. Bearings with lead-Babbitt layer are typically applied in hydrodynamically lubricated bearings.
10. Leaded bronze bearings are the most popular choice in machine engineering because of the good slide ability when boundary lubricated, high stiffness and good machine ability.
11. Thermosets with selected filler become more and more popular in offshore applications because of the high load capacity and good dry sliding properties with no concern of water that may enter the bearing system.
12. Sintered metals impregnated with oil running against steel are widely applied in consumer products because they are lubricated for life.

13. One of the possibilities to improve the life duration of the surface of a rolling guide is by applying a thin hard coating.
14. Thermoplastics in short plastics have advantages over metals in terms of vibration damping, low weight, inexpensive and the ability to run without lubrication.
15. Concerns about plastic bearings are the low stiffness, poor heat conductivity, large thermal expansion and large machining tolerances.
16. Examples of semi crystalline thermoplastics are POM, PA, PE-UHMW.
17. Semi-crystalline materials can be used up to some tens of degrees below the glass-transition temperature.
18. Examples of amorphous polymers are PVC, ABS, PMMA, PC.
19. Simple models to characterize visco-elasticity are the Kelvin model and the Maxwell model.
20. Visco-elasticity is modelled by a combination of Hookean springs and Newtonian dashpots, in which the spring represents elasticity and the dashpot the damping.
21. Thermoplastics in sliding motion against steel do not need to be lubricated however, lubrication may significantly reduce friction.
22. High performance plastics show high wear resistance and low friction.
23. In many self-lubricating plastics PTFE is used as a filler to achieve low friction and good wear resistance. The surface roughness of the counter surface is important to form an effective PTFE transfer film.
24. The fatigue strength of a component cyclically loaded in bending can be improved significantly by carburizing.
25. Thermosets have much higher melting temperature than thermoplastics.
26. Ceramic balls applied in deep groove ball bearings running at high speed are favourable over steel balls because of the much lower centrifugal forces.
27. Silicon Nitride balls in contact with steel are favourable over steel balls because of the higher Hertzian load capacity.
28. Thin modern hard coatings such as PVD and CVD coatings are sensitive to delamination when applied in cyclically loaded concentrated contacts.
29. A good material selection factor for the Hertzian load capacity of a concentrated line contact is (Rp0.2)2/E'.
30. In many self-lubricating plastics, PTFE is used as a filler to achieve low friction and good wear resistance. Lubrication is not needed but if applied it will further improve the wear resistance. U
31. A good material selection factor for the Hertzian load from a high speed rotating ball in a ball bearing is (Rp0.2)3/(E')2/? where ? is the density.
32. A good material selection factor for a slide bearing in order to achieve a high load capacity which is limited by thermal failure is K dT/ ? where K is the heat conduction coefficient, dT the maximum contact temperature and ? the coefficient of friction.
33. Self lubricating plastics are thermoplastics dispersed with solid lubricants such as PTFE, MoS2 and graphite.
34. When lubricated with fluids, unfilled plastics show higher wear resistance than the relatively expensive self-lubricating plastics.

35. The load capacity of plastic-plastic combinations is limited by the poor heat conduction.

36. The surface durability of spur gears is calculated using Hertz theory.

37. Amorphous plastics generally exhibit higher strength, rigidity and wear resistance that semi crystalline plastics and show in general good chemical resistance to oils and grease.

38. High performance plastics, engineering plastics and general purpose plastics are classified on the basis of their stiffness.

Answers

7.1)

a) The load capacity of plastic bearings is limited by the pv-value. If the rotational speed (rev/s) is fixed the sliding speed increases proportional to the bearing diameter and thus the maximum load capacity is gained with a relative small bearing diameter ($P=\mu Fv$, $v=\pi dn$).

b) The contact patch created by plastic deformation becomes smaller with a thin wall thickness of the bearing bushing, resulting in a higher real contact pressure and a more heat development per unit of surface.

c) The bearing running at low velocity and high contact pressure exhibits the highest pv-value because plastic bearings show the lowest friction coefficient at the maximum contact pressure. Furthermore, with a high load at low velocity, the contact patch created by elastic deflection of the bushing by the shaft load is larger.

7.2) In Table 7.2 page 250 are the common bearing materials listed ranged by the material hardness. The hardness of the counter material, in general the shaft, should be approximately 3 times harder than the hardness of the bearing material.

- A large difference in hardness, in general implicit less sensitivity to adhesion
- Abrasion of the hard counter material is limited to polishing wear rather than scratching.
- Improved embed ability of hard abrasive particles in the relative softer bearing material.
- Edge pressures from misalignment or shaft deflections are averaged out by plastic deformation of the relative soft bearing material.

7.3)

a) With (eq. 4.10 page 101) it can be established that the load $F/F_1 > 200$ and the deformation is consequently plastic. With this information it follows that the track width is $b=2r$ from $H = F/\pi r^2$. The track width turns out to be approximately 0.55 mm.

b) The friction in the contact between the ceramic coating and the steel is lower than when the steel of the tool comes into contact with the steel plate. Through adhesion, the friction and wear will suddenly increase sharply. Another method suitable for electrical insulating coatings is the measurement of electrical conduction.

c) In Case 3.2 page 234, an example is given for the wear volume of a ball as a function of the flattening h. With h = 8 µm follows for the wear volume $V = 1 \cdot 10^{-3}$ mm^3. Substitution in (eq. 6.1 page 232) gives a track length of s = 67 m. With a sliding velocity of 0.01 m/s the expected tool life would be approximately 110 minutes.

d) Through the adhesive transfer of material the friction suddenly increases.

7.4) Although metals in general can sustain high temperatures and have a good heat conduction, it is the lubricant that is needed in metal-metal contacts in sliding motion that may fail. Lubricating oils can be applied up to 150°C, however the oxidation stability of the lubricating oil may limit the exposure time to this temperature. Dry/solid lubricants, for example MoS2 based, can be used with contact temperatures up to 400°C, in vacuum much higher.

Some high-performance polymers are suitable for use at high temperatures up to 150...300°C, but have a relatively low compressive strength at higher temperatures and have poor heat conductivity.

Ceramics are very hard and can withstand high temperatures up to 400°C, but are brittle, show high friction coefficients in combination with steel (µ=0.2-0.8) and are also poor heat conductors. Carbon based ceramic coatings (DLC) have a good thermal conductivity and relative low surface energy that make them very suitable to perform at high temperatures and in vacuum.

7.5) Figure 7.4 page 254 shows that the friction coefficient increases with temperature until a maximal value is reached; above that value the friction coefficient falls back. In order to achieve maximum traction, an operating temperature is needed which ensures a maximum friction coefficient. When the maximum friction coefficient is exceeded, fading occurs whereby the friction strongly decreases and a high level of melting takes place. Fading can also occur in the brakes, i.e. 'brake fade". A Formula 1 car has no anti-lock braking system (ABS), which means it is possible that a racing driver ends up locking a wheel when he brakes. It extends the braking distance and the tire will undergo terrible local wear, resulting in a "flat spot".

During the formation lap, most drivers zigzag along the track to warm up the tires. At the end of this lap, the drivers park their cars at the start position and start the race a few seconds later. Tires that have reached the right temperature become very sticky, resulting in a considerable amount of rubber pick-up from other tires which in the course of the race end up immediately next to the ideal line on the track. Whoever takes the ideal racing line experiences few problems with this. But a driver who tactically makes way for a faster colleague regularly, encounters problems because of this. It takes a few laps before the pieces of picked up rubber have cleared again from the tires.

Wet Weather tires do not come to temperature in cold water. To compensate, they are made from a softer tire compound than dry weather tires. Furthermore, the tires differ because of the groove profile which dissipates water sideways. Qualifier tires are very special tires of a super soft compound with a life duration of one or two laps. At one time, this sort of tire was used to achieve a super qualifying lap time.

During the race, pitstops can be made for the following reasons:

- to change tires (according to plan, this happens once or several times per race, or more frequently in changeable weather)
- refuelling (according to plan, one or more times per race)
- repairs (always unexpected) or adjustments to front and/or rear wings (always unexpected)

To change the tires, a small army of at least fifteen fitters is needed to return the car to the race within 4 seconds: two fitters for the jacks at front and back, one for the 'lollipop' plus three fitters per tire (number one undoes the central wheel nut, number two removes the old tire and number three fits the new one. The 'lollipop man' (literally, from lolly) ensures with a board on a stick that the driver knows what he has to do during the stop (e.g. 'BRAKE' and 'FIRST GEAR').

Mostly, refuelling takes place at the same time as tire changes. Such a combined pitstop takes a few seconds longer and depends on the amount of fuel to be replaced. The petrol for a Formula 1 car does not differ much from that of a standard car. The octane number is a little higher, i.e. 102 instead of 98 for a simple super petrol. Current regulations forbid the addition of output-enhancing 'additives'. However, additives can be added to optimise the fuel. The participating oil companies must submit samples of all fuel to be used during the year to the FIA. Spot checks may be carried out during a racing weekend.

7.6) True: 3 - 4 - 5 - 6 - 9 - 10 - 11 - 12 - 14 - 15 - 16 - 18 - 19 - 20 - 21 - 23 - 24 - 26 - 28 - 29 - 31 - 32 - 33 - 34 - 35 - 36

Problems Chapter 8

Problem 8.1: Lubrication regimes

The slide surface of a cam-follower mechanism is partially submerged in an oil bath. After one year's operation, no wear can be observed. The finishing grooves on the slide surface are still visible.

a) Explain this phenomenon.
b) If the lubrication regime is not changed, could failure eventually occur?

Problem 8.2: EP-additives

a) Describe the way/when EP-additives work.
b) What type of wear can be prevented with EP-additives?
c) What does EP stand for and why is this nomenclature disputable?

Problem 8.3: Cone on plate viscometer

The cone on plate viscometer is the most popular method for gaining viscosity information at specific shear rates. Factors such as small sample size and ease of cleaning have helped make the cone and plate approach so popular. The oil for which the viscosity needs to be determined is placed between the cone and the plate.

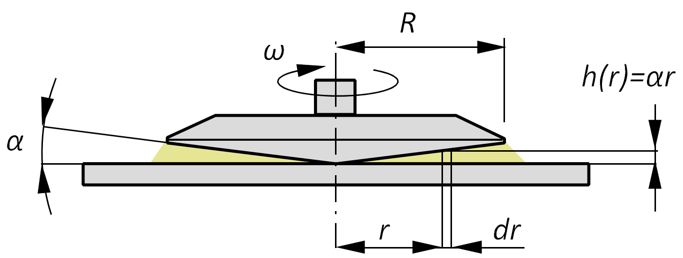

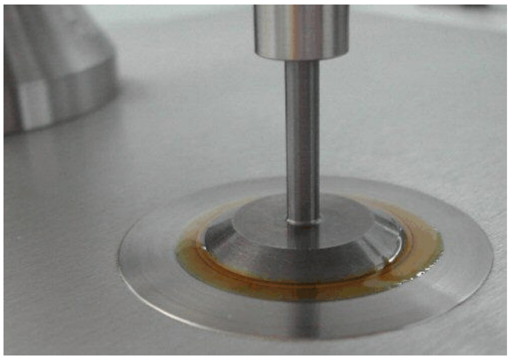

Before the measurement can take place, some time is required to bring the cone, which is at the same temperature as the plane, to the required temperature. To determine the driving torque as a function of the viscosity, the following questions need to be answered.

a) Derive an equation for the shear rate $\partial u/\partial z$ at distance r from the centre.
b) Derive an equation for the viscous shear force $F_f(r)$ of element dr.
c) Derive an equation for the viscous friction torque M.

Problem 8.4: Special lubricants

List a few specific functional requirements of lubricants for
a) Gear lubrication
b) Hydraulic oils
c) Cutting oils.

Answers

8.1)

a) As a result of elastohydrodynamic lubrication the surfaces do not make contact.

b) Through the elastic deformation that is likely to occur in a concentrated contact, surface fatigue may eventually set in.

8.2)

a) The friction between the asperity summits creates a high (flash) temperature. Under the influence of the high temperature, the EP additives form a chemical protective oxide layer with high shearing strength which can prevent pure metal contact.

b) Without this protective layer, the asperity summits may be welded together and then break apart again with continuous movement (scuffing).

c) EP stands for Extreme Pressure, whereas the chemical reaction establishes itself through the Extreme Temperature (flash temperature) between intermeshing asperity summits.

8.3)

a) $\tau = \eta \dfrac{\partial u}{\partial z} \qquad u(r) = \omega r \qquad h(r) = \alpha r \qquad \dfrac{\partial u}{\partial z} = \dfrac{\omega r}{\alpha r} = \dfrac{\omega}{\alpha}$

It is found that a uniform shear rate is generated across the entire sample for any given rotational speed.

b) $F_f(r) = \tau\ 2\pi r\ dr, \qquad \tau = \eta\, \omega / \alpha$

c) $M = \int_0^R r\ \tau\ 2\pi r\ dr = \int_0^R r\ \eta \dfrac{\omega}{\alpha}\ 2\pi r\ dr = \dfrac{2\pi}{3} \dfrac{\eta \omega R^3}{\alpha}$

A doubling of the cone radius R results in a spindle torque increase of a factor eight. This is of great benefit when measuring low viscosity products where an instrument's minimum measurable torque is limited.

8.4)

a) Gear lubricants: extreme pressure additives to prevent scuffing, high pressure coefficient to enable elasto-hydrodynamic lubrication, anti foaming.

b) Hydraulic oil, corrosion resistance, biodegradable.

c) Cutting oil: great lubricity, extreme pressure (EP), cooling, corrosion, compatibility.

Chapter 9

Problem 9.1: Reynolds' equation

Which assumptions have been made in deriving the Reynolds equation?

Problem 9.2: Aquaplaning

A thin water film develops between a car tire and the road surface. Because of the water film, the traction forces between the tire and the road surface are almost lost.

a) What is the effective surface velocity that causes aquaplaning? Assume that there is no slip yet (V=ωR).

b) Several measures are considered to make contact with the road surface. Indicate to which extent these actions make sense by considering the effective surface velocity in the following instances:

- pushing the gas pedal (ωR=10V),
- active braking (ωR=0),
- putting the car into reverse gear (ωR=-10V),
- pushing in the clutch (0≤ωR≤V).

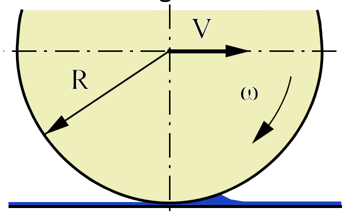

Problem 9.3: Cam-follower mechanism

For an optimal lifetime performance and reliability of a cam-follower mechanism, EHL is required between the cam and the rotating follower. The minimum film thickness in a line contact can be calculated using (eq. 4.51 page 122).

a) Demonstrate in which position of the cam - I or II - the EHL will fail first if no slip occurs and when the angular velocity of the cam is constant.

b) see a) but in the event of 100% slip.

c) The film thickness h_c to be calculated gives an indication if EHL may occur. Where does the minimum film thickness for EHL depends on?

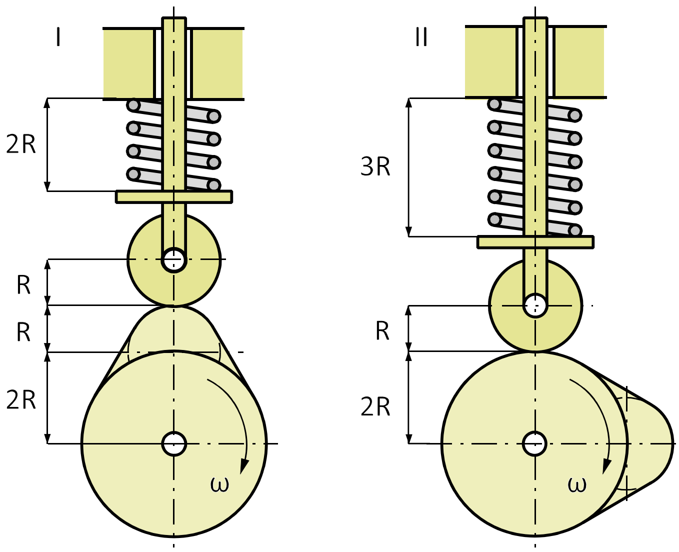

Problem 9.4: Grinding of rollers

A large rotating grinding stone is used with plain hydrodynamic journal bearings. (Rolling bearings generally display high frequency vibrations which compromise the accuracy of movement and hence the surface quality of the grinding). To improve the surface quality, the rotational velocity a grinding stone is increased. At this high rotational velocity the grinding stone starts to vibrate at a frequency equalling half the rotational velocity.

a) What will be the origin of this vibration?
b) What measures can be taken to prevent the vibration without sacrificing any of the rotational speed?
c) Someone suggests replacing the hydrodynamic bearing of the grinding stone by a hydrostatic bearing. Is this a good advice?

Problem 9.5: Circumferentially grooved hydrodynamic bearing

Sometimes bearings are used that contain a central circumferential lubricant feed groove. Examine by how much the load capacity of this type of bearing decreases as a result of the groove. Use the dimensions of the bearing given in Case 9.3a. Consider the circumferentially grooved bearing as two bearings with L/D=0.5.

Problem 9.6: Squeezing Disk brake

Before the brake shoes of a disk brake make contact with the brake disks some rain water will have to be dispersed. The time required to do this and the factors influencing the time will be examined here.

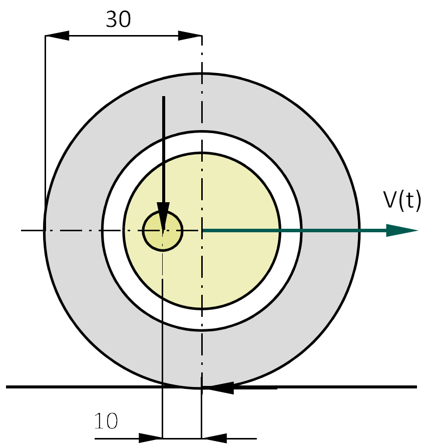

The geometry of a brake shoe is approximated by a round disk with a radius of R=40 mm. The viscosity of water is η=0.001 Pa s. The squeeze force amounts to approximately 6 kN. Because of inaccuracies in shape and roughness of the slide surfaces, mechanical contact already exists at h_2=3 µm.

a) Explain why this problem can be considered a “pure” squeezing film.
b) Calculate the time delay as a result of the squeeze effect and the relative increase in brake distance resulting from the squeeze effect, if the driving speed is 100 km/h.
c) How can this time delay be reduced?
d) To limit the wear on the brake shoes and brake disks, manufacturing the brake disks with a hard wearing material and finish them very smoothly is suggested. What do you think of this proposal?

Problem 9.7: Tube expansion

To expand the diameter of a tube a tapered cone is forced through the bore. The objective is to maintain a thin lubrication film between the pipe and the tapered cone. Consider only the wedge effect and determine the parameters that will influence film thickness h_c.

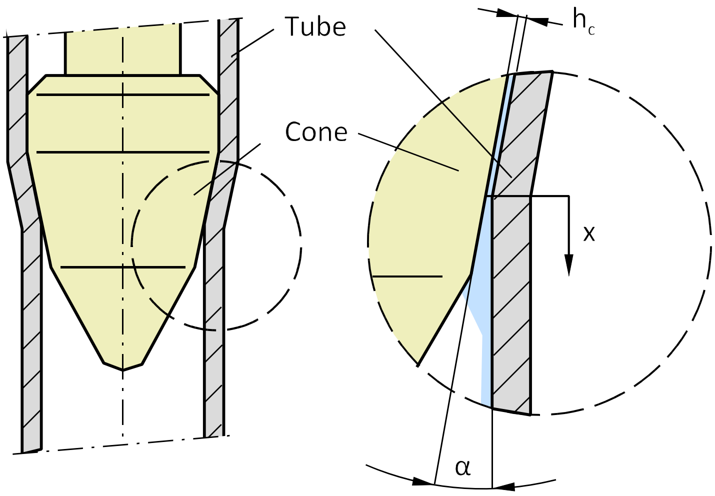

a) Explain why a parallel film will be created.

b) Derive an equation for dp/dx and p(x)

c) Convert from the equation for p(x) an equation for the film thickness h_c.

d) Will the calculated film thickness actually occur?

Problem 9.8: Rail-wheel contact

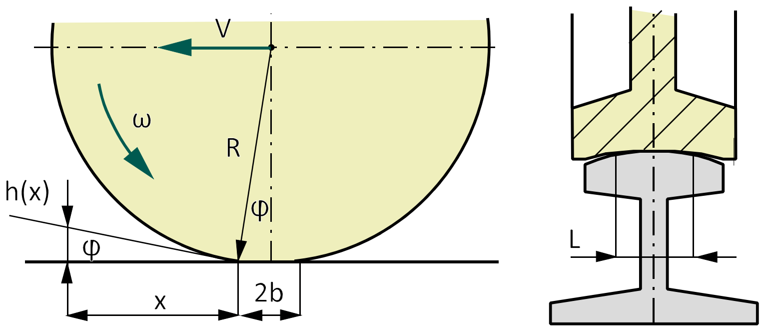

a) In the wedge-shaped inlet region of a rail wheel contact, by approximation $h(x)=\varphi x$ (φ in radians) applies. Derive on the basis of geometric considerations the value of φ (consider φ to be small).

b) Heavy rainfall has created a thin water film. The wheel and the rail remain in contact (blocked film). Derive an equation for the pressure gradient in the inlet region, considering a one-dimensional flow and $h(x)=\varphi x$. There is no slip.

c) Why will the pressure in reality not infinitely increase when x=0 ?

d) Assume that a thin parallel film is generated. Draw a possible actual hydrodynamic film pressure distribution (inlet and conjunction area).

e) Now derive an equation for the pressure gradient in the inlet area by equating the flow in the inlet area with the flow in the conjunction area.

f) Calculate the pressure p(x=0). The film thickness in the inlet region is now $h(x)=h_0+\varphi x$.

g) Consider that the load capacity of the film is almost entirely determined by the pressure in the conjunction area. What, then, is the load capacity?

Answers

9.1) Laminar flow, Newtonian fluid, predominated viscous shear forces, iso-viscous and constant pressure across the film, no slip condition, Euler's coordinate system.

9.2)

a) Aquaplaning $U_e=V+\omega R=2V$.

b) pushing the throttle wide open $|U_e|=11V$, active braking $|U_e|=V$, switching to reverse gear $|U_e|=9V$, holding down clutch $V<|U_e|<2V$. Conclusion: braking or pushing down the clutch, preference for pushing in the clutch to gain speed again when contact is re-established.

9.3) Cam-follower mechanism

a) Position I: Both contact surfaces move along with the film profile at equal velocity ($U_1=U_2=U_F=3\omega R$), so that no lubricant can be dragged into the converging wedge: $U=U_1+U_2-2U_F=0$.

Position II: The film profile is stationary: $U_F=0$. Without slip, both contact surfaces drag the lubricant along as $U_1=U_2=2\omega R$ into the converging wedge: $U=U_1+U_2=4\omega R$

Conclusion: With a rotating follower, EHL will fail first in position 1.

b) Position I: The film profile and the cam surface move to the right with $U_1=U_F=3\omega R$. Let the coordinate system move along again with the film profile: $U=U_1-2U_F=-3\omega R$

Position II: The film profile and the follower stand still $U=U_1=2\omega R$

In position I, the effective sliding velocity is greatest. However, the contact geometry in this position is less favourable. The film thickness will now be established more accurately for both positions.

$$\frac{(h_c)_1}{(h_c)_2}=\left(\frac{3}{2}\right)^{8/11}\left(\frac{1/2}{2/3}\right)^{2/11}\left(\frac{2}{1}\right)^{-1/11}=1.34\cdot 0.90\cdot 0.94=1.14$$

Conclusion: With the stationary follower, EHL will fail first in position II, $(h_c)_1>(h_c)_2$.

c) The required value of h_c can be derived from the roughness of both surfaces.

9.4)

a) The effect of cavitation is limited because of the small eccentricity, resulting in the load vector and the deflection vector being almost perpendicular to each other. This results in unstable behaviour, in this case at half the rotation speed, called half-omega whirl.

b) By choosing a larger bearing clearance the eccentricity will increase, which means the operational speed can be maintained at the higher level.

c) With a hydrostatic pressure in the bearing cavitation is suppressed. If any additional hydrodynamic pressure can build up, the system becomes unstable. A large plain bearing area that enables the build up of hydrodynamic pressure must therefore be avoided.

9.5)

The Sommerfeld number of a bearing with ε=0.15 and L/D=1 amounts to S=9.12, with L/D=0.5 it will be Φ=5.08 (Program 8.2). The load capacity of the bearing is proportional with the product of the Sommerfeld number and the bearing length. This results in the quotient: F(L/D=0.5)/F(L/D=1)=(5.08/9.12)(0.5/1.0)=0.28, i.e. the load capacity of a bearing with L/D=0.5 is 28% of a bearing with L/D=1.0. For the circumferential grooved bearing, it follows that the load capacity will amount to 2·28%=56% of the bearing having an axial groove.

9.6) Disk-brake

a) With a parallel film and in the case of the absence of a wedge-shaped inlet region, no wedge effect will occur.
b) Substitution of I=F·t in () and assuming $(h_2/h_1)^2<1$ gives t=0.12 sec, s=v·t=3.3m.
c) The time delay due to the squeeze effect can be reduced by providing grooves into the brake shoes.
d) A smooth finish reduces the film thickness h_2 with the result that the squeeze time $t \sim 1/h_2^2$ will strongly increase. Halving the film thickness at which contact take place will produce a squeeze time that is four times as large.

9.7) Tube expansion

a) Through plastic deformation the pressure in the film equals the extrusion pressure of the tube. With the uniform pressure $p=p_e$, dp/dx=0 then $q_x=Uh_c/2$ where h_c is the uniform Couette film thickness.
b) The isoviscous solution method for a wedge shaped inlet and uniform interface is presented in (?).
c) In reality, the viscosity will increase due to the pressure-viscosity coefficient, resulting in a thicker film.

9.8) Rail-wheel contact

a) Rφ=b, φ=b/R.
b) In a wedge shaped film with h(x=0)=0 the pressure gradient dp/dx becomes infinite.
c) The calculation does not take into account surface roughness, sideway flow and EHL.
d) This solution method is shown in (?).
e) Substitution of U_e=-2ωR and φ=b/R in (?) results in p_c

$$p_c = -\frac{3\eta U}{\varphi h_0}, \quad \varphi = \frac{b}{R}, \quad U = -2\omega R; \qquad p_c = \frac{6\,\eta\,\omega R^2}{b \quad h_0}$$

f) $F = p_c \; 2bL$

Chapter 10

Problem 10.1: Windscreen wiper

Hydrodynamic lubrication takes place between a windscreen wiper and the windscreen of a car. Without hydrodynamic lubrication, when the windscreen is dry, the wiper will move in jolts over the windscreen due to stick-slip. With hydrodynamic lubrication, the very thin layer of water between the wiper and the window will evaporate shortly after the wiper has passed over it.

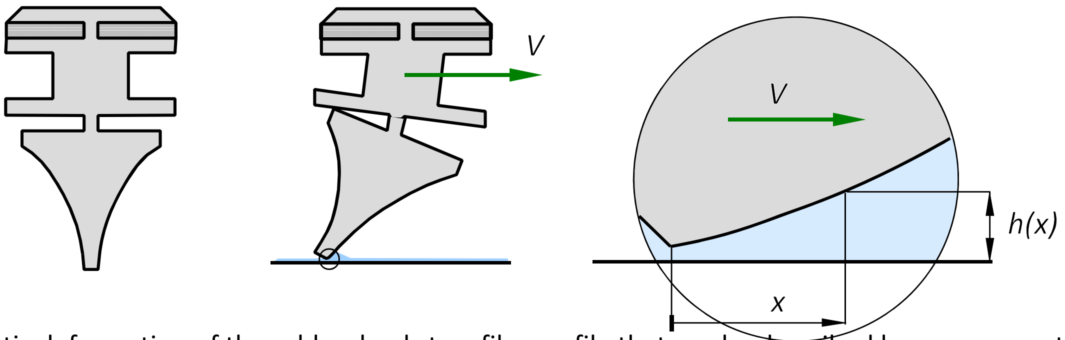

The elastic deformation of the rubber leads to a film profile that can be described by an exponential function, $h(x)=h_0e^{\alpha x}$ with α=20.000m^{-1}. The film cavitates in x=0. The press-on force of the 40cm long wiper blade amounts to 6 N, the velocity of the wiper V=1m/s, the viscosity of water is η=0.001 Pa.s.

a) Give an equation for the pressure gradient with the integration constant h_c. (h_c is the film thickness in the location of dp/dx=0).

b) Derive from the equation of the pressure gradient dp/dx the pressure distribution p(x).

c) Solve the relationship between the constant of integration h_c and h_0.

d) Derive an equation for the load capacity per unit of length.

e) Calculate the minimal film thickness between the windscreen wiper and the window?

f) Calculate the thickness of the water layer that will evaporate immediately after the wiper has passed?

g) Calculate the maximum value of the hydrodynamic pressure p_{max} that will occur.

Answers

10.1) Windscreen wiper

a)

$$\frac{dp}{dx}=6\eta U\frac{h-h_c}{h^3} \qquad p(x)=6\eta U\int_0^x\frac{h-h_c}{h^3}dx, \qquad h=h_0e^{\alpha x}$$

b)

$$\int_0^x\frac{1}{(h_0e^{\alpha x})^2}dx=\frac{1}{h_0^2}\int_0^x e^{-2\alpha x}dx=-\frac{1}{2\alpha h_0^2}\left(e^{-2\alpha x}-1\right)$$

$$\int_0^x\frac{1}{(h_0e^{\alpha x})^3}dx=\frac{1}{h_0^3}\int_0^x e^{-3\alpha x}dx=-\frac{1}{3\alpha h_0^3}\left(e^{-3\alpha x}-1\right)$$

$$p(x)=6\eta U\left(-\frac{1}{2\alpha h_0^2}\left(e^{-2\alpha x}-1\right)+\frac{h_c}{3\alpha h_0^3}\left(e^{-3\alpha x}-1\right)\right)$$

c)

$$p(\infty)=0: \quad 0=6\eta U\left(-\frac{1}{2\alpha h_0^2}(0-1)+\frac{h_q}{3\alpha h_0^3}(0-1)\right), \quad h_c=\frac{3}{2}h_0$$

d)

$$\frac{F}{L}=\int_0^\infty p(x)dx=\frac{6\eta U}{2\alpha h_0^2}\left(-\frac{e^{-2\alpha x}}{-2\alpha}+\frac{e^{-3\alpha x}}{-3\alpha}\right)\Bigg|_0^\infty=-\frac{1}{2}\frac{\eta U}{\alpha^2 h_0^2}$$

e)

$$F=6N, \quad L=0.4m, \quad \alpha=20.000m^{-1}, \quad \eta=0.001\ Ns/m^2, \quad U_e=-1m/s$$

$$h_0=\frac{1}{\alpha}\sqrt{\frac{\eta UL}{2F}}=0.29\,10^{-6}m$$

f) $h_c=3/2\,h_0$

g)

$$h_c=h_0e^{\alpha x}, \quad e^{\alpha x}=h_c/h_0, \quad x=\ln(h_c/h_0)/\alpha, \quad x\approx 20.10^{-6}m$$

$$p_{max}=p(20.10^{-6})=2025\,Pa$$

Problems Chapter 11

Problem 11.1: E.P. 4-pocket journal bearing with capillary restrictors

From a four-pocket journal bearing is given: p_s= 6MPa (60bar), β_0=0.5, D=40mm, L/D=1, $L_T/L=L_A/L$=0.25, $\Delta R/R$=1/1000, ε_{max}=0.5, η=0.2Pa·s, l/d=40.

a) Calculate A_e/A.

b) Calculate the bearing stiffness and load capacity.

c) Calculate the flow and required pumping power.

d) Calculate the dimensions of the capillary restrictors.

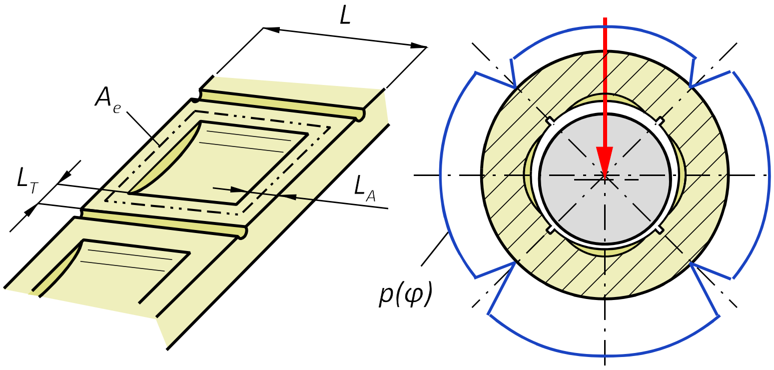

Problem 11.2: E.P. 4-pocket thrust bearing with capillary restrictors

A lock gate can also be carried by a thin water film instead of wheels running on rails. The Prins Willem Alexander lock gate in the river IJ in Amsterdam are the first in the world (1995) designed in that way. The lock gates is carried on both ends by a self-aligning circular thrust bearing with four pockets. Dependent on the tilt, a pressure distribution is generated as illustrated in the figure below.

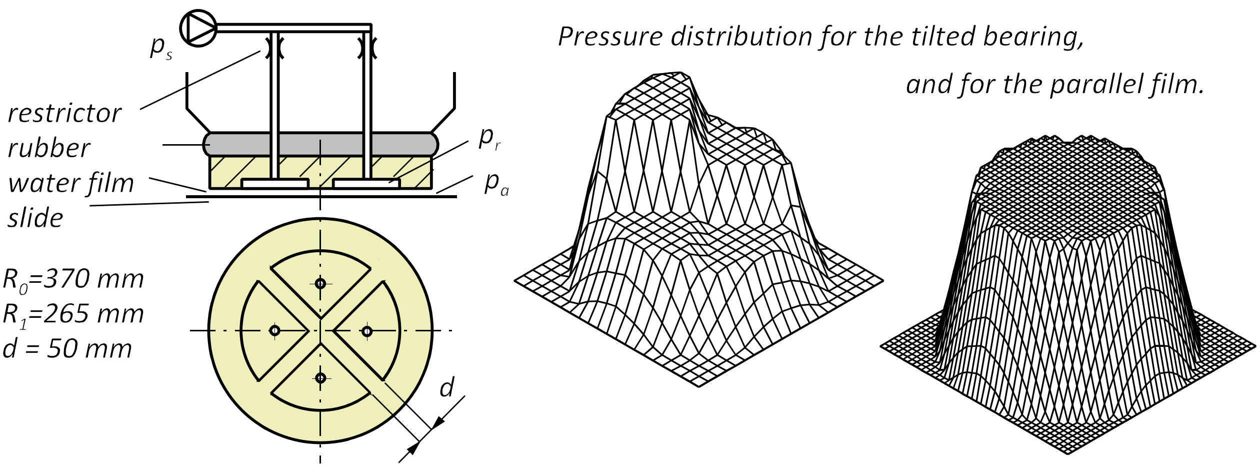

The lock gate is seven metres high, 25 metres long and three metres width. The dry mass of the lock gate amounts to approximately 180 tonnes. In the water, the weight is reduced by the air pockets in the door to 50 tonnes. Under the nominal bearing load of 250 kN on each bearing, a water film is created with a thickness of 130μm (η_{water} = 0.001 Pa s). The pockets are a few millimetres deep. The door can move with a velocity of v=0.24 m/s. Because the bearings have to carry a double overload, restrictors are included which will reduce the feed pressure p_s with a nominal load to the pocket pressure p_r=0.4 p_s (p_a=0). Both bearings are fed by the same pump.

a) Give an approximation (±10%) for the required pumping power. (Assume a linear pressure distribution and calculate the required pocket pressure, supply pressure, the flow and finally the pumping power).

b) Calculate the friction coefficient by viscous shearing in the thin water film?

c) During tests with a prototype hydrostatic thrust bearing, the friction coefficient proved to be μ=0.001. This higher value is a result of the in practice incomplete separation of the bearing surfaces. If the friction coefficient in contact equals μ_{BL}=0.1 and the friction coefficient with a full film is negligible compared to this value, what part of the load is then transferred by contact?

d) The maximal pump pressure (with minimal flow) is equal to p_s=2.4 MPa (24 bar). If with a pump pressure of 2 MPa a load of 250 kN is carried, how great would be the admissible load when i) the bearing surfaces are narrowly still separated ($h \rightarrow 0$), ii) the bearing surfaces are in complete contact ($h=0$)?

e) Someone proposes the incorporation of one restrictor in the central feed rather than the separate restrictors connected to the individual pockets. The advantage would be that only one restrictor is required for each bearing, with less risk blockages thanks to the larger flow inlet. What would the consequence be?

Problem 11.3: E.P. bearings with shallow pocket

A choice must be made between one of two types of long rectangular hydrostatic thrust bearings.

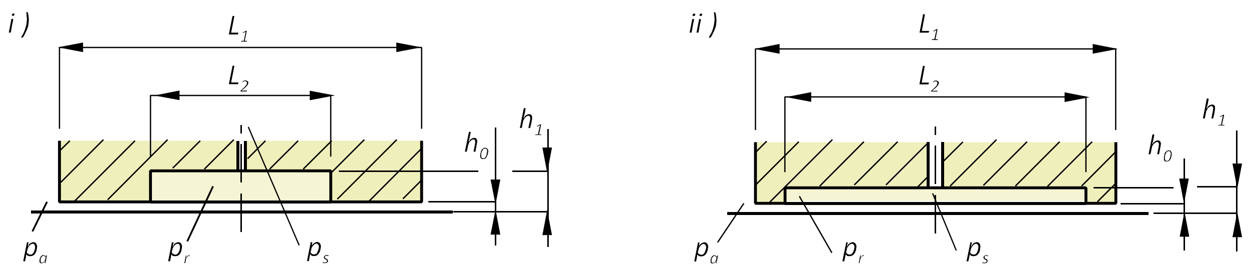

i) a hydrostatic bearing with external restrictor. The pocket depth in this bearing is more then 10 times larger than the film thickness h_0.

ii) a hydrostatic bearing with shallow pocket. The pocket depth in this bearing is approximately the same as the film thickness h_0.

The length of the bearing is so great that a one-dimensional flow can be assumed. With nominal load, the pressure factor $\beta_0(h_0)$=0.5. Answer the questions below for both bearing configurations.

a) Draw the pressure distribution in both bearings.

i) with film thickness h_0

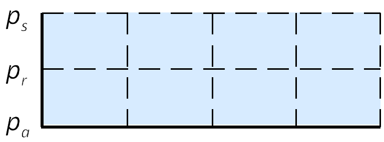

ii) with film thickness h_0

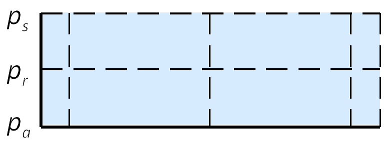

i) with film thickness $h_{min} \rightarrow 0$

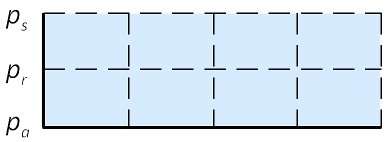

ii) with film thickness $h_{min} \rightarrow 0$

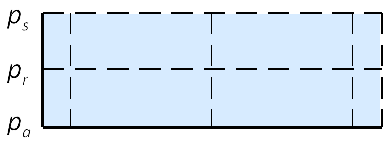

i) with film thickness $h_{min} = 0$

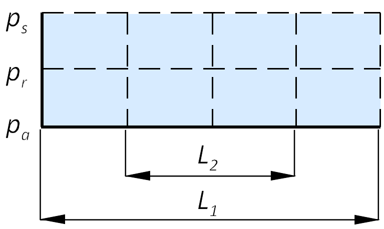

ii) with film thickness $h_{min} = 0$

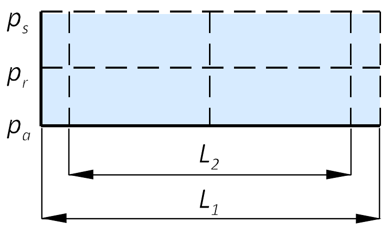

b) What is the nominal load F, expressed in L_1, L_2 and p_s?

c) What is the flow rate Q, expressed in h_0, p_s, B, L_1 and L_2?

d) What is the required pump power N, expressed in h_0, F, η, B, L_1 and L_{21}=L_2/L_1?

e) What should L_{21} be when a minimal pump power is required for F, h_0, η, B and L_1 as given?

f) What is h_1 / h_0 if L_{21} = 1/2?

g) Take for bearing type i) L_{21} =1/3 and for bearing type ii) L_{21}. = 5/6. Take for both bearings equal B, L_1, F, η and $h_{0.}$ Then calculate the pressure ratio $p_{s,i}$ /$p_{s,ii}$, flow ratio Q_i/Q_{ii} and the power ratio N_i /N_{ii}.

h) What is the load increase F_{max}/F when $h_{min} \rightarrow 0$?

Answers

11.1) E.P. journal bearing

a)

$$A_E = (L-L_A)(\pi D/4-L_T),\; A=LD,\; 0.9A_E/A=0.36$$

b)

$$S'=0.54,\; S=S'Ap_s/h_0=325\cdot10^6\,N/m,\; F=S\,\varepsilon\,\Delta R=4.88\,kN$$

c)

$$Q=4\frac{h^3}{12\eta}\frac{\beta p_s}{0.25L}((L-0.25L)2+(\frac{\pi D}{4}-0.25L)2),\; N=Qp_s$$

d)

$$\frac{Q}{4}=\frac{\pi d^4}{128\eta}\frac{(1-\beta)p_s}{l},\; l/d=40;\quad d{=}xx\;mm,\; l{=}xx\,mm$$

11.2) E.P. thrust bearings

a)

$$F=\pi R_1^2 p_r+\pi(R_2^2-R_1^2)\frac{p_r}{2}=\frac{\pi}{2}(R_1^2+R_2^2)p_r,\quad p_r=7.7\,bar,\quad p_r=0.4p_s,\quad p_s=19.3\,bar$$

$$Q=\frac{h^3}{12\eta}\frac{p_r}{R_2-R_1}2\pi\frac{R_1+R_2}{2},\quad Q=9.6\,m^3/h,\quad N=2Qp_s,\quad N=10\,kW$$

b)

$$F_f=\tau A=\eta\frac{U}{h}(\pi(R_2^2-R_1^2)+dl)\qquad l=2R_1+2(R_1-d),\quad \mu=2.10^{-6}$$

c)

$$\mu=\alpha\,\mu_{mech.}+(1-\alpha)\,\mu_{hydr.}\qquad \alpha\approx0.01$$

d)

$$\text{i)}\;\; F=\frac{250}{0.4}\frac{24}{20}=750\;\;kN\qquad\qquad \text{ii)}\;\; F=p_s(\pi R_1^2-dl)=410\;\;kN$$

e) With this method, the tilting stiffness of the bearing would be lost because the pressure in all four pockets would become independent of the bearing tilt.

11.3) E.P. bearing with shallow pocket

a)

i) with film thickness h_0

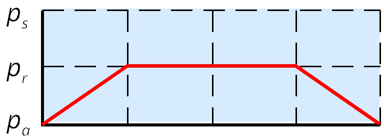

ii) with film thickness h_0

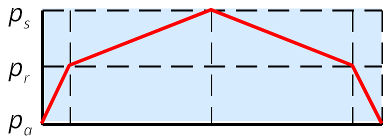

i) with film thickness $h_{min} \to 0$

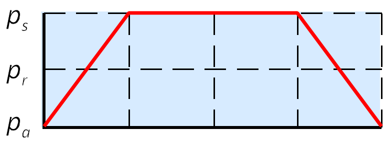

ii) with film thickness $h_{min} \to 0$

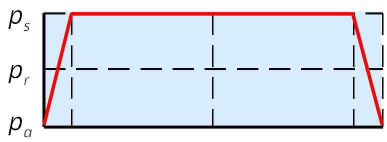

i) with film thickness $h_{min} = 0$

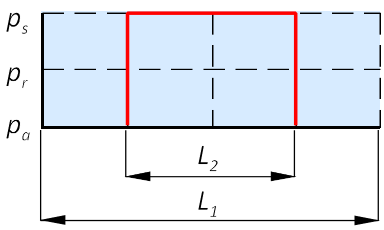

ii) with film thickness $h_{min} = 0$

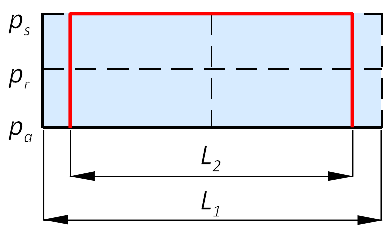

b) *i*) $\dfrac{F}{L} = \dfrac{L_1 + L_2}{4} p_s$ *ii*) $\dfrac{F}{L} = \dfrac{L_1 + 3L_2}{4} p_s$

c) *i*) $\dfrac{Q}{L} = \dfrac{h_0^3 p_s}{6\eta(L_1 - L_2)}$ *ii*) $\dfrac{Q}{L} = \dfrac{h_0^3 p_s}{6\eta(L_1 - L_2)}$

d) *i*) $N = \dfrac{h_0^3 (4F)^2}{6\eta L L_1^3} \dfrac{1}{(1 - L_{21})(1 + L_{21})^2}$ *ii*) $N = \dfrac{h_0^3 (4F)^2}{6\eta L L_1^3} \dfrac{1}{(1 - L_{21})(1 + 2L_{21})^2}$

e) $\dfrac{dN}{d(L_{21})} = 0$ *i*) $L_{21} = 1/3$ *ii*) $L_{21} = 1/2$

f) $(\dfrac{h_0}{h_1})^3 = \dfrac{1}{L_{21}} - 1, h_1/h_0 = 1$ with zero stiffness! This means that $L_{21} > 1/2$ is required.

g) $\dfrac{p_{s,i}}{p_{s,ii}} = \dfrac{(1 + 2L_{21})_{ii}}{(1 + L_{21})_i} = 2$ $\dfrac{Q_i}{Q_{ii}} = \dfrac{(1 - L_{21})_{ii}}{(1 - L_{21})_i} = \dfrac{1}{2}$ $\dfrac{N_i}{N_{ii}} = \dfrac{p_{s,i} Q_i}{p_{s,ii} Q_{ii}} = 1$

h) $(\dfrac{F_{max.}}{F})_i = 2$ $(\dfrac{F_{max.}}{F})_{ii} = \dfrac{11}{8}$

i) *i*) $\mu = \dfrac{4\eta U}{h_0 p_s} \dfrac{1 - L_{21}}{1 + L_{21}}$

Problems Chapter 12

Problem 12.1: Design of a partially grooved aerostatic journal bearing

The bearing configuration shown below has good self aligning capability as a result of the relatively large distance between the bearings. Both bearings may be designed with different diameters or lengths, which may be profitable with eccentric loading. By applying different diameters the feeding pressure generates an axial force so that one thrust ring suffices for axial positioning. The ring will be separated from the housing by a “constant flow supply” which comes from the leakage of the partly-grooved journal bearing connected in series with the thrust ring.

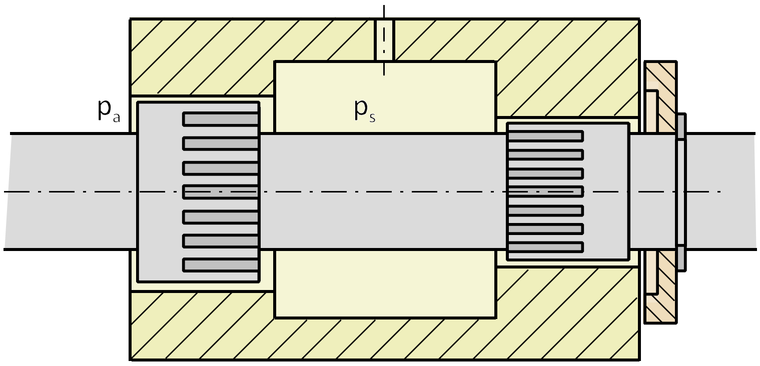

The design shown above is successfully applied in a water lubricated cleaning device with supply pressures over 10MPa (100 bar) but is also applicable for gas lubrication.

a) Calculate the pressure factor β_0 that will occur when the bearings are fed by water and air respectively.

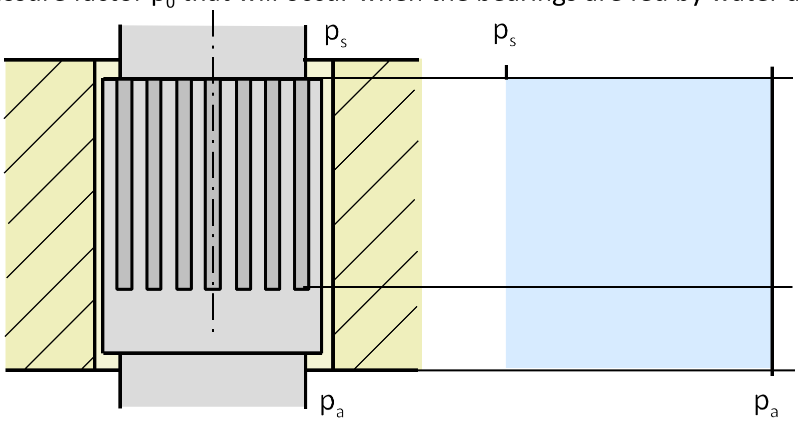

b) Sketch the pressure distribution which may occur if the bearing is fed by water and air respectively, in the figure below.

Answers

12.1) Partially grooved aerostatic journal bearing

a) The formula to calculate the β-value for the incompressible fluid is given by (eq. 11.57 page 429). Substitution of L′=0.9, B′=0.1 and n=4 gives β=0.448. With a parallel film and incompressible fluid the pressure linearly drops from p_s to p_r and from p_r to p_a.

The formula to calculate the β-value for the compressible fluid is derived in the same way as described for the incompressible fluid (eq. 12.10 page 448). Working out this equation finally results in $\beta(L', B', n, p_s/p_a)$. Substitution of L′=0.9, B′=0.1, n=4 and p_s/p_a=6 gives β=0.681. For higher supply pressures, β approaches the asymptotic value 0.669. With a parallel film and compressible fluid the pressure distribution is convex as sketched for the stepped bearing in Figure ?.

b)

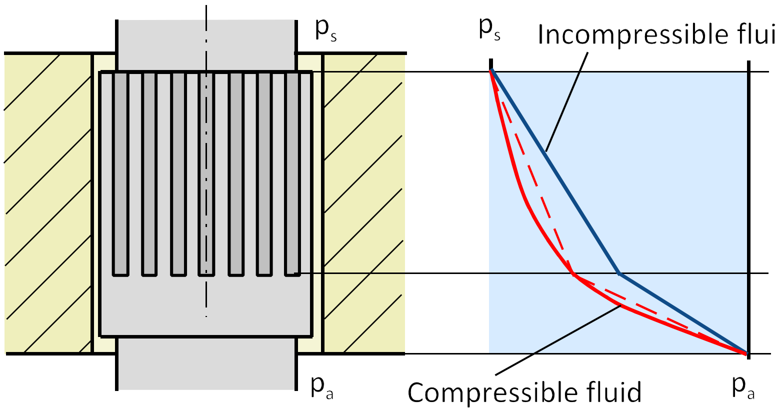

With helically shaped grooves the bearing function remains and the piston becomes driven to rotate. In the other way around, helical grooves and an externally driven rotor will provide a viscous pump. It is evident that designing e.p. air bearings and hydrostatic bearings is a creative job.

Problems Chapter 13

Problem 13.1: Shaft bending by lateral misalignment

There are two types of misalignment: parallel and angular misalignment. With parallel misalignment, the center lines of both shafts are parallel but they are offset. With angular misalignment, the shafts are at an angle to each other.

When a driver like an electric motor is coupled to a screw or any other piece of equipment, it is essential that the shafts are aligned. Any misalignment between the two results in cyclic bending of the shafts and increased bearing load. This may result in premature breakdown of the equipment by fatigue fracture of the shaft or bearing failure.

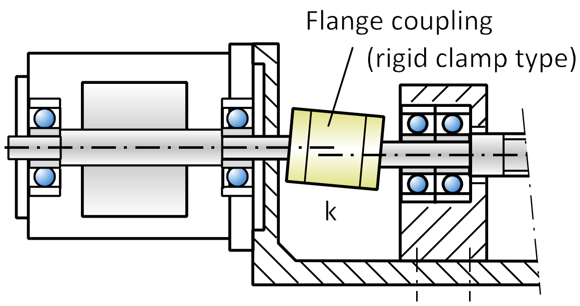

Calculate the bearing load and shaft bending stress as a function of the lateral misalignment δ.

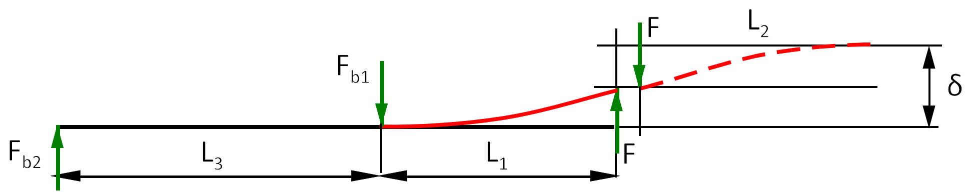

Consider the lateral misalignment that needs to be compensated by elastic deformation of the shafts δ=0.2 mm. The more flexible part of the shaft of the electric motor and that of the spindle of length L_1=L_2 =60 mm and diameter d=12 mm. The distance between the motor bearings is L_3=80 mm.

Problem 13.2: Resonance frequency of a leaf spring guiding

The leaf springs of the linear guide described in Case 13.1 page 473 are accidentally made of a material thickness of 0.3 mm. What consequences does this have for the maximum amplitude of motion?

Answers

13.1)

The formula for lateral stiffness can be derived from the deflection mode shown in Figure ?b. Substitution of $v(L) = \delta/2$ in (?) results in F= 300 N. The moment of bending in the shoulder of the shaft becomes M=FL=17.8 Nm. This results in a bending stress of σ = 105 MPa. The stress concentration locally will result in a much higher local stress.

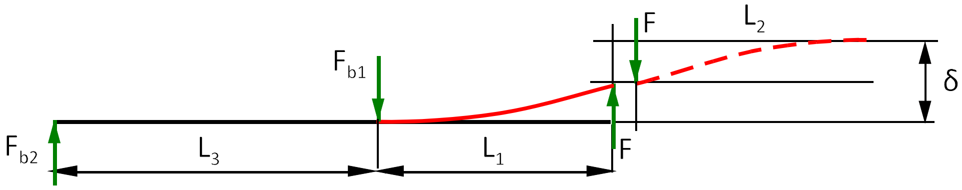

The bearing load becomes $F_{b1} = FL_1/(L_1+L_3)$ =127 N, $F_{b2}=Fb_1 - F$=27 N

13.2)

The stiffness will increase by a factor $(0.3/0.25)^3$, the maximum bending moment will increase by a factor $(0.3/0.25)^2$, the amplitude of motion will increase by a factor $(0.3/0.25)^2/(0.3/0.25)^3=(0.25/0.3)=5/6$. This is a reduction of 17%. The resonant frequency will increase by a factor $(0.3/0.25)^{3/2}$.

Problems Chapter 14

Problem 14.1: Knife edge jewel bearing

The knife edge bearing of a micro balance can be designed as a rolling contact or a sliding contact (Figure 14.3 page 487). Which of the designs has the highest load capacity?

Problem 14.2: Pivot jewel bearing

Calculate the load capacity and friction torque of the pivot bearing described in case 13.1, however with vertical pivot axis.

Answers

14.1) Knife edge jewel bearing

The load capacity is linearly proportional to the effective contact radius (?), $F=C_1 \cdot R'$

Rolling contact: The pivot radius is usually taken three times the bearing radius. The effective contact radius of the line contact becomes $1/R'=1/Rp+1/3Rp$; $R'=3/4Rp$. $G = F = 3/4\ C_1\ Rp$

Sliding contact: The effective contact radius of the line contact becomes: $1/R'=1/Rp$, $R'=Rp$. The normal load becomes $F = C_1\ Rp$. The load capacity becomes $G = 2\ F \sin(\varphi)$. Substitution of $F = C_1\ R_p$ results in $G = 2\ C_1\ R_p \sin(\varphi)$.

The load capacity of the sliding contact and rolling contact are the same when $2 \sin(\varphi)= 3/4$, $\varphi=22$ deg. Since the cone angle 2φ is typically in the range between 80 and 90deg, the load capacity of the sliding contact is larger. For $2\varphi = 90$deg the load capacity of the sliding contact is larger by a factor of $(2 \sin(\varphi)) / (3/4) = 1.9$. Notice that the traction force is not taken into account.

14.2) Pivot jewel bearing

The radii of contact are $r_{1x} = r_{1y} = R_p$, $r_{2x} = r_{2y} = -R_b$. Substitution of the contact radii and the material properties in the Hertz calculator for initial point contacts and setting the constraint for the maximum contact pressure for steel $p_{max} = 4.2$ GPa results in the effective contact radius $R'=0.075$ mm and a maximum Hertzian contact load of $F = 0.35$ N. Substitution of the bearing properties and service conditions in the calculator for the Spherical thrust bearing result in the friction torque for the pivot bearing $T = 0.19 \cdot 10^{-3}$ Nmm. The calculated load capacity and friction torque with horizontal pivot axis is $F = 0.46$ N and $T = 4.8 \cdot 10^{-3}$ Nmm (two bearings). The friction torque with horizontal axis is found to be much larger than with vertical pivot axis.

Table A1: Conversion factors to SI Units

Length:				**Power:**			
1 foot (ft)	=	1200/3937	m	1 ft-lb/s	=	1.356	W
1 inch (in)	=	25.4E-03	m	1 hp	=	746	W
1 mile	=	(5280 feet)					
Mass:				**Volume:**			
1 slug	=	14.59	kg	1 gal (US)	=	3.785E-03	m^3
1 pound (lb)	=	0.454	kg	1 gal (UK)	=	4.546E-03	m^3
				1 barrel	=	(42 gallon)	
Force:				**Temperature:**			
1 pound (lb)	=	4.448	N	Celsius (°C)	=	(°F - 32)5/9	
1 dyne	=	1E-05	N	Kelvin (K)	=	°C + 273	
1 kgf	=	9.81	N				
Pressure:				**Dynamic viscosity:**			
1 lb/in^2	=	6895	Pa	1 cP	=	1E-03	Pa·s
1 bar	=	1E+05	Pa	1 poise (P)	=	(100 cP)	
1 psi	=	(1 lb/in^2)					
PV:				**Kinematic viscosity:**			
1 psi·fps	=	2.1E03	Pa·m/s	1 cSt	=	1E-06	m^2/s
1 psi·fpm	=	35.0E+05	Pa·m/s	1 stokes (St)	=	(100 cSt)	

Table A2 Deflections and slopes of uniform cantilever beams

Loading	deflection	slope
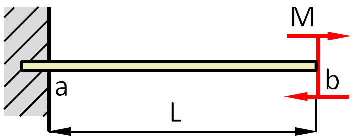	$\delta_b = \frac{ML^2}{2EI}$	$\theta = \frac{ML}{EI}$
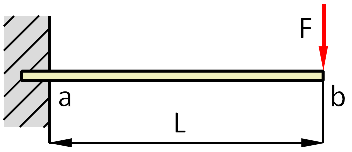	$\delta_b = \frac{FL^3}{3EI}$	$\theta = \frac{FL^2}{2EI}$

Table A3 Moments of inertia I_x, I_y and Polar moments of inertia I_p

Cross section	Bending	Torsion
Elementary equations for uniform beams subjected to bending and torsion respectively:	$M_x = S_x \sigma_b, \quad S_x = \frac{I_x}{y_{max}}$ $I_x = \int y^2\, dA$ $\delta = \frac{ML^2}{2EI}, \quad \theta = \frac{ML}{EI}$	$T = S_t \tau_{max}, \quad S_t = \frac{I_p}{r}$ $I_p = I_x + I_y$ $\phi = \frac{TL}{GI_p}, \quad G = \frac{E}{2(1+\nu)}$
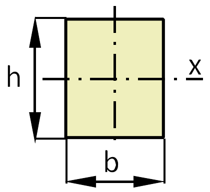	$I_x = \frac{1}{12} b h^3$ $S_x = \frac{1}{6} b h^2$	
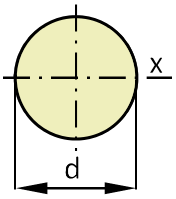	$I_x = \frac{\pi}{64} d^4$ $S_x = \frac{\pi}{32} d^3$	$I_p = \frac{\pi}{32} d^4$ $S_t = \frac{\pi}{16} d^3$
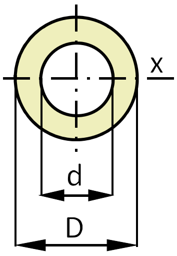	$I_x = \frac{\pi}{64}(D^4 - d^4)$ $S_x = \frac{\pi}{32} \frac{D^4 - d^4}{D}$	$I_p = \frac{\pi}{32}(D^4 - d^4)$ $S_t = \frac{\pi}{16} \frac{D^4 - d^4}{D}$

von Mises equivalent stress $\sigma_e = \sqrt{\sigma + 3(\alpha_0 \tau^2)}$

- $\alpha_0 = 1$ when σ and τ are both static or fully reversed,
- $\alpha_0 = 0.7$ when σ is fully reversed and τ remains static
- $\alpha_0 = 1.5$ when σ remains static and τ is fully reversed

Table A4 Approximate formulae for spring stiffness

Spring	Stiffness
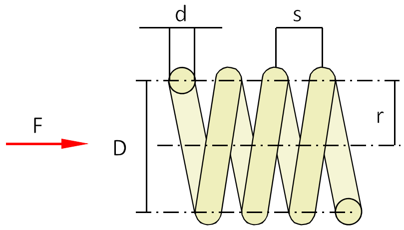	$F = \frac{\pi}{16}\frac{d^3}{r}\tau$ $f = \frac{64\, n\, r^3 F}{d^4 G}$
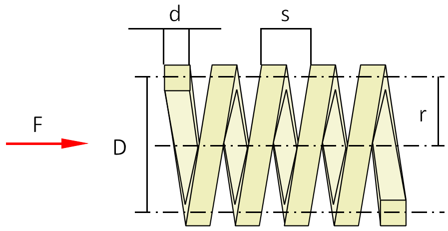	$F = \frac{d^3}{4.8\, r}\tau$ $f = \frac{44.9\, n\, r^3 F}{d^4 G}$
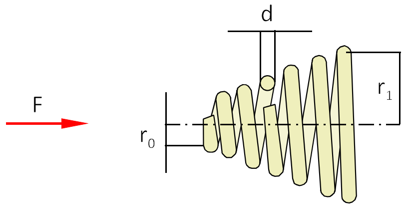	$F = \frac{\pi}{16}\frac{d^3}{r_1}\tau$ $f = \frac{16\, n\, (r_1+r_0)(r_1^2+r_0^2)\, F}{d^4 G}$
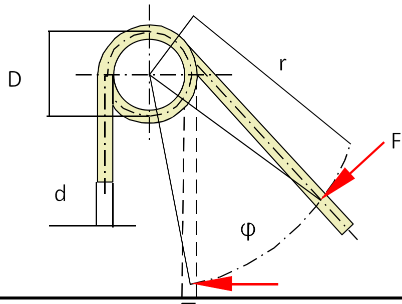	$F = \frac{\pi}{32}\frac{d^3}{r}\sigma$ $\varphi = \frac{2\, D\, \pi\, n}{E\, d}\,\sigma\,\frac{180}{\pi}$ φ [deg.]
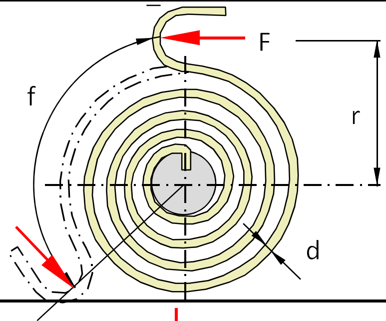	$F = \frac{\pi}{32}\frac{d^3}{r}\sigma$ $f = \frac{2\, r\, l}{E\, d}\sigma$ l = eff spring length
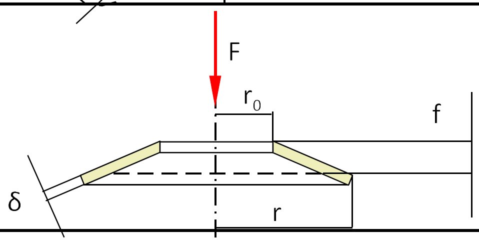	$F = \frac{\delta^2}{1 - 2/3\, r_0/r}\sigma$ $f = \frac{0.65\, r^2}{E\, \delta\, (1 - 2/3\, r_0/r)}\sigma$

Table A5 Buckling limit of compression loaded beams [Gero & Timoshenko, 1985]

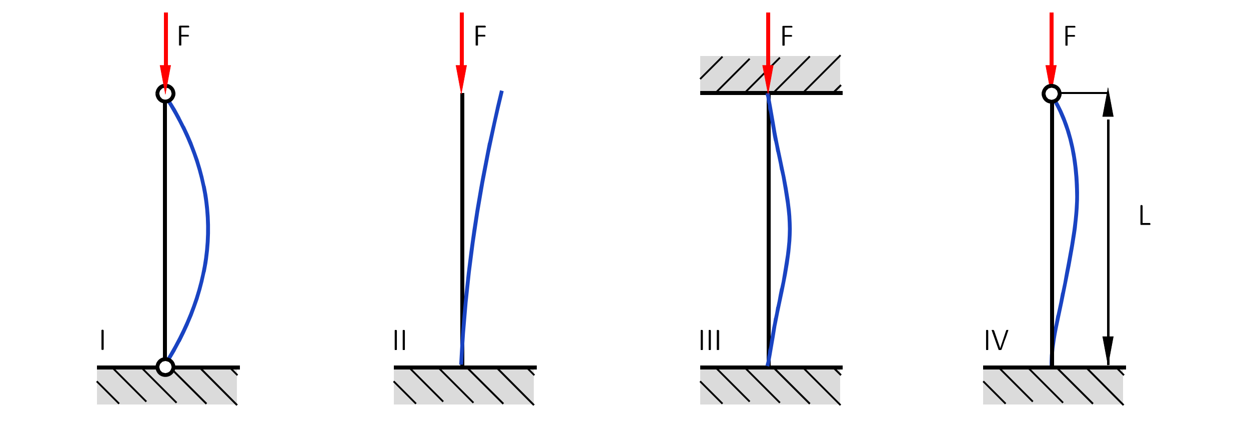

I	II	III	IV
$\frac{FL^2}{EI} = \pi^2$	$\frac{FL^2}{EI} = \frac{\pi^2}{4}$	$\frac{FL^2}{EI} = 4\pi^2$	$\frac{FL^2}{EI} = 2.046\pi^2$

Table A6 Approximate design functions S-shaped beams [Koster, 1996]

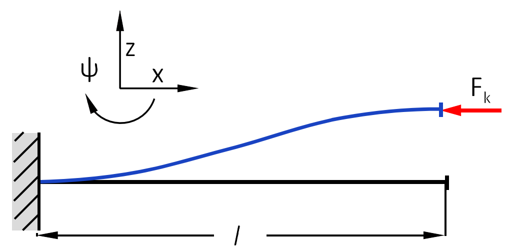

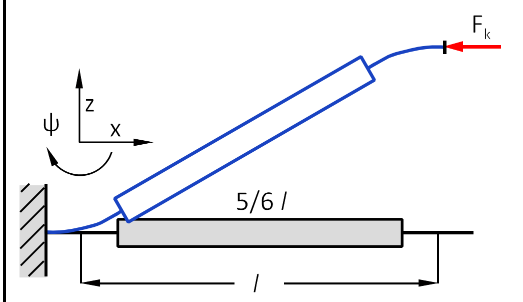

	leaf spring	wire spring	leave spring	wire spring
longitudinal stiffness c_{xx}	$\frac{EA}{l}$	$\frac{EA}{l}$	$\frac{3EA}{l}$	$\frac{3EA}{l}$
lateral stiffness c_{zz}	$\frac{12EI}{l^3}$	$\frac{12EI}{l^3}$	$\frac{72}{5}\frac{EI}{l^3}$	$\frac{72}{5}\frac{EI}{l^3}$
bending stress $\sigma_{\psi z}$	$\frac{3Etz}{l^2}$	$\frac{3Edz}{l^2}$	$\frac{3Etz}{l^2}$	$\frac{3Edz}{l^2}$
buckling load F_k	$\frac{4\pi^2 EI}{l^2}$	$\frac{4\pi^2 EI}{l^2}$	$\frac{36\pi^2 EI}{l^2}$	$\frac{36\pi^2 EI}{l^2}$

[1)] The configuration with reinforced mid-section considered in this table shows an increase of the buckling load by a factor of nine while the lateral stiffness has increased with only 20%.

Table A7 Moments of Inertia

Moment of inertia:	$I = \int \rho^2 dm$	Radius of gyration :	$i = \sqrt{I/m}$
Parallel axis theorem :	$I = I_z + a^2 m$	Torque :	$T = I\alpha \quad \alpha = \dot{\omega}$

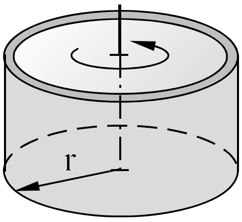

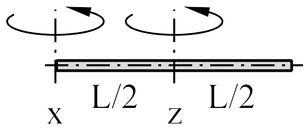

$$I_z = \frac{1}{12} m L^2$$

$$I_x = I_z + \left(\frac{L}{2}\right)^2 m$$

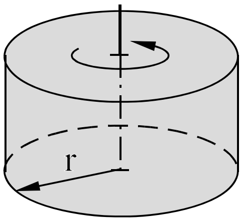

$$I = \frac{1}{2} m r^2$$

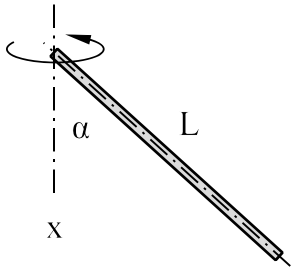

$$I_x = \frac{1}{3} m (L \sin \alpha)^2$$

$$I = \frac{2}{5} m r^2$$

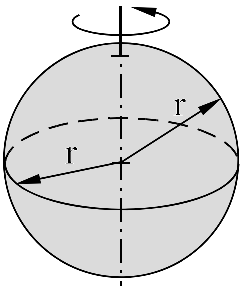

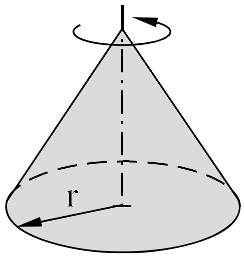

$$I = \frac{3}{10} m r^2$$

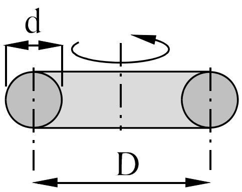

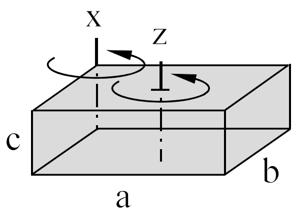

$$I_z = \frac{1}{12} m (a^2 + b^2)$$

$$I_x = \frac{1}{3} m (a^2 + b^2)$$

Linear motion	**Rotational motion**
Position x	Angular position φ
Velocity v	Angular velocity ω
Acceleration a	Angular acceleration α
Load F [N]	moment M [Nm]
mass m [kg]	moment of inertia I [kg m^2]
Impulse p = m v [kg m/s]	Angular Momentum H = I ω [kg m^2/s]
F = m a [N = kg m/s^2]	M = I α [Nm = kg m^2 rad/s^2]
W = F s [N m = J]	W = M φ [Nm rad = J]
E_k = ½ mv^2 [J]	E_k = ½ I ω^2 [J]
P = W/t = F s / t [J/s = W]	P = W/t = M ω [J/s = W]

Table A8 ISO Tolerances for holes and shafts

Metric screw threads ISO 724 (DIN 13 T1)

$H = 0.86603P$ $h_3 = 0.61343P$ $H_1 = 0.54127P$ $R = H/6$

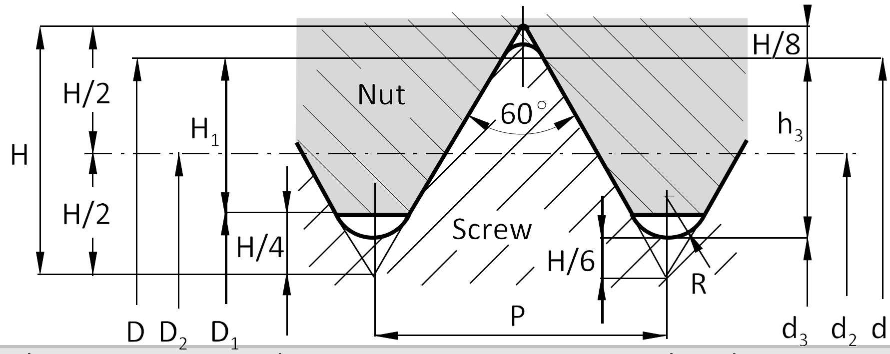

Nominal size d = D	Pitch P	root radius r	pitch diameter $d_2 = D_2$	minor diameter d_3	minor diameter D_1	thread height h_3	thread height H_1	stress area A_s	drill diam. mm
M 1	0.25	0.036	0.838	0.693	0.729	0.153	0.135	0.460	0.75
M 1.2	0.25	0.036	1.038	0.893	0.929	0.153	0.135	0.732	0.95
M 1.6	0.35	0.051	1.373	1.171	1.221	0.215	0.189	1.27	1.25
M 2	0.40	0.058	1.740	1.509	1.567	0.245	0.217	2.07	1.60
M 2.5	0.45	0.065	2.208	1.948	2.013	0.276	0.244	3.39	2.05
M 3	0.50	0.072	2.675	2.387	2.459	0.307	0.271	5.03	2.50
M 4	0.70	0.101	3.545	3.141	3.242	0.429	0.379	8.78	3.30
M 4.5	0.75	0.108	4.013	3.580	3.688	0.460	0.406	11.3	3.80
M 5	0.80	0.115	4.480	4.019	4.134	0.491	0.433	14.2	4.20
M 6	0.100	0.144	5.350	4.773	4.917	0.613	0.541	20.1	5.00
M 8	0.125	0.180	7.188	6.466	6.647	0.767	0.677	36.6	6.80
M 9	1.25	0.180	8.188	7.466	7.647	0.767	0.677	48.1	7.80
M 10	1.50	0.217	9.026	8.160	8.376	0.920	0.812	58.0	8.50
M 11	1.50	0.217	10.026	9.160	9.376	0.920	0.812	72.3	9.50
M 12	1.75	0.253	10.863	9.853	10.106	1.074	0.947	84.3	10.20
M 14	2.00	0.289	12.701	11.546	11.835	1.227	1.083	115	12.00
M 16	2.00	0.289	14.701	13.546	13.835	1.227	1.083	157	14.00
M 18	2.50	0.361	16.376	14.933	15.394	1.534	1.353	193	15.50
M 20	2.50	0.361	18.376	16.933	17.294	1.534	1.353	245	17.50
M 22	2.50	0.361	20.376	18..933	19.294	1.534	1.353	303	19.50
M 24	3.00	0.433	22.051	20.319	20.752	1.840	1.624	353	21.00
M 27	3.00	0.433	25.051	23.319	23.752	1.840	1.624	459	24.00
M 30	3.50	0.505	27.727	25.706	26.211	2.147	1.894	561	26.50
M 33	3.50	0.505	30.727	28.706	29.211	2.147	1.894	694	29.50
M 36	4.00	0.577	33.402	31.093	31.670	2.454	2.165	817	32.00
M 42	4.50	0.650	39.077	36.479	37.129	2.760	2.436	1121	37.50
M 48	5.00	0.722	44.752	41.866	42.857	3.067	2.706	1473	43.00
M 56	5.50	0.794	52.428	49.252	50.046	3.374	2.977	2030	50.50

Table A9 ISO Tolerances for holes and shafts

Example fits using ISO hole basis			
	clearance fit	transition fit	interference fit
H6	h5	j6, k6	n5, r5
H7	f7, g6, h6	k6, m6, n6	r6, s6
H8	d9,e8, f8, h9		s8, u8, x8

ISO Tolerances for holes (ISO 286-2)

Nominal hole sizes (mm)													
>	3	6	10	18	30	40	50	65	80	100	120	140	160
≤	6	10	18	30	40	50	65	80	100	120	140	160	180
micrometer													
H6	+8 0	+9 0	+11 0	+13 0	+16 0		+19 0		+22 0		+25 0		
H7	+12 0	+15 0	+18 0	+21 0	+25 0		+30 0		+35 0		+40 0		
H8	+18 0	+22 0	+27 0	+33 0	+39 0		+46 0		+54 0		+63 0		

ISO Tolerances for shafts (ISO 286-2)

Nominal shaft sizes (mm)													
>	3	6	10	18	30	40	50	65	80	100	120	140	160
≤	6	10	18	30	40	50	65	80	100	120	140	160	180
micrometer													
f6	-10 -18	-13 -22	-16 -27	-20 -33	-25 -41		-30 -49		-36 -58		-43 -68		
f7	-10 -22	-13 -28	-16 -34	-20 -41	-25 -50		-30 -60		-36 -71		-43 -83		
g6	-4 -12	-5 -14	-6 -17	-7 -20	-9 -25		-10 -29		-12 -34		-14 -39		
g7	-4 -16	-5 -20	-6 -24	-7 -28	-9 -34		-10 -40		-12 -47		-14 -54		
h5	-0 -5	-0 -6	-0 -8	-0 -9	-0 -11		-0 -13		-0 -15		-0 -18		
h6	-0 -8	-0 -9	-0 -11	-0 -13	-0 -16		-0 -19		-0 -22		-0 -25		
h7	-0 -12	-0 -15	-0 -18	-0 -21	-0 -25		-0 -30		-0 -35		-0 -40		
h9	-0 -30	-0 -36	-0 -43	-0 -52	-0 -62		-0 -74		-0 -87		-0 -100		
j6	+6 -2	+7 -2	+8 -3	+9 -4	+11 -5		+12 -7		+13 -9		+14 -11		
k6	+9 +1	+10 +1	+12 +1	+15 +2	+18 +2		+21 +2		+25 +3		+28 +3		
m6	+12 +4	+15 +6	+18 +7	+21 +8	+25 +9		+30 +11		+35 +13		+40 +15		
n5	+13 +8	+16 +10	+20 +12	+24 +15	+28 +17		+33 +20		+38 +23		+45 +27		
n6	+16 +8	+19 +10	+23 +12	+28 +15	+33 +17		+39 +20		+45 +23		+52 +27		
p6	+20 +12	+24 +15	+29 +18	+35 +22	+42 +26		+51 +32		+59 +37		+68 +43		
r6	+23 +15	+28 +19	+34 +23	+41 +28	+50 +34		+60 +41	+62 +43	+73 +51	+76 +54	+88 +63	+90 +65	+93 +68